Faculty of Nuclear Sciences and Physical Engineering
Czech Technical University in Prague

DISSERTATION THESIS

Applications of Path Integrals in Quantum Theory and Statistical Physics

Praha 2016 Václav Zatloukal

Bibliografický záznam:

Autor:	Ing. Václav Zatloukal České vysoké učení technické v Praze Fakulta jaderná a fyzikálně inženýrská Katedra fyziky
Název práce:	Aplikace dráhových integrálů v kvantové teorii a statistické fyzice
Studijní program:	Matematické inženýrství
Studijní obor:	Matematická fyzika
Školitel	Ing. Petr Jizba, PhD. České vysoké učení technické v Praze Fakulta jaderná a fyzikálně inženýrská Katedra fyziky
Akademický rok:	2015/2016
Počet stran:	120
Klíčová: slova	dráhový integrál, kvantová mechanika, statistická fyzika

Bibliographic Entry:

Author:	Ing. Václav Zatloukal Czech Technical University in Prague Faculty of Nuclear Sciences and Physical Engineering Department of Physics
Title of Dissertation:	Applications of Path Integrals in Quantum Theory and Statistical Physics
Degree Programme:	Mathematical Engineering
Field of Study:	Mathematical Physics
Supervisor:	Ing. Petr Jizba, PhD. Czech Technical University in Prague Faculty of Nuclear Sciences and Physical Engineering Department of Physics
Academic Year:	2015/2016
Number of Pages:	120
Keywords:	path integral, quantum mechanics, statistical physics

Acknowledgement

I am grateful to my doctoral advisor Dr. Petr Jizba for his support, and for inspiring discussions. I am also pleased to thank Prof. Hagen Kleinert for his supervision during my research stay in Berlin. Last but not least, I would like to sincerely acknowledge fruitful discussions and support, which I received from my temporal advisors and their institutions, namely: Prof. Angel Alastuey (École normale supérieure de Lyon), Prof. Zbigniew Haba (University of Wroclaw), Dr. Jiannis Pachos (University of Leeds), and Dr. Gavin Brennen (Macquarie University, Sydney).

Abstrakt:

Tato práce si klade za cíl prezentovat metody dráhového integrálu a následně je využít ke studiu rozličných problému kvantové a statistické fyziky, či dokonce obohatit stávající obecnou teorii. Po stručném přehledu historických souvislostí a výsledků jsou diskutována čtyři témata, z nichž každé je zastoupeno odpovídající publikací. Nejprve za pomoci dráhového integrálu elegantně odvodíme vysokoteplotní Wigner-Kirkwoodův rozvoj, který je používán v kvantové statistické fyzice. Dále zavedeme lokálněčasový dráhový integrál coby alternatívu k Feynmanovu dráhovému integrálu a prozkoumáme vliv frakčních derivací na distribuční funkce difuzních procesů. Nakonec se budeme zabývat o něco exotičtějším tématem a to kvantovými procházkami s abelovskými a neabelovskými anyonovými částicemi v rovnoměrném i neuspořádaném prostředí za použití diskrétního dráhového integrálu, jenž zahrnuje netriviální topologické efekty.

Abstract:

This thesis aims to introduce the techniques of path integration and apply them to various problems in quantum and statistical physics, or even refine the general theory. After a concise overview of the historical development and its main results, four topics, each represented by a published article, are presented. First, we rederive the high-temperature Wigner-Kirkwood expansion of quantum statistical mechanics to illustrate the efficiency of the path integral formalism. We follow by establishing the local-time path integral as an alternative to the Feynman path integral, and study the effect of fractional derivatives on the distribution functions of diffusion processes. Finally, we consider a more exotic problem of quantum walks with Abelian and non-Abelian anyonic particles in both uniform and random environments, using a discrete path-integral-inspired approach that incorporates nontrivial topological effects.

Contents

1 Opening remarks

This doctoral thesis provides a comprehensive introduction into the concept of path integration, and gathers several latest results in the field, which the author, his doctoral advisor, and other collaborators obtained between the years 2011 and 2016.

In the following chapter, the key ideas upon which the path integral (PI) has been successfully developed, are presented, starting from the mathematical theory of stochastic processes. The exposition is brief but self-contained, so that it allows to study more specialized chapters 3, 4, 5 and 6.[1] Each of these chapters focuses on an original research topic that is introduced to the reader in a compact form to facilitate his/her study of the corresponding articles [13, 14, 15, 16]. The articles are enclosed in their full length in the appendix of this thesis, where a note about collaborators, and about the scope of the thesis author's own contribution is added.[2]

The four topics contribute primarily to the field of statistical quantum physics. They include "Path-integral approach to the Wigner-Kirkwood expansion", "Local-time representation of path integrals", "Green function of the double-fractional Fokker-Planck equation", and "Transport properties of anyons in random topological environments". While the first three items should be easily accessible even to non-experts in the respective fields, who are only reasonably phrased with the basics of path integration, the last topic is more exotic, and hence it requires and deserves a longer preparation, and introduction of the concepts employed.

In the concluding chapter 7, I summarize the results of this doctoral thesis, and discuss their significance for the field of path integrals, or, more broadly, the role they play in the context of statistical and quantum physics.

[1] There exist indeed many applications of PIs in quantum and statistical physics, as well as outside of physics, e.g., in biochemistry or economics. An interested reader is encouraged to consult the monographs [1, 2, 3, 4, 5, 6, 7]. Apart from these, there are chapters with introduction or applications of PIs included in almost every modern textbook on quantum mechanics and quantum field theory (see, e.g., [8, 9, 10, 11, 12]).

[2] The manuscripts in the appendix may slightly differ from the corresponding published articles due to some minor changes implemented by the editorial offices.

2 Introduction to path integrals

At a first glance, path integration can be viewed simply as a method to tackle partial differential equations of the parabolic type. These are so ubiquitous in physics, and other scientific disciplines, that, no wonder, PI finds applications in fields that look, by the common sense, rather unrelated: e.g., quantum mechanics vs. financial markets vs. polymers [2]. The fact that one method can be used for many different purposes hints that the idea behind that method is powerful, and can be fruitful in potential applications.

In short, PI is a sum over histories weighted by appropriate factors, be it histories of a pollen grain in the water, an electron drifting through a double slit, or the evolution of the price of an asset at the stock market.[3] To start intuitively, consider a particle (a pollen grain in the water, or a dust particle in the air) which exhibits random motion. In the simplest case, this motion can be described as a sequence of jumps with their lengths distributed normally, i.e., according to the law

$$\sqrt{(\Delta \mathbf{x})^2} \sim \left(\frac{M}{2\pi\Delta t}\right)^{D/2} e^{-\frac{M(\Delta \mathbf{x})^2}{2\Delta t}}, \tag{1}$$

where D is the dimensionality of space, Δt is the time interval between jumps, and M is a constant that measures the typical size of the jumps.

Assuming that the jumps are independent events, we can compose them in a straightforward way via convolution [17] to obtain the conditional probability

$$P_{\text{free}}(\mathbf{x}, t; \mathbf{x}_0, t_0) = \left(\frac{M}{2\pi(t-t_0)}\right)^{D/2} e^{-\frac{M(\mathbf{x}-\mathbf{x}_0)^2}{2(t-t_0)}}, \tag{2}$$

that a particle located at position $\mathbf{x}_0$ at time t_0 will be found at time $t > t_0$ at position $\mathbf{x}$. It is understood that for times $t < t_0$, $P_{\text{free}} = 0$ identically. (The subscript "free" is used to distinguish this transition probability from a more general case that includes an external potential, which will be discussed below.)

The distribution function P_{free} obeys the following parabolic partial differential equation:

$$\frac{\partial}{\partial t} P_{\text{free}} = \frac{1}{2M} \Delta_{\mathbf{x}} P_{\text{free}} \quad , \quad P_{\text{free}}(\mathbf{x}, t_0; \mathbf{x}_0, t_0) = \delta^{(D)}(\mathbf{x} - \mathbf{x}_0), \tag{3}$$

[3] Note that each of these examples is fundamentally different in nature: first describes a material entity whose trajectory can be directly contemplated; second features a wave-particle quantum whose trajectories are not independent alternative events, but rather happen all at the same time to construct an interference pattern; whereas the last entity is virtual, a number on the computer screen, which we attempt to predict using the PI method.

where $\Delta_{\mathbf{x}} \equiv \frac{\partial^2}{\partial x_1^2} + \ldots \frac{\partial^2}{\partial x_D^2}$ is the Laplace operator. This equation is the simplest form of the *diffusion*, or *Fokker-Planck*, equation, which describes diffusion of particles through a medium. It can also be found under the name *heat equation* as it governs the heat flow in an environment with generic temperature distribution. Owing to the specific initial condition, the solution of Eq. (3) is in fact the Green function (or the fundamental solution) of the operator $\frac{\partial}{\partial t} - \frac{1}{2M}\Delta$.

With quantum-mechanical applications in mind, we will consider a more general form of Eq. (3), namely

$$\frac{\partial}{\partial t} P = -\hat{H}_{\mathbf{x}} P, \tag{4}$$

where

$$\hat{H}_{\mathbf{x}} = -\frac{1}{2M}\Delta_{\mathbf{x}} + V(\mathbf{x}) \tag{5}$$

is the Hamiltonian operator. For a generic potential function $V(\mathbf{x})$, the latter equation does not possess an explicit solution, such as Formula (2). One can only formally write (in the Dirac bra-ket notation)

$$P(\mathbf{x}, t; \mathbf{x}_0, t_0) = e^{-(t-t_0)\hat{H}_{\mathbf{x}}} \delta^{(D)}(\mathbf{x} - \mathbf{x_0}) \equiv \langle \mathbf{x} | \, e^{-(t-t_0)\hat{H}} \, | \mathbf{x}_0 \rangle \, . \tag{6}$$

At this stage, the PI representation enters via the *Suzuki-Trotter* formula, which states, suppressing technical details, that the exponential of a sum of two operators can be written as a limit

$$e^{A+B} = \lim_{N\to\infty} \left(e^{A/N} e^{B/N} \right)^N . \tag{7}$$

This includes the trivial commutative case $e^{a+b} = e^a e^b$. Hence, the transition probability P may be cast in the form

$$\begin{aligned} P(\mathbf{x}, t; \mathbf{x}_0, t_0) &= \lim_{N\to\infty} \langle \mathbf{x} | \left(e^{-\frac{t-t_0}{N}\frac{-\Delta}{2M}} e^{-\frac{t-t_0}{N}V} \right)^N | \mathbf{x}_0 \rangle \\ &= \lim_{N\to\infty} \int d^D x_1 \ldots d^D x_{N-1} \prod_{k=1}^{N} \langle \mathbf{x}_k | \, e^{-\varepsilon \frac{-\Delta}{2M}} e^{-\varepsilon V} \, | \mathbf{x}_{k-1} \rangle \, , \end{aligned} \tag{8}$$

where we have introduced resolutions of unity in the position representation,

$$1 = \int_{\mathbb{R}^D} d^D x \, |\mathbf{x}\rangle \langle \mathbf{x}| \, , \tag{9}$$

and, for brevity, denoted $\mathbf{x} \equiv \mathbf{x}_N$ and $\varepsilon \equiv (t - t_0)/N$.

While the potential part can be immediately rearranged,

$$e^{-\varepsilon V(\hat{\mathbf{x}})} \, |\mathbf{x}_{k-1}\rangle = |\mathbf{x}_{k-1}\rangle \, e^{-\varepsilon V(\mathbf{x}_{k-1})}, \tag{10}$$

the remaining kinetic part is elucidated through the formula

$$\langle \mathbf{x}_k |\, e^{-\varepsilon \frac{-\Delta}{2M}}\, |\mathbf{x}_{k-1}\rangle = P_{\text{free}}(\mathbf{x}_k, \varepsilon; \mathbf{x}_{k-1}, 0) = \left(\frac{M}{2\pi\varepsilon}\right)^{D/2} e^{-\frac{M(\mathbf{x}_k - \mathbf{x}_{k-1})^2}{2\varepsilon}}. \tag{11}$$

The latter is a straightforward application of Eq. (2), which, in fact, can be derived from Eq. (3) via Fourier transform in the variable $\mathbf{x}$.

The transition probability P now reads

$$P(\mathbf{x}, t; \mathbf{x}_0, t_0) = \lim_{N\to\infty} \int_{\mathbb{R}^D} d^D x_1 \ldots d^D x_{N-1} \left(\frac{M}{2\pi\varepsilon}\right)^{ND/2} e^{-\varepsilon \sum_{k=1}^{N} \left[\frac{M}{2}\left(\frac{\mathbf{x}_k - \mathbf{x}_{k-1}}{\varepsilon}\right)^2 + V(\mathbf{x}_{k-1})\right]}, \tag{12}$$

which is customarily denoted by

$$\int_{\mathbf{x}(t_0)=\mathbf{x}_0}^{\mathbf{x}(t)=\mathbf{x}} \mathcal{D}\mathbf{x}(t') e^{-\int_{t_0}^{t} dt' \left[\frac{M}{2}\dot{\mathbf{x}}^2 + V(\mathbf{x})\right]}. \tag{13}$$

This is the path integral (PI), a sum over all trajectories (particle's histories) that originate from position $\mathbf{x}_0$ at time t_0 and terminate at $\mathbf{x}$ at time t, weighted by certain exponential factors.

The integration over a space of functions (fluctuating trajectories) was originally introduced by Wiener [18] to describe the Brownian motion, and since then it forms the basis of the theory of stochastic processes. There, the expression (13) would be regarded as a mean value of the functional

$$\exp\left[-\int_{t_0}^{t} dt' V(\mathbf{x})\right] \tag{14}$$

with respect to the Wiener probability measure

$$\sim \exp\left[-\int_{t_0}^{t} dt' \frac{M}{2}\dot{\mathbf{x}}^2\right] \tag{15}$$

(the $\sim$-sign captures the prefactor in front of the exponential in Eq. (12)), taken over the space of trajectories with specified endpoints.

Let us stress that Formula (13) for $P(\mathbf{x}, t; \mathbf{x}_0, t_0)$ does not *solve* Eq. (4). It serves merely as a *representation* for transition amplitudes which can be resolved in particular simple cases to produce a closed formula, or at least used to derive general approximation schemes (e.g., the saddle-point approximation). In any case, the PI representation (13) views certain parabolic differential equations from a different angle and provides one with a valuable intuition about the problem in hand.

In non-relativistic quantum mechanics, the central equation is the Schrödinger equation

$$\frac{\hbar}{i}\frac{\partial}{\partial t}\psi(\mathbf{x},t) = -\hat{H}_{\mathbf{x}}\psi(\mathbf{x},t), \tag{16}$$

with the Hamiltonian operator

$$\hat{H}_{\mathbf{x}} = -\frac{\hbar^2}{2M}\Delta_{\mathbf{x}} + V(\mathbf{x}). \tag{17}$$

It differs from the diffusion equation (4) only in the introduction of the Planck constant $\hbar$, and, more importantly, in the appearance of the imaginary unit i. The latter implies that the wave function ψ is complex-valued in general.

With the initial condition

$$\psi(\mathbf{x},t_0) = \delta^{(D)}(\mathbf{x}-\mathbf{x}_0), \tag{18}$$

Eq. (16) can be again formally solved,

$$K(\mathbf{x},t;\mathbf{x}_0,t_0) \equiv \psi(\mathbf{x},t) = \langle\mathbf{x}|\, e^{-\frac{i}{\hbar}(t-t_0)\hat{H}}\, |\mathbf{x}_0\rangle\,, \tag{19}$$

to yield the transition amplitudes K, that is, the matrix elements of the evolution operator $e^{-\frac{i}{\hbar}(t-t_0)\hat{H}}$ in the position basis.

The same sequence of steps that led to the PI representation (13) can now be applied to treat Eq. (19), and yield the PI representation of the transition amplitudes

$$K(\mathbf{x},t;\mathbf{x}_0,t_0) = \int_{\mathbf{x}(t_0)=\mathbf{x}_0}^{\mathbf{x}(t)=\mathbf{x}} \mathcal{D}\mathbf{x}(t') e^{\frac{i}{\hbar}\int_{t_0}^{t} dt' \left[\frac{M}{2}\dot{\mathbf{x}}^2 - V(\mathbf{x})\right]}, \tag{20}$$

named *Feynman PI* after Richard Feynman who was the first to use PI in quantum physics [19, 20].[4] The right-hand-side is again a shorthand notation for the infinite-fold integration, Eq. (12), where the substitutions $M \to M/\hbar^2$ and $\varepsilon \to i\varepsilon/\hbar$ have been performed (the so-called *Wick rotation*). Note that due to the imaginary unit in the exponent of Eq. (20), the integrals fail to converge absolutely, which causes troubles when one tries to apply rigorously the results of the mathematical measure theory. Yet, integrals of the form

$$\int_{\mathbb{R}} e^{ix^2} dx \tag{21}$$

(cf. *Fresnel integrals*) do converge non-absolutely, resulting in $\sqrt{i\pi}$.

[4] Feynman was the first physicist who *used* PI to formulate quantum mechanics and developed the complete method (see [1]), although the basic idea is present already in the work of Dirac [21], who appreciated the role of Lagrangian in short-time evolution of the wave function, and even suggested the time-slicing procedure for finite, i.e., non-infinitesimal, times analogous to Formula (12).

The weights of the paths $\mathbf{x}(t')$ in Formula (20) are complex units $e^{i\mathcal{A}[\mathbf{x}]/\hbar}$, the phase of which is identified with the classical action, i.e., the time integral of the Lagrangian

$$\mathcal{A}[\mathbf{x}] = \int_{t_0}^{t} dt' L(\mathbf{x}, \dot{\mathbf{x}}), \tag{22}$$

divided by $\hbar$. PI allows to formulate quantum physics in terms of Lagrangians instead of Hamiltonians, which proves to be very helpful in the development of the quantum field theory [10].

2.1 Phase space path integral

The Feynman PI (20) is formulated in terms of configuration-space trajectories and the Lagrangian. On the contrary, the canonical approach to quantum mechanics starts from the phase space of the positions and momenta, where the central role is played by the Hamiltonian of the system. To make contact between the two approaches, it is illuminating to consider the *phase space PI*, i.e., an equivalent PI formulated in terms of the phase-space trajectories.

Let us start with the quantum-mechanical propagator (19), written in the form

$$K(\mathbf{x}, t; \mathbf{x}_0, t_0) = \langle \mathbf{x} | \left(e^{-\frac{i}{\hbar}\varepsilon \hat{H}} \right)^N | \mathbf{x}_0 \rangle , \tag{23}$$

where $\varepsilon N = t - t_0$, and $\hat{H} = H(\hat{\mathbf{x}}, \hat{\mathbf{p}})$ is a generic Hamiltonian operator. Utilizing the $\mathbf{x}$-space resolutions of unity as in Eq. (8), and the $\mathbf{p}$-space resolutions of unity

$$1 = \int_{\mathbb{R}^D} d^D p \, |\mathbf{p}\rangle \langle \mathbf{p}| , \tag{24}$$

where

$$\langle \mathbf{x} | \mathbf{p} \rangle = \frac{e^{\frac{i}{\hbar}\mathbf{p}\cdot\mathbf{x}}}{(2\pi\hbar)^{D/2}}, \tag{25}$$

the propagator may be cast as

$$\begin{aligned} K &= \int d^D x_1 \dots d^D x_{N-1} \prod_{k=1}^{N} \langle \mathbf{x}_k | \, e^{-\frac{i}{\hbar}\varepsilon \hat{H}} \, | \mathbf{x}_{k-1} \rangle \\ &= \int d^D x_1 \dots d^D x_{N-1} \int \frac{d^D p_1}{(2\pi\hbar)^{D/2}} \cdots \frac{d^D p_N}{(2\pi\hbar)^{D/2}} \prod_{k=1}^{N} \langle \mathbf{x}_k | \, e^{-\frac{i}{\hbar}\varepsilon \hat{H}} \, | \mathbf{p}_k \rangle \, e^{-\frac{i}{\hbar}\mathbf{p}_k \cdot \mathbf{x}_{k-1}}. \end{aligned} \tag{26}$$

For large N, ε becomes infinitesimal, and so we can approximate[5]

$$\langle \mathbf{x}_k |\, e^{-\frac{i}{\hbar}\varepsilon \hat{H}}\, | \mathbf{p}_k \rangle \approx \langle \mathbf{x}_k |\, (1 - \frac{i}{\hbar}\varepsilon \hat{H})\, | \mathbf{p}_k \rangle = \frac{e^{\frac{i}{\hbar}\mathbf{p}_k \cdot \mathbf{x}_k}}{(2\pi\hbar)^{D/2}} \big[1 - \frac{i}{\hbar}\varepsilon H(\mathbf{x}_k, \mathbf{p}_k)\big] \approx \frac{e^{\frac{i}{\hbar}[\mathbf{p}_k \cdot \mathbf{x}_k - \varepsilon H(\mathbf{x}_k, \mathbf{p}_k)]}}{(2\pi\hbar)^{D/2}}. \tag{27}$$

Hence, we obtain an expression for the propagator

$$K = \int d^D x_1 \ldots d^D x_{N-1} \int \frac{d^D p_1}{(2\pi\hbar)^D} \cdots \frac{d^D p_N}{(2\pi\hbar)^D} e^{\frac{i}{\hbar}\varepsilon \sum_{k=1}^{N} \left[\mathbf{p}_k \cdot \frac{\mathbf{x}_k - \mathbf{x}_{k-1}}{\varepsilon} - H(\mathbf{x}_k, \mathbf{p}_k)\right]}, \tag{28}$$

which is customarily abbreviated

$$\int_{\mathbf{x}(t_0)=\mathbf{x}_0}^{\mathbf{x}(t)=\mathbf{x}} \mathcal{D}\mathbf{x}(t')\mathcal{D}\mathbf{p}(t') e^{\frac{i}{\hbar}\int_{t_0}^{t} dt' [\mathbf{p}\cdot\dot{\mathbf{x}} - H(\mathbf{x},\mathbf{p})]}. \tag{29}$$

This is the phase space PI. Note that while the $\mathbf{x}$-trajectories start and end up at prescribed fixed points, there is no such constraint on the $\mathbf{p}$-trajectories.

The phase space PI representation (29) is more general than the Feynman PI (20), as it holds, at least formally, for a generic Hamiltonian. If we take, in particular,

$$H = \frac{\mathbf{p}^2}{2M} + V(\mathbf{x}), \tag{30}$$

and integrate out the momenta in Eq. (28), we recover, indeed, the Feynman representation, Formula (20).

Let us also remark that the PI (29) is a good starting point to exploit the path-integral representation in the Hamiltonian-constraint-based relativistic quantum mechanics. Although the following considerations are somewhat formal, it is instructive to follow them in order to observe the heuristic power of PIs.

First of all, we note that Formula (26) holds true even if we change the equidistant "ε"-time slicing to an arbitrary variable time slicing, $\varepsilon \to t_k - t_{k-1}$, where $t_N \equiv t$. Averaging over all time slicings amounts to integrating over $t_1, \ldots, t_{N-1}$, which introduces in Eq. (28) an "irrelevant" infinite constant.[6] Using, in addition, a trivial identity

$$e^{-\frac{i}{\hbar}\varepsilon H(\mathbf{x}_k, \mathbf{p}_k)} = \int dE_k e^{\frac{i}{\hbar}\varepsilon E_k} \delta\big(E_k + H(\mathbf{x}_k, \mathbf{p}_k)\big), \tag{31}$$

we obtain the PI expression

$$K \propto \int_{(t_0,\mathbf{x}_0)}^{(t,\mathbf{x})} \mathcal{D}\mathbf{x}\mathcal{D}t\mathcal{D}\mathbf{p}\mathcal{D}E e^{\frac{i}{\hbar}\int_{(t_0,\mathbf{x}_0)}^{(t,\mathbf{x})} [E dt + \mathbf{p}\cdot d\mathbf{x}]} \delta[E + H(\mathbf{x}, \mathbf{p})], \tag{32}$$

[5] We tacitly assume that H does not involve products of $\mathbf{x}$ and $\mathbf{p}$. Such product have to be treated more carefully, as their translation to the PI action depends on the choice of operator ordering.

[6] Irrelevant in the sense that it does not contain any structure relevant for the problem.

where the δ-functional is defined by its discretized form

$$\delta[E + H(\mathbf{x}, \mathbf{p})] \sim \prod_{k=1}^{N} \delta\big(E_k + H(\mathbf{x}_k, \mathbf{p}_k)\big). \tag{33}$$

The path integration is performed over all spacetime trajectories that connect the points $(t_0, \mathbf{x}_0)$ and $(t, \mathbf{x})$, and over all four-momentum trajectories. Parametrization of the trajectories plays no role, as neither the action nor the δ-functional depends on it.

Let us denote the spacetime points by $x = (t, \mathbf{x})$, the four-momentum by $p = (E, \mathbf{p})$, and introduce the relativistic Hamiltonian

$$H_{\mathrm{rel}}(x, p) = E + H(\mathbf{x}, \mathbf{p}). \tag{34}$$

With these definitions, and regarded as a function of x, the right-hand side of Eq. (32) assumes the form

$$\tilde{\psi}(x) \equiv \int_{x_0}^{x} \mathcal{D}x\mathcal{D}p e^{\frac{i}{\hbar}\int_{x_0}^{x} p\cdot dx} \delta[H_{\mathrm{rel}}]. \tag{35}$$

This PI has been introduced in [22] under the name "timeless PI".[7] It has an intuitive geometric interpretation as a sum over all (x, p)-trajectories (with fixed x-space endpoints x_0 and x) that are weighted by a universal factor

$$e^{\frac{i}{\hbar}\int_{x_0}^{x} p\cdot dx}, \tag{36}$$

and fulfill at all instances the *Hamiltonian constraint*

$$H_{\mathrm{rel}}(x, p) = 0. \tag{37}$$

The PI (35) makes sense, at least formally, for generic functions H_{rel} of x and p. For example, a free relativistic particle with mass M is described by the relativistic Hamiltonian

$$H_{\mathrm{rel}} = \frac{E^2}{c^2} - \mathbf{p}^2 - M^2c^2. \tag{38}$$

The relativistic formulation of mechanics (both relativistic and non-relativistic) based on the Hamiltonian constraint is explained in detail in Chapter 3 of monograph [23]. A great advantage of this formulation is that it can be extended to the field theory in a rather straightforward and smooth manner. The ensuing formalism for field theories based on the Hamiltonian constraint is elegant and compact, and it raises exciting questions about both classical and quantum field theory [24, 25].[8]

[7] The word "timeless" refers to the fact that the paths are not parametrized. Time is, however, still present as the first component of x.

[8] These articles also developed during my doctoral studies, but their topic is too remote to be included as a part of this thesis.

At the end of this section, let us derive a partial differential equation fulfilled by the wave function $\tilde{\psi}(x)$ represented by the PI (35). In a discretized form,

$$\tilde{\psi}(x) \sim \int \prod_{k=1}^{N-1} d^{D+1}x_k \int \prod_{k=1}^{N} \frac{d^{D+1}p_k}{(2\pi\hbar)^{D+1}} e^{\frac{i}{\hbar}\sum_{k=1}^{N} p_k\cdot(x_k - x_{k-1})} \prod_{k=1}^{N} \delta\big(H_{\rm rel}(x_k, p_k)\big). \tag{39}$$

Observe that

$$-i\hbar\partial_{x_N} e^{\frac{i}{\hbar}p_N\cdot(x_N - x_{N-1})} = p_N e^{\frac{i}{\hbar}p_N\cdot(x_N - x_{N-1})}, \tag{40}$$

i.e., the appearance of p_N inside the PI can be traded for operating by $-i\hbar\partial_{x_N}$ outside the PI. Hence, the right-hand side reads (recall that $x_N \equiv x$)

$$\delta\big(H_{\rm rel}(x, -i\hbar\partial_x)\big) \int \prod_{k=1}^{N-2} d^{D+1}x_k \int \prod_{k=1}^{N-1} \frac{d^{D+1}p_k}{(2\pi\hbar)^{D+1}} e^{\frac{i}{\hbar}\sum_{k=1}^{N-1} p_k\cdot(x_k - x_{k-1})} \prod_{k=1}^{N-1} \delta\big(H_{\rm rel}(x_k, p_k)\big), \tag{41}$$

where integrations over p_N and x_{N-1} have been performed. The latter identified x_{N-1} with x. In the limit $N \to \infty$, we find

$$\tilde{\psi}(x) = \delta\big(H_{\rm rel}(x, -i\hbar\partial_x)\big) \int_{x_0}^{x} \mathcal{D}x\mathcal{D}p\, e^{\frac{i}{\hbar}\int_{x_0}^{x} p\cdot dx} \delta[H_{\rm rel}] = \delta\big(H_{\rm rel}(x, -i\hbar\partial_x)\big)\tilde{\psi}(x). \tag{42}$$

Applying the relativistic Hamiltonian operator on both sides of this equation, and taking into account the identity

$$\alpha\,\delta(\alpha) = 0 \tag{43}$$

extended to operator-valued α, we arrive at the partial differential equation

$$H_{\rm rel}(x, -i\hbar\partial_x)\tilde{\psi}(x) = 0. \tag{44}$$

This equation can be viewed as a generalization of the Schrödinger equation to the relativistic formalism. For $H_{\rm rel}$ given by Eq. (34), which describes non-relativistic systems, we recover the standard Schrödinger equation

$$\left[-i\hbar\partial_t + H(\mathbf{x}, -i\hbar\partial_{\mathbf{x}})\right]\tilde{\psi}(t, \mathbf{x}) = 0, \tag{45}$$

while in the case of a free relativistic particle, Eq. (38), we obtain the Klein-Gordon equation

$$\left[-\frac{\hbar^2}{c^2}\partial_t^2 + \hbar^2\partial_{\mathbf{x}}^2 - M^2c^2\right]\tilde{\psi}(t, \mathbf{x}) = 0. \tag{46}$$

Let us remark that the operator $\delta\big(H_{\rm rel}(x, -i\hbar\partial_x)\big)$ serves as a projector on the space of solutions of Eq. (44). Indeed, for any wave function $\phi(x)$, the wave function $\delta(\hat{H}_{\rm rel})\phi(x)$ satisfies

$$\hat{H}_{\rm rel}\big(\delta(\hat{H}_{\rm rel})\phi(x)\big) = 0, \tag{47}$$

due to the identity (43).

3 Path-integral approach to the Wigner-Kirkwood expansion

Path integrals that contain only real quantities, such as in Eq. (13), occur naturally in statistical quantum mechanics, where the central role is played by the Gibbs operator

$$e^{-\beta\hat{H}}. \tag{48}$$

Here, $\beta = 1/(k_B T)$ is the inverse temperature, and k_B the Boltzmann constant. For a fixed number of particles, the partition function is obtained by taking the trace of the Gibbs operator,

$$Z(\beta) = \mathrm{Tr}\, e^{-\beta\hat{H}}, \tag{49}$$

whence the equilibrium density matrix is just a normalized version of the Gibbs operator,

$$\frac{e^{-\beta\hat{H}}}{Z(\beta)}. \tag{50}$$

PI representation of the matrix elements of the Gibbs operator (sometimes called the *Feynman-Kac* formula) follows from Eqs. (6) and (13) by setting $t - t_0 = \beta$, $t' = \tau/\hbar$, and $M \to M/\hbar^2$:

$$\rho(\mathbf{x}_a, \mathbf{x}_b, \beta) \equiv \langle \mathbf{x}_b |\, e^{-\beta\hat{H}}\, | \mathbf{x}_a \rangle = \int_{\mathbf{x}(0)=\mathbf{x}_a}^{\mathbf{x}(\beta\hbar)=\mathbf{x}_b} \mathcal{D}\mathbf{x}(\tau) e^{-\frac{1}{\hbar}\int_0^{\beta\hbar} d\tau \left[\frac{M}{2}\dot{\mathbf{x}}^2 + V(\mathbf{x})\right]}. \tag{51}$$

(We rescaled the parameter t' to comply with the form that is usual in the literature – see Ref. [2].) Note that the integrand in the exponent of this PI is the classical Hamiltonian (the energy of the system), expressed in terms of the position variable $\mathbf{x}$ and the velocity $\dot{\mathbf{x}}$.

In the article of Appendix A, Ref. [13], we develop the *Wigner-Kirkwood* expansion [26, 27], which approximates the PI (51) in the regime of small β, i.e., high temperatures. In fact, we consider a slightly more general situation, in which the kinetic term in the PI (51) assumes the form $\sum_{j=1}^{D} \frac{M_j}{2}\dot{x}_j^2$, to allow for various particle species.

It is illuminating to introduce dimensionless time and space variables, s and $\boldsymbol{\xi}$, by

$$\begin{aligned} \mathbf{x} &= \mathbf{x}_a + \Lambda\boldsymbol{\xi}, \\ \tau &= \beta\hbar s, \end{aligned} \tag{52}$$

where $\Lambda = \mathrm{diag}(\lambda_1, \ldots, \lambda_D)$ is a diagonal matrix with the entries

$$\lambda_j = \sqrt{\frac{\beta\hbar^2}{M_j}}, \tag{53}$$

which are identified as the thermal de Broglie wavelengths. The PI representation of $\rho(\mathbf{x}_a, \mathbf{x}_a, \beta)$ (we have set $\mathbf{x}_b = \mathbf{x}_a$ for simplicity) now reads

$$\rho(\mathbf{x}_a, \mathbf{x}_b, \beta) = \frac{1}{\det \Lambda} \int_{\boldsymbol{\xi}(0)=\mathbf{0}}^{\boldsymbol{\xi}(1)=\mathbf{0}} \mathcal{D}\boldsymbol{\xi}(s) e^{-\int_0^1 ds \left[\frac{1}{2}\dot{\boldsymbol{\xi}}^2 + \beta V(\mathbf{x}_a + \Lambda\boldsymbol{\xi})\right]}. \tag{54}$$

For small β, it is legitimate to expand the potential into a Taylor series around the point $\mathbf{x}_a$, and, moreover, expand in β the potential part of the PI weight factors. The result is a power series in β and $\hbar$, multiplied by the classical (i.e., $\hbar$-independent) factor $e^{-\beta V(\mathbf{x}_a)}$. This series features derivatives of the potential V, and model-independent coefficients Q (see Eqs. (14–16) in the article of Appendix A).

In the one-dimensional case, the Q coefficients can be given a more explicit form of Eq. (26) in App. A. This expression is simple enough to be implemented on a computer. Hence, using the *Mathematica* software, we managed to drive the Wigner-Kirkwood expansion up to the 18th order in β, with first eight orders shown explicitly in Table I of the article in App. A.

As an example, we considered the one-dimensional anharmonic oscillator, and calculated high-temperature expansions of certain thermodynamic quantities. We also commented on the possibility to generalize our results to off-diagonal matrix elements ($\mathbf{x}_b \neq \mathbf{x}_a$). This can be done in principle, but the complexity of calculations proved to be beyond the scope of the paper.

4 Local-time representation of path integrals

Before introducing the concept of local times, let us first talk about the role of PI's in the quantum field theory.

4.1 Path integrals in quantum field theory

Quantum field theory, in its modern formulation, is also based on the concept of integration over a space of functions [9, 10]. Here, however, the fluctuating trajectories $\mathbf{x}(t)$ (where t is a one-dimensional parameter) are replaced by fluctuating *fields* $\phi(x^\mu)$, where $x^\mu \equiv x$ is a space-time point, and ϕ may be a real or complex, or even Lie-algebra or Grassmann-valued quantity.

One way to introduce field-theoretic PI is to start with a generic self-adjoint operator $A(x^\mu, \partial/\partial x^\mu)$ with spectral lower bound, that acts on a space of real-valued functions (for simplicity), and consider its Green function G, i.e., a function, which satisfies the equation

$$A(x, \partial/\partial x)G(x, x_0) = \delta(x - x_0). \tag{55}$$

(Here, the δ-function is, of course, multidimensional.)

To draw analogy with finite-dimensional matrices, we can rewrite the left-hand side as

$$A(x, \partial/\partial x)G(x, x_0) = \int dx' \delta(x - x') A(x', \partial/\partial x')G(x', x_0), \tag{56}$$

which is now interpreted as a continuous matrix multiplication of two continuous matrices, $\delta(x - x')A(x', \partial/\partial x')$ and $G(x', x_0)$, over the index x'.

All discrete-matrix formulas can now be, at least on the formal level, extended to the continuous case. Of particular utility is the identity

$$\begin{aligned} &-\frac{1}{2}\int dx\, \phi(x)A(x, \partial/\partial x)\phi(x) + \int dx\, J(x)\phi(x) = \\ &= -\frac{1}{2}\int dx\, \left[\phi(x) - \int dx'\, G(x, x')J(x')\right] A(x, \partial/\partial x) \left[\phi(x) - \int dx''\, G(x, x'')J(x'')\right] \\ &+\frac{1}{2}\int dx\, dx'\, J(x)G(x, x')J(x'), \end{aligned} \tag{57}$$

which can be used to calculate the continuous infinite-dimensional Gaussian integral:

$$\begin{aligned} W_0[J] &\equiv \mathcal{N}_0 \int \mathcal{D}\phi(x) \exp\left[-\frac{1}{2}\int dx\, \phi(x)A(x, \partial/\partial x)\phi(x) + \int dx\, J(x)\phi(x)\right] = \\ &= \exp\left[\frac{1}{2}\int dx\, dx'\, J(x)G(x, x')J(x')\right], \end{aligned} \tag{58}$$

where the normalization $\mathcal{N}_0$ is determined from the requirement $W_0[0] = 1$. The infinite-dimensional integral, taken over all field configurations $\phi(x)$, is the *field-theoretic PI*.[9] The quantity W_0 is a functional of the *source* $J(x)$, which is an arbitrary function of x.

In quantum field theory, the term quadratic in ϕ in Eq. (58) is identified with a classical free-field action

$$\mathcal{A}_0[\phi] = \frac{1}{2}\int dx\, \phi(x) A(x, \partial/\partial x)\phi(x). \tag{59}$$

Interactions are then introduced into the action as higher-order terms, e.g., $\int dx\, \phi^4(x)$. With a total classical action $\mathcal{A}_0[\phi]+\mathcal{A}_{\rm int}[\phi]$ in hand, the quantum field theory is developed from the *generating functional*

$$W[J] \equiv \mathcal{N}\int \mathcal{D}\phi(x) \exp\left[-\mathcal{A}_0[\phi] - \mathcal{A}_{\rm int}[\phi] + \int dx\, J(x)\phi(x)\right], \tag{60}$$

where the normalization $\mathcal{N}$ is again such that $W[0] = 1$. For non-interacting theory, $\mathcal{A}_{\rm int}[\phi] = 0$, and $W[J]$ reduces to $W_0[J]$.

The real form of the exponent in Eq. (60) is characteristic for the *Euclidean field-theoretic PI*, which finds applications in statistical quantum (but also classical) physics. In elementary particle physics, natural definition of the generating functional contains an additional imaginary factor i, and the ensuing PI is named *Minkowski PI*. The two are related by the Wick rotation, much like PI's (13) and (20) (see Ref. [10] for details).

The generating functional is used to generate the correlation (or n-point) functions of the quantum field theory via functional differentiation:

$$\mathcal{N}\int \mathcal{D}\phi\, \phi(x_1)\ldots\phi(x_n)\, e^{-\mathcal{A}_0[\phi]-\mathcal{A}_{\rm int}[\phi]} = \frac{\delta}{\delta J(x_n)}\cdots\frac{\delta}{\delta J(x_1)} W[J]|_{J=0}. \tag{61}$$

For non-interacting theories, the generating functional is given explicitly by Eq. (58), and so the right-hand side of Eq. (61) is calculable in closed form as an expression constructed from the Green function $G(x, x')$ (cf. the *Wick theorem*). The correlation functions (or Fourier transforms of these) are pictorially represented by the *Feynman diagrams* to facilitate their assembly.

For interacting theories, however, an explicit formula for the generating functional is, in most cases, not known. The standard way to tackle the problem is then to employ

[9] Some author use the term *functional integral* for the field-theoretic PI. On the other hand, some other authors refer to quantum-mechanical PI as functional integral. In the absence of a universal agreement about the nomenclature, we find it more safe to use the term *path integral* with an appropriate adjective in front.

again functional derivatives to pull the interaction part of the action outside the PI, i.e., to cast

$$W[J] = \frac{\mathcal{N}}{\mathcal{N}_0} e^{-\mathcal{A}_{\rm int}[\delta/\delta J]} W_0[J]. \tag{62}$$

After expanding the variational differential operator $e^{-\mathcal{A}_{\rm int}[\delta/\delta J]}$ in series, the n-point functions of the interacting theory can be expressed in terms of the m-point functions ($m \geq n$) of the corresponding free-field theory. There exist rather sophisticated techniques to organize and manipulate the ensuing *perturbation series* (see, e.g., Ref. [28]), which, however, we will not discuss in this thesis.

In fact, we will not be concerned with the quantum field theory on its own. For our studies of the local times, it will suffice to consider the field-theoretic PI representation of the Green function from Eq. (55), i.e., of the free-field two-point function,

$$\begin{aligned} G(x, x_0) &= \frac{\delta}{\delta J(x)} \frac{\delta}{\delta J(x_0)} W_0[J]|_{J=0} \\ &= \frac{\int \mathcal{D}\phi(x')\phi(x)\phi(x_0) \exp\left[-\frac{1}{2}\int dx' \phi(x') A(x', \partial/\partial x')\phi(x')\right]}{\int \mathcal{D}\phi(x') \exp\left[-\frac{1}{2}\int dx' \phi(x') A(x', \partial/\partial x')\phi(x')\right]}, \end{aligned} \tag{63}$$

where the normalization $\mathcal{N}_0$ has been now written out explicitly.

4.2 Local times of path integrals

Throughout this section, we shall consider the spatial dimensionality $D = 1$. Drawing our attention back to PI (13), one can ask the following question: Given a point X in $\mathbb{R}$, what portion of time do the trajectories $x(t')$ spend, on average, in the vicinity of X? (The situation is depicted in Fig. 1.) Formally, we look for the mean value

$$\int_{x(t_0)=x_0}^{x(t)=x} \mathcal{D}x(t') L(X)\, e^{-\int_{t_0}^{t} dt' \left[\frac{M}{2}\dot{x}^2 + V(x)\right]} \tag{64}$$

of the *local time* functional

$$L[x(t')](X) \equiv \int_{t_0}^{t} dt' \delta(X - x(t')), \tag{65}$$

evaluated over all trajectories connecting the points (t_0, x_0) and (t, x).

Averages of the products $L(X_1) \ldots L(X_N)$, where N is arbitrarily large, are the N-point functions of a new stochastic process indexed by the variable X — the local time process [29]. The trajectories $L(x)$ of this process are continuous functions, which are positive, and compactly supported.

Our aim is to rewrite the PI (13) as an integral over the local-time profiles $L(x)$ with appropriate weight factors. This goal has been achieved in the article of Appendix B,

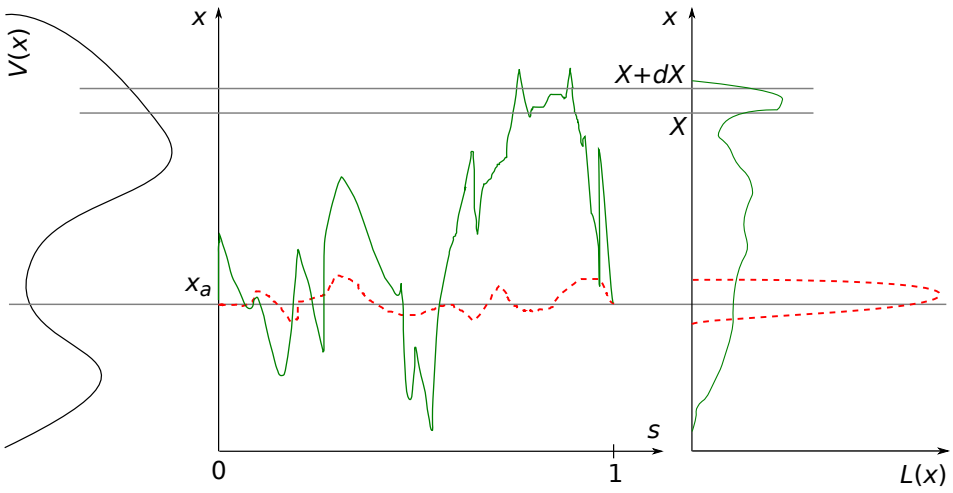

Figure 1: Generic trajectories $x(s)$, in a rescaled time variable $s = t'/t$, and their corresponding local-time profiles $L(x)$, for $x_0 = x \equiv x_a$.

Ref. [14]. Our primary motivation there originated in statistical quantum mechanics. We have seen in Sec. 3, how matrix elements of the Gibbs operator, Eq. (51), can be approximated at high temperatures. In this regime, quantum fluctuations of the PI trajectories $x(s)$ are small (the red dashed representative curve in Fig. 1), and they are constrained in the vicinity of the endpoint x_a (if we consider, for simplicity, $x_b = x_a$). As temperature decreases, the inverse temperature β grows, and this makes the quantum fluctuations more and more significant (the green solid curve at Fig. 1). The PI weight factors are then being dominated by the potential part of the action, as is most easily visible from the rescaled representation Eq. (54).

To successfully approximate the PI (51) at low temperatures, it is therefore essential to have a good information about the time that the PI trajectories spend in the vicinity of a given point X. When X is the minimum of the potential function $V(x)$, and the trajectory $x(\tau)$ stays in its neighborhood for a long time, then the weight factor

$$\exp\left[-\frac{1}{\hbar}\int_0^{\beta\hbar} d\tau\, V(x(\tau))\right] \tag{66}$$

is relatively large, compare to the trajectories that stay further away from the potential minimum.

Let us be more precise, and rewrite the potential part of the action as

$$\int_0^{\beta\hbar} d\tau\, V(x(\tau)) = \int_{\mathbb{R}} dX\, L(X)V(X), \tag{67}$$

where $L(X)$ is given by Eq. (65) with $t_0 = 0$, $t = \beta\hbar$, and $t' \equiv \tau$. The PI representation of the matrix elements of the Gibbs operator, Eq. (51), now reads

$$\rho(x_a, x_b, \beta) = \int_{x(0)=x_a}^{x(\beta\hbar)=x_b} \mathcal{D}x(\tau) e^{-\frac{1}{\hbar}\int_0^{\beta\hbar} d\tau \frac{M}{2}\dot{x}^2} e^{-\frac{1}{\hbar}\int_{\mathbb{R}} dX\, L(X)V(X)}. \tag{68}$$

This is still a Feynman PI, i.e., a PI over trajectories $x(\tau)$. Our task is now to rewrite it as a PI over the local-time profiles $L(x)$,

$$\rho(x_a, x_b, \beta) = \int \mathcal{D}L(x) \widetilde{\mathcal{W}}[L; \beta, x_a, x_b] e^{-\frac{1}{\hbar}\int_{\mathbb{R}} dX\, L(X)V(X)}, \tag{69}$$

where the trajectories $L(x)$ are positive and compactly supported, and their weights $\widetilde{\mathcal{W}}$ are expected to depend on x_a, x_b, and β. In fact, due to the normalization of the local time,

$$\int_{\mathbb{R}} dx\, L(x) = \beta\hbar, \tag{70}$$

we may assume the form

$$\widetilde{\mathcal{W}}[L; \beta, x_a, x_b] = \delta\left(\int_{\mathbb{R}} dx\, L(x) - \beta\hbar\right) \mathcal{W}[L; \beta, x_a, x_b]. \tag{71}$$

To find an explicit expression for the weight factors, we adopt an indirect approach via a differential equation, and the field-theoretic PI representation, guided by the fact that the trajectories in the desired local-time PI representation have x as their independent variable.

Let us outline the main steps of the derivation. Details can be found in Sec. IV of the article in Appendix B.

First, observe that the quantity $\rho(x_0, x, \beta) = \langle x| e^{-\beta\hat{H}} |x_0\rangle$ satisfies the differential equation (the diffusion, or heat equation)

$$(\partial_\beta + \hat{H}_x)\rho(x_0, x, \beta) = 0, \tag{72}$$

with the initial condition

$$\rho(x_0, x, 0_+) = \delta(x - x_0). \tag{73}$$

In the Laplace picture, defined by

$$\widetilde{\rho}(x_0, x, E) = \int_0^\infty d\beta\, e^{-\beta E} \rho(x_0, x, \beta), \tag{74}$$

we have the equation

$$(E + \hat{H}_x)\widetilde{\rho}(x_0, x, E) = \delta(x - x_0). \tag{75}$$

Recalling Eq. (55), we identify $\widetilde{\rho}$ with the Green function of the differential operator $E + \hat{H}_x$, and hence we can represent it via Eq. (63) as

$$\widetilde{\rho}(x_0, x, E) = \frac{\int \mathcal{D}\phi(x')\phi(x)\phi(x_0) \exp\left[-\frac{1}{2}\int dx'\phi(x')(E + \hat{H}_{x'})\phi(x')\right]}{\int \mathcal{D}\phi(x') \exp\left[-\frac{1}{2}\int dx'\phi(x')(E + \hat{H}_{x'})\phi(x')\right]}. \tag{76}$$

The E in the denominator makes a serious obstacle to the inversion of the Laplace transform. To circumvent this obstacle, we employ the *replica trick*

$$\frac{a}{b} = \lim_{D\to 0} ab^{D-1}, \tag{77}$$

which allows us to rewrite the right-hand side of Eq. (76) as a single field-theoretic PI over a D-component field (see Eq. (13) in the article of App. B).[10]

Further steps are detailed in App. B. Due to the form of the Hamiltonian,

$$\hat{H}_x = -\frac{\hbar^2}{2M}\frac{d^2}{dx^2} + V(x), \tag{78}$$

we may take advantage of the radial symmetry in the replica space, and reduce the PI trajectories to their radial part $\eta(x)$.

The final formula for the local-time PI representation of the matrix elements of the Gibbs operator reads (denoting $x_a \equiv x_0$, $x_b \equiv x$)

$$\rho(x_a, x_b, \beta) = \lim_{X_\pm\to\pm\infty} \lim_{D\to 0} \lim_{\eta_\pm\to 0} \int_{\eta(X_-)=\eta_-}^{\eta(X_+)=\eta_+} \mathcal{D}\eta(x)\, \delta\left(\int_{X_-}^{X_+} \eta^2 dx - \beta\right) \mathcal{W}[\eta]\, e^{-\int_{X_-}^{X_+} V(x)\eta^2 dx}, \tag{79}$$

where the weight factors are given by

$$\mathcal{W}[\eta; x_a, x_b, \beta] = \frac{2}{D}(\eta_-\eta_+)^{\frac{1-D}{2}} \eta(x_a)\eta(x_b) \exp\left\{-\int_{X_-}^{X_+} dx \left[\frac{\hbar^2}{2M}\eta'^2 + \frac{M}{\hbar^2}\frac{\Delta(x)}{8\eta^2}\right]\right\}. \tag{80}$$

(Cf. Formula (28) in App. B.) The limit $D \to 0$ originates from the replica trick, while $\eta_\pm$ and $X_\pm$ are merely suitable regulators on the η and x-axes, respectively. At each x-slice, the integral over $\eta(x)$ runs from 0 to $+\infty$, and η itself is related to the local time L via

$$\eta^2(x) = \frac{L(x)}{\hbar}. \tag{81}$$

[10] We emphasize that D refers to the number of components of the replica field, and not to the number of spatial dimensions, which has been set to one.

Finally, Δ is a piecewise constant function

$$\Delta(x) = \begin{cases} -1 & \text{for } x \in [\min(x_a, x_b), \max(x_a, x_b)] \\ (D-1)(D-3) & \text{otherwise.} \end{cases} \tag{82}$$

We have therefore obtained the form of the local-time PI anticipated on heuristic grounds in Eq. (69), with the local-time profiles expressed naturally in terms of the quantity η, i.e., the square root of L. Looking closely at the weight factors (80), we conclude that η follows the *Bessel stochastic process*, confirming previous results [30]. For the physics community, it may be enlightening to identify the total exponent in PI (79), including the weight factor, with the action for the *radial harmonic oscillator* with variable frequency $V(x)$ (see Ref. [31] or Sec. IV.C in App. B).

In our article, we also discussed the connection of the local-time PI with the Sturm-Liouville theory (Sec. IV.D in App. B), and incorporated arbitrary functionals of the local time into our PI representation (Sec. V).

Finally, let us concentrate on the behaviour of the Gibbs operator at low temperatures, which was the original motivation for taking the adventure of deriving the local-time PI. For $T \to 0$ (i.e., $\beta \to \infty$), the spectral decomposition demonstrates that[11]

$$\rho(x_a, x_b, \beta) = \sum_n e^{-\beta E_n} \psi_n(x_a) \psi_n(x_b) \overset{\beta \to \infty}{\sim} e^{-\beta E_{\rm gs}} \psi_{\rm gs}(x_a) \psi_{\rm gs}(x_b), \tag{83}$$

where $\psi_{\rm gs}$ is the ground state, and $E_{\rm gs}$ the ground state energy.

It is not at all obvious how this result could be derived from the Feynman PI (51), but, and this is a great advantage of our approach, it can be obtained from the local-time PI (79). On the heuristic level, relegating the details to Sec. VI of the article in App. B, we observe that the total action in PI (79), i.e., the expression in the exponent, reads

$$\int_{X_-}^{X_+} dx \left[\frac{\beta \hbar^2}{2M} \eta'^2 + \beta V(x) \eta^2 + \frac{M}{\beta \hbar^2} \frac{\Delta(x)}{8\eta^2} \right], \tag{84}$$

where we have rescaled η by a factor of $\sqrt{\beta}$. In the large-β limit, the last term is negligible, and the PI in (79) is dominated (cf. the *saddle-point method*) by the trajectory that minimizes the functional

$$\int_{X_-}^{X_+} dx \left[\frac{\hbar^2}{2M} \eta'^2 + V(x) \eta^2 \right] = \langle \eta | \, \hat{H} \, | \eta \rangle \,, \tag{85}$$

[11] It is useful to remind that in one-dimensional quantum mechanics, all bound states ψ_n can be chosen real [32].

under the normalization constraint

$$\int_{X_-}^{X_+} \eta^2 dx = \langle \eta | \eta \rangle = 1. \tag{86}$$

But such η is, according to the Rayleigh-Ritz variational principle, exactly the ground-state wave function ψ_{gs}.

5 Fractional diffusion

At the beginning of Sec. 2, we formed the heat equation (4), and derived for its Green function the PI representation (13). In Sec. 2.1, we introduced the phase space PI (29), and demonstrated that it can serve as a representation for the Green function of a more general differential equation (44). In addition, according to Sec. 4.1, the latter Green function can be represented also by means of the field-theoretic PI (63).

In fact, there exists still one more (widely-used) PI representation applicable to Eq. (44), which we shall now derive. In abstract notation, Eq. (44) reads

$$\hat{H}_{\rm rel}|\tilde{\psi}\rangle = 0, \tag{87}$$

where $\hat{H}_{\rm rel} = H_{\rm rel}(\hat{x},\hat{p})$, $x \equiv (t,\mathbf{x})$, and $p \equiv (E,\mathbf{p})$. Its Green function $\hat{G}$ satisfies, by definition,

$$\hat{H}_{\rm rel}\,\hat{G} = 1, \tag{88}$$

that is,

$$\hat{G} = \hat{H}_{\rm rel}^{-1}. \tag{89}$$

Now, an inverse can be handled with the *Schwinger parametrization* trick,

$$\hat{H}_{\rm rel}^{-1} = \int_0^\infty ds\, e^{-s\hat{H}_{\rm rel}}, \tag{90}$$

and therefore we find, in the position space,

$$G(x,x_0) = \int_0^\infty ds\, \langle x|\, e^{-s\hat{H}_{\rm rel}}\, |x_0\rangle\,. \tag{91}$$

Regarding s as a time parameter, and x as a collection of all position variables, the transition amplitudes on the right-hand side can be readily represented by the familiar phase-space PI (29), where we set $t_0 = 0$, $t = -i\hbar s$, and make the replacements $\mathbf{x} \to x$, $\mathbf{p} \to p$. Namely,

$$\langle x|\, e^{-s\hat{H}_{\rm rel}}\, |x_0\rangle = \int_{x(0)=x_0}^{x(s)=x} \mathcal{D}x(s')\mathcal{D}p(s')\, e^{\int_0^s ds'\left[\frac{i}{\hbar}p\cdot\dot{x} - H_{\rm rel}(x,p)\right]}. \tag{92}$$

Eqs. (91) and (92) provide once more a PI representation of the Green function $G(x,x_0)$.

In the rest of this section, will be concerned with the operator

$$H_{\rm rel}(\hat{p}) = (i\hat{E})^{1-\gamma} + D_\lambda(\hat{\mathbf{p}}^2)^{\lambda/2}, \tag{93}$$

where D_λ is a constant, and with the corresponding differential equation

$$\left[\partial_t^{1-\gamma} + D_\lambda(-\Delta)^{\lambda/2}\right] P(t,\mathbf{x}) = \delta(t)\delta^{(D)}(\mathbf{x}), \tag{94}$$

where $\Delta \equiv \partial_{\mathbf{x}}^2$ is the Laplace operator (we have set $\hbar = 1$). The parameters γ and λ are in general real numbers, and so the operators on the left-hand side are *fractional differential operators* [35], which we define in the Fourier space via

$$\begin{aligned} \partial_t^{1-\gamma} e^{iEt} &= (iE)^{1-\gamma} e^{iEt} \\ (-\Delta)^{\lambda/2} e^{i\mathbf{p}\cdot\mathbf{x}} &= (\mathbf{p}^2)^{\lambda/2} e^{i\mathbf{p}\cdot\mathbf{x}}. \end{aligned} \tag{95}$$

Equation (94) is called *fractional Fokker-Planck equation*, or *double fractional Fokker-Planck equation* to emphasize the presence of both, temporal and spatial, fractional derivatives. For $\gamma = 0$ and $\lambda = 2$, it reduces to the standard diffusion equation, Eq. (3).

The function $P(t, \mathbf{x})$ is the probability distribution of a fractional (or *anomalous*) diffusion process (see monograph [36]) starting at time $t = 0$ at the spatial origin. Since $\hat{H}_{\rm rel}$, as given by Eq. (93), is x-independent, the knowledge of P is equivalent to the knowledge of the Green function G,

$$G(x, x_0) = G(x - x_0, 0) = P(x - x_0). \tag{96}$$

Making use of the Schwinger representation (91), the distribution function P can be cast

$$P(t, \mathbf{x}) = \int_0^\infty ds\, e^{-s\left[\partial_t^{1-\gamma} + D_\lambda (-\Delta)^{\lambda/2}\right]} \delta(t) \delta^{(D)}(\mathbf{x}). \tag{97}$$

The temporal and spatial differential operators certainly commute. Therefore, the exponential factorizes,

$$e^{-s\left[\partial_t^{1-\gamma} + D_\lambda (-\Delta)^{\lambda/2}\right]} = e^{-s\,\partial_t^{1-\gamma}} e^{-s\,D_\lambda (-\Delta)^{\lambda/2}}, \tag{98}$$

and we obtain

$$P(t, \mathbf{x}) = \int_0^\infty ds\, P_T(t, s) P_X(\mathbf{x}, s), \tag{99}$$

where

$$P_T(t, s) = e^{-s\,\partial_t^{1-\gamma}} \delta(t) = \int_{-\infty}^{\infty} \frac{dE}{2\pi} e^{-s\,(iE)^{1-\gamma}} e^{iEt}, \tag{100}$$

and

$$P_X(\mathbf{x}, s) = e^{-s\,D_\lambda (-\Delta)^{\lambda/2}} \delta^{(D)}(\mathbf{x}) = \int_{\mathbb{R}^D} \frac{d^D p}{(2\pi)^D} e^{-s\,D_\lambda (\mathbf{p}^2)^{\lambda/2}} e^{i\mathbf{p}\cdot\mathbf{x}}. \tag{101}$$

The functions P_T and P_X, with s treated as a parameter, are known as *Lévy stable distribution functions* [33]. They occur naturally as attractors in the *generalized central limit theorem* [34].[12]

[12] By the classical central limit theorem, the properly normed sum of a set of random variables, each with finite variance, will tend towards a normal distribution as the number of variables increases. If the assumption on finite variance is relaxed, the limiting distribution may be a stable distribution.

The word "stable" refers to the following property of these distributions: A sum of two Lévy-distributed random variables is again Lévy-distributed. The emblematic feature of the Lévy stable distributions is that they favour rare event, i.e., large values of the random variable, when compared with the Gaussian distribution. Whereas the "tails" of the Gaussian distribution drop-off exponentially, the tails of a generic Lévy distribution are "heavy" — they follow an inverse power law.

In the article of Appendix C, Ref. [15], we investigate various properties of the distribution function $P(t, \mathbf{x})$, and of its constituents $P_T(t, s)$ and $P_X(\mathbf{x}, s)$, and visualise them with a number of plots. We note that the representation (99) can be viewed as a weighted superposition of the single-fractional distributions P_X, with the pseudotime parameter s smeared according to the distribution P_T. The double-fractional diffusion process is therefore not Markovian with respect to the physical time t, but possesses a memory quantified by the smearing kernel P_T. This fact can be traced back to the appearance of the fractional time derivative, which is, in fact, an integral operator

$$\partial_t^{1-\gamma} f(t) = \int_{-\infty}^{\infty} dt' \int_{-\infty}^{\infty} \frac{dE}{2\pi} (iE)^{1-\gamma} e^{iE(t-t')} f(t') = \int_{-\infty}^{t} dt' \frac{(t-t')^{\gamma-2}}{\Gamma(\gamma-1)} f(t'). \qquad (102)$$

(We have used Formula 3.382.7 from Ref. [37], but have not discussed subtle regularization issues.)

Other possibility to cast the distribution function P is by means of the Fox H special function, which is conveniently defined by a contour integral (details can be found in Sec. II.B of App. C).

Also, the PI (92) can be used to represent the function P. However, for an x-independent operator $\hat{H}_{\text{rel}}$, such PI is rather redundant, and would only be useful if we wanted to introduce a potential term of some form.

5.1 Origin of fractional powers in strongly interacting many-body systems

We should explain the physical origin of the fractional powers of the space and time derivatives in Equation (94) above. Such powers occur naturally in many-particle systems if the interaction strength or the range becomes very large.

Many-particle systems are described by a second-quantized field theory with a free-particle action

$$\mathcal{A}_0 = \int d^4x \, \phi^\dagger(t, \mathbf{x}) \left[i\hbar\partial_t + \frac{\hbar^2}{2M}\Delta - V(\mathbf{x}) \right] \phi(t, \mathbf{x}), \qquad (103)$$

and an interaction of the type

$$\mathcal{A}_{\rm int} = \frac{g}{4!}\int d^4x\,(\phi^\dagger\phi)^2. \tag{104}$$

Introducing the generating functional of *connected* correlation functions [10],

$$Z[J] = -\ln W[J], \tag{105}$$

where W is given by Eq. (60), the field expectation values are obtained by functional differentiation,

$$\Phi(x) \equiv \langle\phi(x)\rangle = \frac{\delta Z[J]}{\delta J(x)}. \tag{106}$$

The *effective action* of the field theory is defined via the functional Legendre transform

$$\Gamma[\Phi] = Z[J] - \int d^4x\,J(x)\Phi(x). \tag{107}$$

As long as the interaction strength g is small, the initial action $\mathcal{A} = \mathcal{A}_0 + \mathcal{A}_{\rm int}$ is a good approximation to the effective action (cf. the *mean-field approximation*). By extremizing $\mathcal{A}[\Phi]$, we obtain the *Gross-Pitaevski equation*

$$\left[i\hbar\partial_t + \frac{\hbar^2}{2M}\Delta - V(\mathbf{x}) - g\Phi^\dagger\Phi\right]\Phi(t,\mathbf{x}) = 0 \tag{108}$$

In general, the perturbation expansion leads to an effective action in the form of a power series in $g\Phi^\dagger\Phi$. This series is divergent and must be resummed. For large interaction strength g, this produces anomalous power behaviours in the field strength as well as in the momenta [28]. Therefore, by extremizing the resummed effective action, we arrive at the *fractional Gross-Pitaevski equation* [38, 39]

$$\left[(i\partial_t)^{1-\gamma} + D_\lambda(-\Delta)^{1-\eta/2} - V(\mathbf{x}) - \frac{\delta+1}{4}g_c|\Phi|^{\delta-1}\right]\Phi(t,\mathbf{x}) = 0, \tag{109}$$

where g_c is the renormalized coupling constant.

The free-field part of this field equation is of the fractional Fokker-Planck type, Eq. (94), in which momentum and energy appear with powers different from $\lambda = 2$ and $\gamma = 0$, respectively.

In real physical systems, the large interparticle interaction strength can be achieved by tuning the external magnetic field to hit the *Feshbach resonance* [40].

6 Quantum walks with anyons

In this last chapter, we will study a discrete quantum process — the *quantum walk*. It can be described by a sum over the walker's histories, i.e., by a discrete type of path integral. The particles that will take part in this walk will have exotic statistical properties, generalizing those of bosons and fermions. They will be referred to as *anyons*. We will investigate the influence of this exotic exchange statistics, and of a certain disorder in the surrounding environment on the properties of the quantum walk.

There are several concepts that need to be introduced. We will start from a classical random walk to define the quantum walk by analogy. Then we will talk about a disorder-induced phenomenon of *Anderson localization*, and conclude the preliminary discussion by introducing anyons, and their basic properties. Finally, we will combine everything together in the investigation of "transport properties of anyons in random topological environment", which is the title of the article in Appendix D, Ref. [16].

6.1 Classical random walk

The diffusion equation (3) is used to describe a continuous-time motion of a particle (or rather a statistical ensemble of particles) through a continuous medium. The discrete analogue of this process is commonly referred to as the *random walk*, or, colloquially, the *drunken sailor problem*. In the discrete setting, the walker makes jumps, one at a time, on a spatial lattice, and there is a certain probability distribution ascribed to the directions of subsequent jumps.

Let us assume, for simplicity, that the lattice is one-dimensional (the set of integers), and that the walker hops onto a neighboring site with probability $1/2$ in both directions. Starting at time $t_0 = 0$ at position $x_0 = 0$, the probability to find the walker at time $t \in \mathbb{Z}_+$ at site $x \in \mathbb{Z}$ is given by the binomial distribution

$$p_{\mathrm{RW}}(x,t) = \frac{1}{2^t}\binom{t}{\frac{t+x}{2}}. \tag{110}$$

This result can be derived either from the recurrence relation

$$p_{\mathrm{RW}}(x,t) = \frac{1}{2}p_{RW}(x+1,t-1) + \frac{1}{2}p_{RW}(x-1,t-1) \tag{111}$$

supplemented by the initial condition $p_{\mathrm{RW}}(x,0) = \delta_{x,0}$, or directly by counting the number of paths that reach the point x in t steps, each path being weighted by the factor $(1/2)^t$.

Note that the first method is a discrete analogue of the diffusion equation (3), while the latter method resembles path integration. Indeed, in the limit of infinitesimal time

steps and lattice spacing, the random walk process goes over to the Brownian motion, the binomial distribution (110) converges to the normal distribution, Eq. (2), and the difference equation (111) turns into the differential equation (3) [41].

The spreading rate of a random walk is commonly quantified by the *variance* as a function of time,

$$\sigma^2(t) \equiv \sum_{x\in\mathbb{Z}} p(x,t)\left(x - \sum_{x'\in\mathbb{Z}} p(x',t)x'\right)^2. \tag{112}$$

In particular, for the probability distribution $p = p_{\mathrm{RW}}$, the second term in the brackets vanishes due to the symmetry $x \to -x$ of Formula (110). Hence, we find the recurrence relation

$$\sigma^2_{\mathrm{RW}}(t) = \sigma^2_{\mathrm{RW}}(t-1) + 1, \tag{113}$$

with the initial condition $\sigma^2_{\mathrm{RW}}(0) = \sum_x \delta_{x,0}x^2 = 0$. This is solved by

$$\sigma^2_{\mathrm{RW}}(t) = t, \tag{114}$$

yielding a linear increase of the random-walk variance in time.

6.2 Quantum walk

Quantum walk is a quantum-mechanical analogue of the classical random walk [42]. In the quantum setting, lattice points are represented by vectors in a discrete-position Hilbert space

$$\mathcal{H}_{\mathrm{space}} = \{|x\rangle\}_{x\in\mathbb{Z}}, \tag{115}$$

and the hopping of the walker is generated by a unitary *coin* operator U, which acts in a two-dimensional Hilbert space

$$\mathcal{H}_{\mathrm{coin}} = \{|0\rangle, |1\rangle\}. \tag{116}$$

For definiteness, we take the *Hadamard coin*, represented in the $\{|0\rangle, |1\rangle\}$ basis by the matrix

$$U = \frac{1}{\sqrt{2}}\begin{pmatrix} 1 & 1 \\ 1 & -1 \end{pmatrix}. \tag{117}$$

The state of the walker is described by a wave-function

$$|\psi(t)\rangle \in \mathcal{H}_{\mathrm{space}} \otimes \mathcal{H}_{\mathrm{coin}}, \tag{118}$$

which evolves in discrete time steps according to

$$|\psi(t)\rangle = (T_0 U)^t |\psi(0)\rangle. \tag{119}$$

Here, T_0 is the conditional shift operator,

$$T_0 \equiv \sum_{x\in\mathbb{Z}} \left(|x-1\rangle\langle x| \otimes |0\rangle\langle 0| + |x+1\rangle\langle x| \otimes |1\rangle\langle 1|\right), \tag{120}$$

which propagates $|0\rangle$-coin modes "to the left", and $|1\rangle$-coin modes "to the right". (See Fig. 2 below.)

Let us assume the initial state to be localized,

$$|\psi(0)\rangle = |0\rangle\langle 0|_{\text{space}} \otimes |0\rangle\langle 0|_{\text{coin}}\,. \tag{121}$$

In order to obtain the walker's position distribution after t steps, we form the reduced spatial density matrix

$$\rho_{\text{space}}(t) = \text{Tr}_{\text{coin}}\, |\psi(t)\rangle\langle\psi(t)|\,, \tag{122}$$

where the coin degree of freedom has been traced out, and consider its diagonal elements[13]

$$p_{\text{QW}}(x,t) \equiv \langle x|\,\rho_{\text{space}}(t)\,|x\rangle\,. \tag{123}$$

Enumerating all possible walker's histories, which follow the instructions implemented by operators T_0 and U, we can derive the following path-integral-like representation of the position distribution:

$$p_{\text{QW}}(x,t) = \sum_{(\vec{a},\vec{a}')\rightsquigarrow x} \frac{(-1)^{z(\vec{a},\vec{a}')}}{2^t}, \tag{124}$$

where $(\vec{a},\vec{a}') \rightsquigarrow x$ denotes all pairs of paths that lead from the origin to the site x in t steps, and the phase factors z are given, for the Hadamard coin, Eq. (117), by

$$z(\vec{a},\vec{a}') = \sum_{k=1}^{t-1} (a_k a_{k+1} + a'_k a'_{k+1}). \tag{125}$$

Formula (124) certainly resembles a PI. It is a sum over histories weighted by appropriate phase factors. In fact, the sum is finite and it runs over pairs of paths, as we are representing the density matrix (122), and not the state $|\psi(t)\rangle$ itself. The quantum nature of the problem is reflected in the fact that the weights $(-1)^z$ can be both positive and negative, which results in complicated interference effects.

[13] Note that

$$\langle x|\,\rho_{\text{space}}\,|x\rangle = \text{Tr}_{\text{space}}\left(|x\rangle\langle x|\,\rho_{\text{space}}\right),$$

i.e., diagonal elements are the expectation values of the position operator $|x\rangle\langle x|$ in the quantum state ρ_{space}.

Although an explicit form of p_{QW} is not known, computer simulations and approximation methods show that quantum walker behaves quite differently from the classical one [43]. In particular, the variance of the quantum walk distribution exhibits a quadratic growth in time,

$$\sigma^2_{\mathrm{QW}}(t) \sim t^2, \tag{126}$$

which should be compared with the linear behaviour of the classical random walk, Eq. (114). Such speed-up effects are ubiquitous in the quantum information science [44], which aims to build a quantum computer that would be orders of magnitude faster than its classical counterpart we use today.

6.3 Anderson localization

In general, the transition amplitudes of a quantum particle are obtained from the Feynman PI, Eq. (20). In the case when the potential $V(\mathbf{x})$ is disordered, the phase factors corresponding to different paths sum up in such a way that they cause destructive interference effect. If the disorder is strong enough, the destructive interference can even stop the particle from propagating.

This phenomenon is rather general, and applies not only to quantum waves, but also, e.g., to electromagnetic and acoustic classical waves [45]. It was proposed by P. W. Anderson in [46], hence the name *Anderson localization*.

When the quantum particle is localized, its wave function assumes a characteristic exponential shape

$$|\psi(t,\mathbf{x})|^2 \propto e^{-|\mathbf{x}|/\xi_{\mathrm{loc}}}, \tag{127}$$

where ξ_{loc} is the *localization length*. The form of the right-hand side not only peaks the particle around the origin, but, more importantly, does not change in time, i.e., the peak does not broaden.

In Section 6.5, we propose an unusual mechanism that introduces random phases on top of the quantum walk protocol, Eq. (119), and analyze under what circumstances this mechanism leads to the localization of the walker. (Detailed analysis is carried out in the article of Appendix D.) But first of all, we need to say a few words about anyons.

6.4 Anyons

Anyons were introduced as hypothetical particles in two-dimensional spaces [47] with exchange statistics that generalizes that of bosons and fermions. What makes 2D systems extraordinary is a rich structure of the fundamental group of the n-particle configuration manifold (see also [48]).

Although purely theoretical in the beginning, anyons gained physical significance after it was realized that effective quasi-particles in the fractional quantum Hall effect carry fractional charge, and obey an exotic exchange statistics [49, 50].

The defining property of anyons is that the wave function which represents a system of identical particles acquires a generic phase factor when two particles are exchanged. The phase factors form a unitary representation of the *braid group*, which can be either Abelian (complex units $e^{i\phi}$), or non-Abelian (unitary matrices). Accordingly, anyons are divided into two classes: *Abelian*, and *non-Abelian*. The first class has been studied in the context of statistical physics and thermodynamics [51], while the second class has been argued to play an essential role in the quest for building a (topological) quantum computer [52].

6.5 Anyonic quantum walks in random topological environments

The anyonic statistics is capable of generating additional phases in our quantum walk of Sec. 6.2. For this purpose, we place static anyons onto the links between neighbouring sites, and envisage the walker to be a distinguished anyon of the same kind (see Figure 2). We demand, for simplicity, that the walker moves in a counter-clockwise sense around

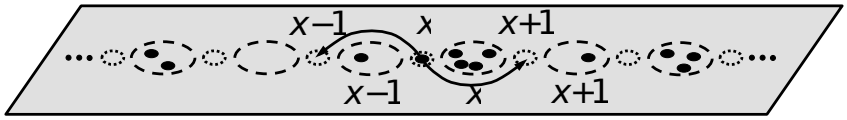

Figure 2: Walking anyon braids around islands populated by static anyons.

thus formed islands populated by the static anyons. Our model is quasi-one-dimensional in the sense that although the admissible positions of the walker lie in a line, the second dimension is needed to perform the counter-clockwise braiding.

The conditional shift operator T_0, defined in Eq. (120), is now extended to a conditional shifting and braiding operator

$$T \equiv \sum_{x\in\mathbb{Z}} \left(|x-1\rangle\langle x| \otimes |0\rangle\langle 0| \otimes b_{x-1} + |x+1\rangle\langle x| \otimes |1\rangle\langle 1| \otimes b_x \right), \tag{128}$$

where $\{b_x\}_{x\in\mathbb{Z}}$ are the braid matrices that form a unitary representation of the braid group, which may be either Abelian, for Abelian anyons, or non-Abelian, for non-Abelian anyons. The braid matrices act on an additional Hilbert space, the *fusion space* $\mathcal{H}_{\text{fusion}}$,

which implements the anyonic exchange statistics.[14]

The walker's wave functions is a vectors in the total Hilbert space

$$\mathcal{H}_{\text{space}} \otimes \mathcal{H}_{\text{coin}} \otimes \mathcal{H}_{\text{fusion}}, \tag{129}$$

whose time evolution is determined by

$$|\psi(t)\rangle = (TU)^t \, |\psi(0)\rangle \,, \tag{130}$$

where U is the Hadamard matrix (117).

The spatial distribution of the anyonic walker after t steps is given by

$$p_{\text{AQW}}(x,t) = \langle x| \, \rho_{\text{space}}(t) \, |x\rangle \,, \tag{131}$$

where

$$\rho_{\text{space}}(t) = \text{Tr}_{\text{fusion}} \text{Tr}_{\text{coin}} \, |\psi(t)\rangle \, \langle\psi(t)| \tag{132}$$

is the reduced density matrix, where the coin and the fusion degrees of freedom have been traced out.

To elucidate the right-hand side of Eq. (131), we rewrite it in a sum-over-histories representation analogous to Eq. (124),

$$p_{\text{AQW}}(x,t) = \sum_{(\vec{a},\vec{a}') \rightsquigarrow x} \frac{(-1)^{z(\vec{a},\vec{a}')}}{2^t} \text{Tr}\mathcal{Y}_{(\vec{a},\vec{a}')}. \tag{133}$$

The pairs of trajectories $(\vec{a},\vec{a}')$ entangle with the worldlines of the static anyons (see Fig. 2 in App. D). When their endpoints are glued together, the ensuing knots and links, and their topological invariants (namely, the *Jones polynomial*), produce the extra factors $\text{Tr}\mathcal{Y}_{(\vec{a},\vec{a}')}$. These arise from the trace over the fusion space, and therefore depend on the type of anyons one considers.

In the article in Appendix D, Ref. [16], we study quantum walks with both, Abelian and non-Abelian, types of anyons. In the Abelian case, we consider various exchange phases $e^{i\phi}$. In the non-Abelian case, we analyze a specific model, the so-called *Ising anyons*. Further distinction is made with respect to the regularity of the background of the static anyons. We consider two cases. First, the uniform density case, where the particles are placed one per island, and second, the disordered case, where the occupations of the islands are random. In the latter case, we can expect some Anderson

[14] Detailed exposition and analysis of the fusion spaces is rather involved and goes well beyond the scope of this introductory chapter. We refer an interested reader to Refs. [52, 53, 54].

localization effects, since the walker picks up random phases when passing around the randomly populated islands.

The results of our analysis are summarized in Fig. 3, where we plot, for these various cases, time dependency of the variance of the walker's position distribution (131).

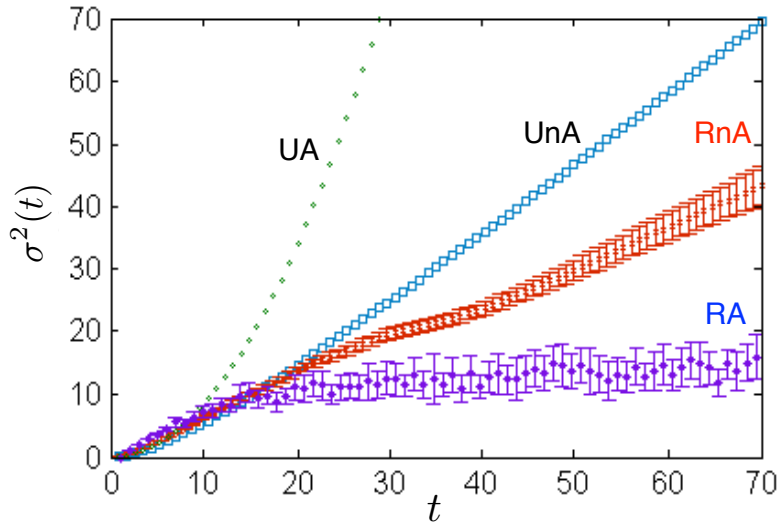

Figure 3: Time dependency of the variance of the walker's position distribution is shown for various settings: (UA) uniform density, Abelian anyons; (RA) random density, Abelian anyons ; (UnA) uniform density, non-Abelian anyons; (RnA) random density, non-Abelian anyons. For random background densities, the plot shows average values, and standard deviation bars.

In the case of Abelian anyons and regular background (UA), the anyonic quantum walk reduces to the ordinary quantum walk of Sec. 6.2, since every trajectory picks up the same overall statistical phase. The variance grows like in Eq. (126),

$$\sigma^2_{\rm UA}(t) = \sigma^2_{\rm QW}(t) \sim t^2, \tag{134}$$

i.e., the walker's spreading is *ballistic*. In the disordered Abelian case (RA), the variance saturates around a constant asymptotic value,

$$\sigma^2_{\rm RA}(t) \sim const, \tag{135}$$

and so we observe the Anderson localization taking place.

For (Ising) non-Abelian anyons in a uniform background (UnA), we find a diffusive behaviour (qualitatively the same as for the classical random walk, Eq. (114)),

$$\sigma^2_{\mathrm{UnA}}(t) \sim t, \tag{136}$$

which persists even for random background densities (RnA),

$$\sigma^2_{\mathrm{RnA}}(t) \sim t, \tag{137}$$

only the slope becomes more gentle.[15]

The classical spreading of the non-Abelian anyonic walker is attributed to the entanglement in the exponentially growing fusion space of non-Abelian anyons.

[15] In the latter case, the specific value of the slope is probably a result of the specific way, in which we introduce randomness, and is not expected to be universal.

7 Conclusions

Path integrals have been around in physics for more than 70 years, and over the time they have become a standard mathematical tool widely used in the quantum theory. In quantum mechanics, the Feynman PI provides a valuable insight into the structure of the theory, and helps to build physical intuition, although for most calculations the Schrödinger's formulation proves to be more efficient. In quantum field theory, however, the PI formulation overshadows the canonical approach on both, the pedagogical and computational, sides.

Many applications of PI's in and also outside of physics have been found and discussed over the past decades. It might thus seem that the field has been explored so exhaustively that finding new applications would be quite hard. Yet, in this thesis, I have tried to persuade the reader that PI techniques are worth to keep in mind when approaching a physical problem, as they can provide surprising shortcuts on the route to the solution. This is due to the intuition and insights gained by the PI point of view.

In this respect, let me recall the first of my research topics, the Wigner-Kirkwood high-temperature expansion (Sec. 3 and Appendix A). Although this expansion has been known for a long time [26, 27], the Feynman PI representation (54) of the relevant quantity makes its derivation very clear and intuitive as it supplies one immediately with an idea to expand in β, and provides also a PI representation of the expansion coefficients, which can be later on simplified, and explicitly calculated. The resulting formulas are so simple that even computer can evaluate them. Therefore, we can drive the expansion in β to relatively high 18th order (in the case of a one-dimensional system).

Nowadays, the majority of theoretical physicists is more or less familiar with the PI methods, and do not hesitate to use them to formulate their theories, or carry out everyday calculations. On the other hand, not so many physicists study the PI on its own. This task is usually relegated to mathematicians, who analyze the corresponding stochastic integrals. The problem with this practice is that the language of mathematicians is more precise, and therefore far more complicated, than the often heuristic language used by physicists. In the end, many valuable results remain unappreciated and unknown to the physics community.

The original motivation for my second research topic, the local times of path integrals (Sec. 4 and Appendix B), was to tackle the low-temperature limit in quantum statistical mechanics. The resulting method, however, is a general substitute for the Feynman PI that will hopefully find concrete applications in the future. It is a practical tool accessible to physicists, and it provides an interesting interpretation of the field-theoretic

PI representation (63) in the framework of quantum mechanics, making a link between the first and the second quantization. In mathematics, the local times of stochastic processes have been studied for a long time. Let us quote, in particular, the works of Ray [55] and Knight [56] who investigated stochastic process that describes the local time of the Brownian motion. We rederived some of their results using the methods of theoretical physics, hence providing a more intuitive understanding of the problem.

The third of my research topics concentrated on fractional diffusion processes, and resulting Lévy stable distributions (Sec. 5 and Appendix C). In the literature, one can find many ways how to represent the solutions of the single as well as the double fractional Fokker-Planck equation [57]. Yet, I believe that our derivation that employs the Schwinger trick is particularly instructive and compact, as it allows to systematically reduce a doubly fractional problem to two single fractional ones. From our article it is also clear how a potential potential term can be treated using the fractional phase-space PI representation, Eq. (92).

A particular discrete quantum process was the object of study in the fourth research project, the quantum walks with anyons (Sec. 6 and Appendix D). Quantum walks can also be approached from the PI perspective, namely, the walker's spatial distribution can be represented by a sum over histories, with the weights depending on the protocol that is used to define the walk. Our modification of standard, and well-investigated, quantum walk scenarios consists in introducing anyons, particles with exotic exchange statistics, which leads to the occurrence of complicated additional phase factors (even non-local in the case of non-Abelian anyons). In turn, through the anyonic quantum walk, we can study transport properties of anyons of different kinds in various environments. We showed that Abelian anyons propagate ballistically in a uniform environment, whereas they localize if the environment is disordered. On the other hand, non-Abelian (Ising-type) anyons exhibit a classical diffusive behaviour, whether the density of the surrounding anyons is uniform or random. This classification could become relevant for identification of the anyonic species in real transport experiments.

One more topic was briefly discussed in Sec. 2.1 of this thesis — the phase-space PI (35) for the relativistic formulation of quantum mechanics based on the Hamiltonian constraint. This could serve as an alternative to the standard Schwinger-representation-based relativistic PI (92).

References

[1] R. P. Feynman and A. R. Hibbs, *Quantum Mechanics and Path Integrals*, McGraw-Hill, New York (1965).

[2] H. Kleinert, *Path Integrals in Quantum Mechanics, Statistics, Polymer Physics, and Financial Markets*, 5th Ed., World Scientific (2009).

[3] L. S. Schulman, *Techniques and Applications of Path Integration*, Dover Publications (2005).

[4] P. Cartier and C. DeWitt-Morette, *Functional Integration: Action and Symmetries*, Cambridge Univ. Press (2010).

[5] J. Zinn-Justin, *Path Integrals in Quantum Mechanics*, Oxford Univ. Press (2010).

[6] P. Exner, *Open Quantum Systems and Feynman Integrals*, Springer (1985).

[7] B. Simon, *Functional Integration And Quantum Physics*, 2nd Ed., Chelsea Pub Co (2004).

[8] H. Kleinert, *Particles and Quantum Fields*, to be published by World Scientific (2016).

[9] R. J. Rivers, *Path Integral Methods in Quantum Field Theory*, Cambridge Univ. Press (1988).

[10] P. Ramond, *Field Theory: A Modern Primer*, 2nd Ed., Westview Press (1997).

[11] M. E. Peskin and D. V. Schroeder, *An Introduction To Quantum Field Theory*, Westview Press (1995).

[12] M. Blasone, P. Jizba and G. Vitiello, *Quantum Field Theory and Its Macroscopic Manifestations: Boson Condensation, Ordered Patterns and Topological Defects*, Imperial College Press (2011).

[13] P. Jizba and V. Zatloukal, *Path-integral approach to the Wigner-Kirkwood expansion*, Phys. Rev. E **89**, 012135 (2014) [arXiv:1309.0206].

[14] P. Jizba and V. Zatloukal, *Local-time representation of path integrals*, Phys. Rev. E **92**, 062137 (2015) [arXiv:1506.00888].

[15] H. Kleinert and V. Zatloukal, *Green function of the double-fractional Fokker-Planck equation: Path integral and stochastic differential equations*, Phys. Rev. E **88**, 052106 (2013) [arXiv:1503.01667].

[16] V. Zatloukal, L. Lehman, S. Singh, J. K. Pachos, and G. K. Brennen, *Transport properties of anyons in random topological environments*, Phys. Rev. B **90**, 134201 (2014) [arXiv:1207.5000].

[17] H. Risken, *The Fokker-Planck Equation: Methods of Solution and Applications*, 2nd Ed., Springer-Verlag (1989).

[18] N. Wiener, *Differential Space*, J. Math. Phys. **2**, 132 (1923).

[19] R. P. Feynman, *The Principle of Least Action in Quantum Mechanics*, PhD Dissertation, Princeton University (1942). (L. M. Brown, ed., *Feynman's Thesis: a New Approach to Quantum Theory*, World Scientific, 2005.)

[20] R. P. Feynman, *Space-Time Approach to Non-Relativistic Quantum Mechanics*, Rev. Mod. Phys. **20**, 367 (1948).

[21] P. A. M. Dirac, *The Lagrangian in Quantum Mechanics*, Physikalische Zeitschrift der Sowjetunion **3**, 6472 (1933).

[22] Dah-Wei Chiou, *Timeless path integral for relativistic quantum mechanics*, Class. Quant. Grav. **30**, 125004 (2013) [arXiv:1009.5436].

[23] C. Rovelli, *Quantum Gravity*, Cambridge Univ. Press (2004).

[24] V. Zatloukal, preprint (2015) [arXiv:1504.08344].

[25] V. Zatloukal, preprint (2016) [arXiv:1602.00468].

[26] E. Wigner, *On the Quantum Correction For Thermodynamic Equilibrium*, Phys. Rev. **40**, 749 (1932).

[27] J. G. Kirkwood, *Quantum Statistics of Almost Classical Assemblies*, Phys. Rev. **44**, 31 (1933).

[28] H. Kleinert and V. Schulte-Frohlinde, *Critical Properties of ϕ^4-Theories*, World Scientific (2001).

[29] M. Marcus and J. Rosen, *Markov Processes, Gaussian Processes, and Local Times*, 1st Ed., Cambridge Univ. Press (2006).

[30] A. N. Borodin, *Brownian local time*, Russ. Math. Surv. **44**, 1-51 (1989).

[31] C. Grosche and F. Steiner, *Handbook of Feynman Path Integrals*, Springer (1998).

[32] A. Messiah, *Quantum Mechanics*, Dover Pubs. (1999).

[33] Ken-iti Sato, *Lévy Processes and Infinitely Divisible Distributions*, Cambridge Univ. Press (1999).

[34] B. V. Gnedenko and A. N. Kolmogorov, *Limit Distributions for Sums of Independent Random Variables*, Addison-Wesley (1954).

[35] I. Podlubny, *Fractional Differential Equations. An Introduction to Fractional Derivatives, Fractional Differential Equations, Some Methods of Their Solution and Some of Their Applications*, Academic Press (1999).

[36] M. M. Meerschaert and A. Sikorskii, *Stochastic Models for Fractional Calculus*, Walter de Gruyter (2011).

[37] I. S. Gradshteyn and I. M. Ryzhik, *Table of Integrals, Series, and Products*, 7th Ed., Elsevier (2007).

[38] H. Kleinert, Eur. Jour. Phys. **100**, 10001 (2012).

[39] H. Kleinert, *Effective action and field equation for BEC from weak to strong couplings*, J. Phys. B **46**, 175401 (2013).

[40] L. P. Pitaevskii and S. Stringari, *Bose-Einstein Condensation*, Clarendon Press (2003).

[41] H. Kleinert, *Gauge Fields in Condensed Matter*, World Scientific (1990).

[42] J. Kempe, *Quantum random walks: An introductory overview*, Contemporary Physics **44** 4, p. 307-327 (2003).

[43] A. Ambainis, E. Bach, A. Nayak, A. Vishwanath, and J. Watrous, *One-dimensional quantum walks*, Proc. 33rd Annual ACM STOC, pp. 6069 (2001).

[44] M. A. Nielsen and I. L. Chuang, *Quantum Computation and Quantum Information*, Cambridge Univ. Press (2000).

[45] C. A. Müller and D. Delande, *Disorder and interference: localization phenomena*, Ch. 9 in "Les Houches 2009 - Session XCI: Ultracold Gases and Quantum Information" ed. by C. Miniatura et al., Oxford Univ. Press (2011) [arXiv:1005.0915].

[46] P. W. Anderson, *Absence of Diffusion in Certain Random Lattices*, Phys. Rev. **109** 5, p. 1492-1505 (1958).

[47] J. Leinaas and J. Myrheim, *On the theory of identical particles*, Il Nuovo Cimento B **37**, 123 (1977).

[48] V. Zatloukal, *Anyons and Their Significance in Quantum Mechanics and Statistical Physics*, Master thesis, Czech Technical University in Prague (2011) [available online at http://zatlovac.eu].

[49] B. I. Halperin, *Statistics of Quasiparticles and the Hierarchy of Fractional Quantized Hall States*, Phys. Rev. Lett. **52**, 1583 (1984).

[50] Daniel Arovas, J. R. Schrieffer, and Frank Wilczek, *Fractional Statistics and the Quantum Hall Effect*, Phys. Rev. Lett. **53**, 722 (1984).

[51] A. Khare, *Fractional Statistics and Quantum Theory*, World Scientic (2005).

[52] J. K. Pachos, *Introduction to Topological Quantum Computation*, Cambridge Univ. Press (2012).

[53] J. Preskill, *Lecture Notes for Physics 219: Quantum Computation*, California Institute of Technology (14 June 2004).

[54] V. Zatloukal, *Anyonic Quantum Walks*, Pre-Master thesis, Czech Technical University in Prague (2010) [available online at http://zatlovac.eu].

[55] D. Ray, *Sojourn times of a diffusion process*, Illinois J. Math. **7** 4, p. 615-630 (1963).

[56] F. B. Knight, *Random walks and a sojourn density process of Brownian motion*, Trans. Amer. Math. Soc. **109** 1, p. 56-86 (1963).

[57] Jun-Sheng Duan, *Time- and space-fractional partial differential equations*, J. Math. Phys. **46**, 013504 (2005).

A Full article: Path-integral approach to the Wigner-Kirkwood expansion

Journal reference:

P. Jizba and V. Zatloukal, *Path-integral approach to the Wigner-Kirkwood expansion*, Phys. Rev. E **89**, 012135 (2014) [arXiv:1309.0206].

Path-integral approach to the Wigner–Kirkwood expansion

Petr Jizba[1,*] and Václav Zatloukal[2,†]

[1,2] *FNSPE, Czech Technical University in Prague, Břehová 7, 115 19 Praha 1, Czech Republic*

[1] *ITP, Freie Universität in Berlin, Arnimallee 14, D-14195 Berlin, Germany*

[2] *Max Planck Institute for the History of Science, Boltzmannstrasse 22, 14195 Berlin, Germany*

We study the high-temperature behavior of quantum-mechanical path integrals. Starting from the Feynman–Kac formula, we derive a new functional representation of the Wigner–Kirkwood perturbation expansion for quantum Boltzmann densities. As shown by its applications to different potentials, the presented expansion turns out to be quite efficient in generating analytic form of the higher-order expansion coefficients. To put some flesh on the bare bones we apply the expansion to obtain basic thermodynamic functions of the one-dimensional anharmonic oscillator. Further salient issues, such as generalization to the Bloch density matrix and comparison with the more customary world-line formulation are discussed. The paper is accompanied by Mathematica code that generates higher order expansion terms for an arbitrary smooth local potential.

I. INTRODUCTION

The Wigner–Kirkwood (WK) expansion was originally presented in two seminal papers [1, 2] and since its very inception it has had two important implications. On the one hand, it has been used for studying the equilibrium statistical mechanics of a nearly classical system of particles obeying Maxwell–Boltzmann statistics. WK expansion is in its essence an expansion of the quantum Boltzmann density in powers of Planck's constant $\hbar$, or equivalently of the thermal de Broglie wavelength $\lambda = \hbar\sqrt{\beta/M}$, where β is the inverse temperature and M is the mass of a particle. On the other hand, it has paved a way for new alternative mathematical techniques and practical calculational schemes that are pertinent to the high-temperature regime in quantum systems.

In this paper, we pursue the study of the WK perturbation method by means of the path integral (PI) calculus. The relevance of the PI treatment in a high-temperature context is due to several reasons: PI's allow to connect evolutionary equations (Bloch equation or Fokker–Planck equation) with the underlying stochastic analysis [3, 4], they are tailor-made for obtaining quasi-classical asymptotics [5, 6], they allow to utilize some powerful transformation techniques to simplify the original stochastic process [5, 7], etc. Besides, PI's also provide an excellent tool for direct numerical simulations of the underlying stochastic dynamics including many-body systems [8, 9]. One of the key advantages of the PI approach is, however, the fact that the techniques and methodologies used can efficiently bypass the explicit knowledge of the exact energy spectrum — the point that hindered earlier attempts to go beyond few leading orders

*Electronic address: p.jizba@fjfi.cvut.cz
†Electronic address: v.zatloukal@fu-berlin.de

in the expansion (see, e.g., Refs. [10–14]). In particular, one can progress without relying on the explicit use of approximate expressions or interpolation formulas for the energy eigenvalues which are often difficult to judge due to lack of reliability in their error estimates.

The idea to use PI's as a means of producing various WK-type expansions and related thermodynamic functions is clearly not new. Indeed, the first systematic discussions and analyzes of these issues emerged already during the early 1970's. Among these belong the early attempts of PI treatments of the high-temperature behavior of partition functions for anharmonic oscillators [15–17] and gradient expansions of free energy [5]. These approaches belong in the class of the so-called *analytic perturbation schemes* which account for an explicit analytic expressions of the coefficient functions. For many practical purposes it is desirable to have explicit analytical expressions for coefficients in the WK perturbation expansion. This is so, for instance, when the symmetry (Lorentz, gauge, global) is supposed to be broken by quantum or thermal fluctuations. Though these issues are more pressing in quantum field theories, they have in recent two decades entered also in the realm of a few-body finite-temperature quantum mechanics. The catalyst has been theoretical investigations and ensuing state-of-the-arts experiments in condensed Bose gases, degenerate Fermi gases, quantum clusters or strongly coupled Coulomb systems. It is not only the zero-temperature regime that is of interest in these systems. Many issues revolve also around finite-temperature or "high"-temperature questions. These include, thermal and thermoelectric transport of ultra-cold atomic gases [18, 19], hydrogen, helium, and hydrogen/helium mixtures and their astrophysical implications [20, 21], Lennard–Jones ^{3}He and ^{4}He gases [22], etc.

Apart from the aforementioned group of PI methods there are also various non-analytic methods among which the most prominent are computational methods, such as PI Monte Carlo and molecular dynamics simulations [23, 24], accompanied by a host of PI reweighted techniques [25]. Another important type of non-analytic method are the approximative schemes, to which belong variational approaches [5, 26, 27] and ergodic approximations [28]. Nice summaries of both analytic and non-analytic PI approaches can be found, e.g., in Refs. [5, 9].

A serious weakness of existent analytic WK expansions and their various disguises (be they based on PI's or not), resides in their inability to progress very far with the expansion order. This makes it difficult to address thermodynamically relevant intermediate-temperature regions that is particularly pertinent in molecular and condensed matter chemistry (binding energies, self-dissociation phenomena, order-disorder transitions, etc.). The best analytic expansions are presently available within the framework of the world-line path integral method (known also as the string inspired method) [29]. In this approach the expansion coefficients are available up to order $\mathcal{O}(\beta^{12})$, subject to the actual interaction potential (cf. Refs. [29–31]). Other more conventional approaches, such as the recursive or non-recursive heat-kernel calculations [32, 33] or higher derivative expansions by Feynman diagrams [34–36], achieve at best the order $\mathcal{O}(\beta^7)$. The key problem is a rapid escalation in the complexity of higher-order terms which is difficult to handle without some type of resummation. In the present paper we derive a new resummation formula that provides a rather simple and systematic way of deriving the coefficient functions. Its main advantages rely on both an analytic control of the high-temperature behavior, and on an accurate description over a wide temperature range via numerical calculations that can be simply carried out at the level of an undergraduate exercise.

The structure of the paper is as follows. To set the stage we recall in the next section some fundamentals of PI formulations of the Bloch density matrix and the ensuing partition function and Boltzmann density. With the help of the space-time transformation that transforms the Wiener-process sample paths to the Brownian-bridge sample paths we obtain the PI that represents a useful alternative to the original Feynman–Kac representation. Consequently we arrive at a new functional representation of the Boltzmann density which is more suitable for tackling the high-temperature regime than the genuine Wigner–Kirkwood formulation (see Sections II A, II B and III). While the method resembles in principle the Wentzel–Brillouin–Kramers (WKB)

solution for the transition amplitude, its details are quite different. In two associated subsections we examine some salient technical issues related to the low-order high-temperature expansion in one dimension. To illustrate the potency of our approach we consider in Section III the high-temperature expansion of the one-dimensional anharmonic oscillator. In particular, we perform the Boltzmann density and ensuing partition function expansions and compute the related thermodynamic quantities. The expansions obtained improve over the classic results of Schwarz [14] and Padé-approximation-based expansion of Gibson [37]. In Section IV we proceed by extending our expansion to the whole Bloch density matrix. The expansion thus obtained is compared with the more conventional Wick's theorem based perturbation expansion based on the Onofri–Zuk Green's functions. There we show that our prescription comprises substantially less (in fact, exponentially less) terms contributing to higher perturbation orders. Also the algebraic complexity of the coefficient functions involved is substantially lower in our approach. Various remarks and generalizations are proposed in the concluding section. For the reader's convenience the paper is supplemented with two appendices which clarify some finer technical details. The paper is also accompanied by Mathematica code that generates the higher-order expansion terms for arbitrary smooth local potentials up to 18th order in β.

Let us add a final note. Most of the presented mathematical derivations are of a heuristic nature — as it should be expected from the mathematical analysis based on the path-integral calculus. For example, it is assumed throughout that the expansions such as (7) or (14) have meaning and represent, at least asymptotically, convergent series. Further, in a number of places, we assume that integration and summation may be interchanged. The basic purpose of this paper is to find explicit formulas for the coefficient functions $Q(\boldsymbol{m}_1, \ldots, \boldsymbol{m}_n)$, and in doing so to reveal the elaborate algebraic and combinatorial structure present in these functions. A more rigorous treatment of the aforementioned mathematical aspects is possible, but would involve different language and techniques than are employed in this paper.

II. WIGNER–KIRKWOOD EXPANSION

In this section we derive the Wigner–Kirkwood expansion by means of path-integral techniques. To this end we consider a D-dimensional non-relativistic quantum mechanical system described with the Hamiltonian

$$\hat{H} \;=\; \sum_{j=1}^{D} \frac{\hat{p}_j^2}{2M_j} + V(\hat{\boldsymbol{x}}) \;, \tag{1}$$

where $V(\boldsymbol{x})$ is a generic smooth potential, and $\hat{p}_j = -i\hbar\frac{\partial}{\partial x_j}$. We define the Gibbs operator $e^{-\beta\hat{H}}$, where $\beta = 1/(k_B T)$ is the inverse temperature, and k_B the Boltzmann constant. The partition function $Z(\beta)$ is defined as the trace of the Bloch (or canonical) density matrix, i.e., in the position representation we have the formula

$$Z(\beta) \;=\; \int_{\mathbb{R}^D} d\boldsymbol{x}\, \langle \boldsymbol{x}|\, e^{-\beta\hat{H}}\, |\boldsymbol{x}\rangle \;=\; \int_{\mathbb{R}^D} d\boldsymbol{x}\;\; \varrho(\boldsymbol{x},\beta)\,. \tag{2}$$

For brevity, we use here and throughout the convention $d\boldsymbol{x} \equiv d^D x$. The un-normalized probability density $\varrho(\boldsymbol{x},\beta)$ is also known as the Boltzmann density.

Matrix elements of the Bloch density matrix can be represented by the path integral as [5, 38]

$$\langle \boldsymbol{x}_b|\, e^{-\beta\hat{H}}\, |\boldsymbol{x}_a\rangle \;=\; \int_{\boldsymbol{x}(0)=\boldsymbol{x}_a}^{\boldsymbol{x}(\beta\hbar)=\boldsymbol{x}_b} \mathcal{D}\boldsymbol{x}(\tau) \exp\left\{ -\frac{1}{\hbar}\int_0^{\beta\hbar} d\tau \left[\sum_{j=1}^{D} \frac{M_j}{2}\, \dot{x}_j^2(\tau) + V(\boldsymbol{x}(\tau)) \right] \right\} \;. \tag{3}$$

which can be viewed as the Wick-rotated quantum-mechanical transition amplitude. Indeed, if one changes the time τ in $i\tau$, one recovers the usual transition amplitude $\langle \boldsymbol{x}_b, \tau_b | \boldsymbol{x}_a, \tau_a \rangle$ satisfying the Schödinger equation with the Hamiltonian $\hat{H}$ (cf. e.g. Refs. [5, 6]). In the literature on stochastic processed is the path-integral representation of the Bloch density matrix also know as the Feynman–Kac formula [39].

For the purpose of the density matrix computation, we shall primarily consider here only diagonal matrix elements, i.e., case when $\boldsymbol{x}_b = \boldsymbol{x}_a$. We shall briefly return to the off-diagonal matrix elements in Section IV. To proceed we perform a change of space and time variables, $\boldsymbol{x} \to \boldsymbol{x}_a + \Lambda\boldsymbol{\xi}$, $\tau \to \beta\hbar s$, where Λ is a diagonal matrix $\mathrm{diag}(\lambda_1, \ldots, \lambda_D)$ with entries $\lambda_j = \sqrt{\beta\hbar^2/M_j}$ (corresponding to the thermal de Broglie wavelength of the jth degree of freedom). The ensuing path integral

$$\langle \boldsymbol{x}_a | \, e^{-\beta\hat{H}} \, | \boldsymbol{x}_a \rangle \;=\; \frac{1}{\det\Lambda} \int_{\boldsymbol{\xi}(0)=\boldsymbol{0}}^{\boldsymbol{\xi}(1)=\boldsymbol{0}} \mathcal{D}\boldsymbol{\xi}(s) \exp\left\{ - \int_0^1 ds \left[\frac{1}{2}\, \dot{\boldsymbol{\xi}}^2(s) + \beta V(\boldsymbol{x}_a + \Lambda\boldsymbol{\xi}(s)) \right] \right\}, \qquad (4)$$

is formulated in terms of dimesionless time s and position $\boldsymbol{\xi}$. Note that the size of quantum fluctuations is now controlled by the parameters λ_j, i.e., the only place (apart from the overall PI normalization factor) where the measure of quantum fluctuations — $\hbar$ is present. Since β and $\hbar^2$ appear in (4) on the same footing, the small regime allows to treat in an unified manner both the semiclassical (small $\hbar$) and/or high-temperature (small β) approximations. By assuming small Λ the potential term can be Taylor-expanded as

$$V(\boldsymbol{x}_a + \Lambda\boldsymbol{\xi}(s)) \;=\; V(\boldsymbol{x}_a) + \sum_{\boldsymbol{m}\neq\boldsymbol{0}} \frac{V^{(\boldsymbol{m})}(\boldsymbol{x}_a)}{\boldsymbol{m}!} \, (\Lambda\boldsymbol{\xi}(s))^{\boldsymbol{m}} \;, \qquad (5)$$

where the D-dimensional index $\boldsymbol{m} = (m^1, \ldots, m^D)$ runs through all choices of m^j's $\in \{0, \ldots, \infty\}$ except for $(m^1, \ldots, m^D) = (0, \ldots, 0)$. The multi-derivative $(\boldsymbol{m})$ is defined through the identity

$$V^{(\boldsymbol{m})}(\boldsymbol{x}_a) \;=\; \left. \frac{\partial^{|\boldsymbol{m}|} V(\boldsymbol{x})}{\partial \boldsymbol{x}^{\boldsymbol{m}}} \right|_{\boldsymbol{x}=\boldsymbol{x}_a} \;\equiv\; \left. \frac{\partial^{m^1+\ldots+m^D} V(\boldsymbol{x})}{\partial x_1^{m^1} \ldots \partial x_D^{m^D}} \right|_{\boldsymbol{x}=\boldsymbol{x}_a} , \qquad (6)$$

with $|\boldsymbol{m}| = m^1 + \ldots + m^D$. Finally, the multi-factorial $\boldsymbol{m}! \equiv m^1! \ldots m^D!$, and the multi-power of a D-dimensional vector $\boldsymbol{v}$ is defined componentwise as $\boldsymbol{v}^{\boldsymbol{m}} \equiv v_1^{m^1} \ldots v_D^{m^D}$. Expanding the exponential, followed by some rearrangement, allows to cast (4) in the form

$$\langle \boldsymbol{x}_a | \, e^{-\beta\hat{H}} \, | \boldsymbol{x}_a \rangle = \frac{e^{-\beta V(\boldsymbol{x}_a)}}{\det\Lambda} \sum_{n=0}^{\infty} (-\beta)^n \sum_{\boldsymbol{m}_1, \ldots, \boldsymbol{m}_n \neq \boldsymbol{0}} \prod_{j=1}^{D} \lambda_j^{m_1^j + \ldots + m_n^j} \frac{V^{(\boldsymbol{m}_1)}(\boldsymbol{x}_a) \ldots V^{(\boldsymbol{m}_n)}(\boldsymbol{x}_a)}{\boldsymbol{m}_1! \ldots \boldsymbol{m}_n!} \, \bar{Q} \;. \qquad (7)$$

At this point, we have introduced the dimensionless quantity

$$\begin{aligned} \bar{Q}(\boldsymbol{m}_1, \ldots, \boldsymbol{m}_n) \;&=\; \frac{1}{n!} \int_0^1 ds_1 \ldots ds_n \int_{\boldsymbol{\xi}(0)=\boldsymbol{0}}^{\boldsymbol{\xi}(1)=\boldsymbol{0}} \mathcal{D}\boldsymbol{\xi}(s) \boldsymbol{\xi}^{\boldsymbol{m}_1}(s_1) \ldots \boldsymbol{\xi}^{\boldsymbol{m}_n}(s_n) \exp\left[- \int_0^1 ds \, \frac{1}{2}\, \dot{\boldsymbol{\xi}}^2(s) \right], \\ &=\; \frac{1}{n!} \int_0^1 ds_1 \ldots ds_n \, \langle \boldsymbol{\xi}^{\boldsymbol{m}_1}(s_1) \ldots \boldsymbol{\xi}^{\boldsymbol{m}_n}(s_n) \rangle \,, \end{aligned} \qquad (8)$$

that does not depend on physical constants or parameters of the system. $\bar{Q}$ is also manifestly symmetric under any permutation of its arguments. Let us stress that the $n = 0$ term in the expansion (7) equals 1.

In (8) we have denoted with $\langle\cdots\rangle$ the $(|\boldsymbol{m}_1|+\ldots+|\boldsymbol{m}_n|)$-point correlation function. It can be evaluated using diagrammatic approach based on the so-called Onofri–Zuk (or "world-line") Green's function [6, 29, 40, 41]

$$\Delta_{ij}(t,u) = -\frac{1}{2}\delta_{ij}\left[|t-u| - (t+u-2tu)\right]. \tag{9}$$

We shall briefly sketch this approach in Sec. IV in connection with the off-diagonal density matrix elements. At any rate, procedure based on Green's function (9) proves rather impractical when higher-order terms are to be calculated. Inasmuch as we shall follow a different route. To this end we rewrite expression (8) as a sum of $n!$ integrals over time-ordered sets $s_1<\ldots<s_n$, slice the path integral at corresponding time instances, and replace the free-particle path integrals by more compact braket notation by virtue of (3). We obtain

$$\bar{Q}(\boldsymbol{m}_1,\ldots,\boldsymbol{m}_n) \;=\; \frac{1}{n!}\sum_{\sigma\in S_n} Q(\boldsymbol{m}_{\sigma(1)},\ldots,\boldsymbol{m}_{\sigma(n)})\,, \tag{10}$$

where the sum runs over all permutations of n indices, and

$$Q(\boldsymbol{m}_1,\ldots,\boldsymbol{m}_n) \;=\; \int_{0<s_1<\ldots<s_n<1} ds_1\ldots ds_n \int_{\mathbb{R}^D} d\boldsymbol{y}_1\ldots d\boldsymbol{y}_n \prod_{\nu=0}^{n} \langle \boldsymbol{y}_{\nu+1}|\exp\left[-(s_{\nu+1}-s_\nu)\frac{\hat{\boldsymbol{q}}^2}{2}\right]|\boldsymbol{y}_\nu\rangle\, \boldsymbol{y}_\nu^{\boldsymbol{m}_\nu}\,. \tag{11}$$

In the preceding we have defined $\boldsymbol{m}_0=\boldsymbol{0}$, $s_0=0$, $s_{n+1}=1$, $\boldsymbol{y}_0=\boldsymbol{y}_{n+1}=\boldsymbol{0}$, and the momentum $\hat{\boldsymbol{q}}=(\hat{q}_1,\ldots,\hat{q}_D)$, conjugated to the (dimensionless) position operator $\hat{\boldsymbol{y}}=(\hat{y}_1,\ldots,\hat{y}_D)$. Here and throughout we use the standard convention: $\hat{q}_j=-i\frac{\partial}{\partial y_j}$ and $\langle\boldsymbol{y}|\boldsymbol{q}\rangle = e^{i\boldsymbol{q}\boldsymbol{y}}/(2\pi)^{D/2}$.

Combinatorial complexity can be reduced significantly by observing that for any function $F(\boldsymbol{m}_1,\ldots,\boldsymbol{m}_n)$ the following identity holds:

$$\sum_{\boldsymbol{m}_1,\ldots,\boldsymbol{m}_n\neq\boldsymbol{0}} \frac{1}{n!}\sum_{\sigma\in S_n} F(\boldsymbol{m}_{\sigma(1)},\ldots,\boldsymbol{m}_{\sigma(n)}) \;=\; \sum_{\boldsymbol{m}_1,\ldots,\boldsymbol{m}_n\neq\boldsymbol{0}} F(\boldsymbol{m}_1,\ldots,\boldsymbol{m}_n)\,. \tag{12}$$

This statement is not trivial, since F is not supposed to be invariant under permutations of the $\boldsymbol{m}$'s. When applied to (7) for

$$F(\boldsymbol{m}_{\sigma(1)},\ldots,\boldsymbol{m}_{\sigma(n)}) \;=\; \prod_{j=1}^{D}\lambda_j^{m_1^j+\ldots+m_n^j}\frac{V^{(\boldsymbol{m}_1)}(\boldsymbol{x}_a)\ldots V^{(\boldsymbol{m}_n)}(\boldsymbol{x}_a)}{\boldsymbol{m}_1!\ldots\boldsymbol{m}_n!}\,Q(\boldsymbol{m}_{\sigma(1)},\ldots,\boldsymbol{m}_{\sigma(n)})\,, \tag{13}$$

the expansion can be then reduced to

$$\langle\boldsymbol{x}_a|\,e^{-\beta\hat{H}}\,|\boldsymbol{x}_a\rangle \;=\; \frac{e^{-\beta V(\boldsymbol{x}_a)}}{\det\Lambda}\sum_{n=0}^{\infty}(-\beta)^n\sum_{\boldsymbol{m}_1,\ldots,\boldsymbol{m}_n\neq\boldsymbol{0}}\prod_{j=1}^{D}\lambda_j^{m_1^j+\ldots+m_n^j}\frac{V^{(\boldsymbol{m}_1)}(\boldsymbol{x}_a)\ldots V^{(\boldsymbol{m}_n)}(\boldsymbol{x}_a)}{\boldsymbol{m}_1!\ldots\boldsymbol{m}_n!}\,Q\,. \tag{14}$$

This result is new. In addition, in Appendix we derive a new explicit expression for the coefficients Q which proves to be very useful in the determination of the higher-order terms. In particular, there we show that

$$Q(\boldsymbol{m}_1,\ldots,\boldsymbol{m}_n) \;=\; K\int_{\mathbb{R}^D}\frac{d\boldsymbol{q}}{(2\pi)^D}\left(\frac{i^{|\boldsymbol{m}_n|}}{1+\frac{\boldsymbol{q}^2}{2}}\frac{\partial^{|\boldsymbol{m}_n|}}{\partial\boldsymbol{q}^{\boldsymbol{m}_n}}\right)\ldots\left(\frac{i^{|\boldsymbol{m}_1|}}{1+\frac{\boldsymbol{q}^2}{2}}\frac{\partial^{|\boldsymbol{m}_1|}}{\partial\boldsymbol{q}^{\boldsymbol{m}_1}}\right)\frac{1}{1+\frac{\boldsymbol{q}^2}{2}}\,, \tag{15}$$

where the multiplicative constant has the form

$$K \;=\; \frac{1}{\Gamma\left(n+1-\frac{D}{2}+\frac{|\boldsymbol{m}_1|+\ldots+|\boldsymbol{m}_n|}{2}\right)}. \tag{16}$$

From Appendix B we can observe that the integral (15) suffers the infrared divergencies precisely in those instances when the Γ-function in K has pole. Consequently, in practical applications one should appropriately regularize (e.g., via dimensional regularization) both K and integral in (15) in order to resolve the indeterminate form of the product.

In passing we may note that because Q is real, it must be equal to zero when $|\boldsymbol{m}_1|+\ldots+|\boldsymbol{m}_n|$ together with all partial sums $m_1^j+...+m_n^j$ $(j=1,\ldots,D)$ is an even number (cf. also Section IV and Appendix B). So the expansion of the density matrix (14) can be reorganized as an expansion in $\hbar^2$. This is emblematic of the Wigner–Kirkwood expansion [1] for systems with differentiable potentials. In the case of the non-differentiable potentials (cavities, billiards, etc.) the generalized derivative of Schwartz must be used instead [42].

Result (14) might be used for calculating higher-order terms beyond $\hbar^2$-correction (terms up to order $\hbar^6$ have been already determined in the literature [44]). Moreover, the structure of (14) clearly emphasizes that expansion is appropriate only when the involved thermal de Broglie wavelengths are much smaller than the typical length of variation of the potential.

A. Calculation of low-order terms in D dimensions

In order to get further insight into structure of (14) we will now calculate first few terms in the expansion. To this end, we notice that a typical term in (15) has the generic structure

$$\begin{aligned}\int_{\mathbb{R}^D}\frac{d\boldsymbol{q}}{(2\pi)^D}\frac{q_1^{2r_1}\ldots q_D^{2r_D}}{\left(1+\frac{\boldsymbol{q}^2}{2}\right)^s} &= \int_0^\infty d\sigma\frac{\sigma^{s-1}}{(s-1)!}e^{-\sigma}\int_{\mathbb{R}^D}\frac{d\boldsymbol{q}}{(2\pi)^D}q_1^{2r_1}\ldots q_D^{2r_D}e^{-\sigma\frac{\boldsymbol{q}^2}{2}}\\ &= \frac{\Gamma(s-\frac{D}{2}-|\boldsymbol{r}|)}{(s-1)!(2\pi)^{D/2}2^{|\boldsymbol{r}|}}\prod_{j=1}^{D}\frac{(2r_j)!}{r_j!}\,,\end{aligned} \tag{17}$$

where $r_1,\ldots,r_D,s\in\mathbb{N}$. If the power of any q_j is odd, the above integral obviously vanishes. For the sake of simplicity, the discussion here will be restricted to the orders in $\mathcal{O}(\beta^3)$, but it can be naturally extended to higher orders (cf. next section). At this level, we need to know (15) for $n=1$ and $n=2$.

Case $n=1$: Here the lowest-order non-trivial contribution comes from $|\boldsymbol{m}_1|=2$, with $m_1^i=\delta_{ij}+\delta_{ik}$. After differentiating

$$\frac{\partial^2}{\partial q_j\partial q_k}\frac{1}{1+\frac{\boldsymbol{q}^2}{2}} = -\frac{\delta_{jk}}{\left(1+\frac{\boldsymbol{q}^2}{2}\right)^2}+\frac{2q_jq_k}{\left(1+\frac{\boldsymbol{q}^2}{2}\right)^3}\,, \tag{18}$$

we can use the formulas (15) and (17) to find

$$Q(\boldsymbol{m}_1) = \frac{1}{(2\pi)^{D/2}}\frac{\delta_{jk}}{6}\,. \tag{19}$$

Case $n=2$: Here the lowest-order non-trivial contribution comes from $|\boldsymbol{m}_1|=|\boldsymbol{m}_2|=1$, with $m_1^i=\delta_{ij}$, $m_2^i=\delta_{ik}$. Consequently, we need to estimate

$$\frac{\partial}{\partial q_k}\left(\frac{1}{1+\frac{\boldsymbol{q}^2}{2}}\frac{\partial}{\partial q_j}\frac{1}{1+\frac{\boldsymbol{q}^2}{2}}\right) = -\frac{\delta_{jk}}{\left(1+\frac{\boldsymbol{q}^2}{2}\right)^3}+\frac{3q_jq_k}{\left(1+\frac{\boldsymbol{q}^2}{2}\right)^4}\,, \tag{20}$$

which gives

$$Q(\boldsymbol{m}_1,\boldsymbol{m}_2) \;=\; \frac{1}{(2\pi)^{D/2}}\frac{\delta_{jk}}{24}\,. \tag{21}$$

By gathering the results (19) and (21) together we can write the expansion (14) in the $n=2$ approximation as

$$\langle \boldsymbol{x}_a|\, e^{-\beta\hat{H}}\,|\boldsymbol{x}_a\rangle \;\sim\; \frac{e^{-\beta V(\boldsymbol{x}_a)}}{(2\pi)^{D/2}\mathrm{det}\Lambda}\left(1-\frac{\beta}{12}\sum_{j=1}^{D}\lambda_j^2\frac{\partial^2 V(\boldsymbol{x}_a)}{\partial x_j^2}+\frac{\beta^2}{24}\sum_{j,k=1}^{D}\lambda_j\lambda_k\frac{\partial V(\boldsymbol{x}_a)}{\partial x_j}\frac{\partial V(\boldsymbol{x}_a)}{\partial x_k}\right). \tag{22}$$

This agrees, for $\lambda_j=\lambda$ (i.e., for equal-mass particles), with the usual low-order Wigner–Kirkwood expansion (see, e.g., Refs. [5, 45]).

B. Expansion for $D=1$

Here we show that the form of the coefficients $Q(m_1,\ldots,m_n)$ can be substantially simplified in 1-dimension ($D=1$). It is rather interesting that the simplification basically involves only arithmetic operations. To see what is involved we denote

$$I(m_1,\ldots,m_n|r,s) \;=\; \int_{\mathbb{R}}\frac{dq}{2\pi}\left(\frac{i^{m_n}}{1+\frac{q^2}{2}}\frac{\partial^{m_n}}{\partial q^{m_n}}\right)\cdots\left(\frac{i^{m_1}}{1+\frac{q^2}{2}}\frac{\partial^{m_1}}{\partial q^{m_1}}\right)\left(\frac{1}{(1+\frac{i}{\sqrt{2}}q)^r}\frac{1}{(1-\frac{i}{\sqrt{2}}q)^s}\right), \tag{23}$$

so that (cf. Eq. (15)): $Q(m_1,\ldots,m_n)=K(m_1,\ldots,m_n)I(m_1,\ldots,m_n|1,1)$. By the m_1-fold differentiation of the last bracket we obtain the recurrence relation

$$\begin{aligned} I(m_1,\ldots,m_n|r,s) \;&=\; \frac{(-1)^{m_1}}{2^{m_1/2}}m_1!\sum_{k_1=0}^{m_1}(-1)^{k_1}\binom{r-1+k_1}{r-1}\binom{s-1+m_1-k_1}{s-1} \\ &\times\; I(m_2,\ldots,m_n|r+1+k_1,s+1+m_1-k_1)\,, \end{aligned} \tag{24}$$

with the initial condition

$$I(\emptyset|r,s) \;=\; \int_{\mathbb{R}}\frac{dq}{2\pi}\frac{1}{(1+\frac{i}{\sqrt{2}}q)^r}\frac{1}{(1-\frac{i}{\sqrt{2}}q)^s} \;=\; \frac{2^{3/2}}{2^{r+s}}\binom{r+s-2}{r-1}. \tag{25}$$

The latter identity is a straightforward consequence of Cauchy's integral theorem where the contour integration is taken at either the pole $i\sqrt{2}$ or $-i\sqrt{2}$. Repeated use of (24), with (25) as the last step, leads to an explicit form for $Q(m_1,\ldots,m_n)$, namely

$$Q \;=\; \frac{(\frac{m_1+\ldots+m_n}{2}+n)!}{\sqrt{2\pi}2^{(m_1+\ldots+m_n)/2}}\sum_{\ell_1=0}^{m_1}\cdots\sum_{\ell_n=0}^{m_n}\prod_{k=1}^{n}\frac{(-1)^{\ell_k}\binom{m_k}{\ell_k}}{(\ell_1+\ldots+\ell_k+k)(m_1-\ell_1+\ldots+m_k-\ell_k+k)}\,. \tag{26}$$

In deriving we have used the duplication formula [46]: $\sqrt{\pi}2^{1-2z}\Gamma(2z)=\Gamma(z)\Gamma(z+1/2)$. Resulting one-dimensional expansion takes the form

$$\langle x_a|\, e^{-\beta\hat{H}}\,|x_a\rangle \;=\; \frac{e^{-\beta V(x_a)}}{\lambda}\sum_{n=0}^{\infty}(-\beta)^n\sum_{m_1,\ldots,m_n=1}^{\infty}\lambda^{m_1+\ldots+m_n}\frac{V^{(m_1)}(x_a)\ldots V^{(m_n)}(x_a)}{m_1!\ldots m_n!}\,Q\,. \tag{27}$$

Apart from the initial constant term $\beta^0\hbar^0$, the latter expansion contains terms proporional to $\beta^i(\hbar^2)^j$, where $i,j\in\mathbb{N}$ and $i/3\le j\le i-1$ (or, equivalently, $j+1\le i\le 3j$).

For the first few orders the coefficients of the expansion can be found rather straightforwardly. In Table I we list the coefficients of the series $e^{\beta V(x)}\sqrt{2\pi}\lambda\,\langle x|\,e^{-\beta\hat{H}}\,|x\rangle$. To order β^8 these can be obtained without any excessive hardship (for further comments see [47]). The higher orders in fixed β can now be simply obtained by grouping terms with equal order of β and performing a number of multi-differentiations for $V(x_a)$ which can be easily done with Maple or Mathematica. To this end we supplement the paper with Mathematica code that allows to generate the higher-order expansion terms (up to 18th order) for arbitrary smooth local potentials.

III. EXAMPLE: ANHARMONIC OSCILLATOR IN $D=1$

In the previous section, we have seen in some detail how the coefficients functions in the Wigner–Kirkwood expansion can be resolved in an explicit form. The basic results there were the formulas (14)–(16). The expressions found are quite general, valid for any smooth potential and in $D=1$ are analytically accessible up to order β^{18}. Nevertheless, for consistency reasons it is useful to examine a problem possessing an exact solution in which it is possible to find closed expressions for the expansion coefficients. The $D=1$ harmonic oscillator provides us with just such an exactly solvable example. Rather than starting directly with a simple harmonic oscillator, it is instructive to start with an *anharmonic* oscillator first and then regain the harmonic oscillator solution in the limit of vanishing coupling constant (i.e., zero anharmonicity limit). In addition, the anharmonic oscillator, which can be regarded as a field theory in one dimension, has long served as a testing ground for new ideas for solving field theories and hence is bolstered by a large body of literature. In this respect it is a natural model which any new approximation scheme should address. For a definiteness we start with the anharmonic potential

$$V(x) \;=\; \frac{M}{2}\omega^2x^2+\frac{g}{4!}x^4, \tag{28}$$

for which the high-temperature expansion (27) yields

$$\begin{aligned}\langle x|\,e^{-\beta\hat{H}}\,|x\rangle \;=\;& \frac{\exp\left[-\beta\left(\frac{M}{2}\omega^2x^2+\frac{g}{4!}x^4\right)\right]}{\sqrt{2\pi}\lambda}\left[1\;-\;\frac{\beta^2\hbar^2\left(gx^2+2M\omega^2\right)}{24M}\right.\\ &+\;\frac{\beta^3\left(5Mx^2\hbar^2\left(gx^2+6M\omega^2\right)^2-18g\hbar^4\right)}{4320M^2}\\ &\left.+\;\frac{\beta^4\hbar^4\left(17g^2x^4+84gMx^2\omega^2+36M^2\omega^4\right)}{5760M^2}\;+\;O\left(\beta^5\right)\right].\end{aligned} \tag{29}$$

The higher-order corrections can be explicitly obtained with the help of Table I (up to order β^8) or with the enclosed Mathematica code quoted in [47] (up to order β^{18}).

In the case of zero anharmonicity ($g=0$), we can check our results against the exact solution of the harmonic oscillator problem. The expansion (29) reduces to

$$\langle x|\,e^{-\beta\hat{H}}\,|x\rangle_{g=0}=\;\frac{\exp\left(-\beta\frac{M}{2}\omega^2x^2\right)}{\sqrt{2\pi}\lambda}\left[1-\frac{1}{12}\beta^2\omega^2\hbar^2+\frac{1}{24}\beta^3Mx^2\omega^4\hbar^2+\frac{1}{160}\beta^4\omega^4\hbar^4+O\left(\beta^5\right)\right], \tag{30}$$

TABLE I: Coefficients of the series $e^{\beta V(x)}\sqrt{2\pi}\lambda\,\langle x|\,e^{-\beta\hat{H}}\,|x\rangle$, at terms $\beta^i(\hbar^2)^j$, calculated according to formulas (26) and (27). Here $0\le i\le 8$ and $0\le j\le 7$, which allows to determine the series up to the 8th order in β. Coefficients of terms $(\hbar^2)^j$, which are polynomials in β, can be read off completely only for $j\le 2$. (For instance, the $\hbar^6$-term is lacking a contribution from β^9.)

	$\hbar^0$	$\hbar^2$	$\hbar^4$	$\hbar^6$	$\hbar^8$	$\hbar^{10}$
β^0	1	0	0	0	0	0
β^1	0	0	0	0	0	0
β^2	0	$-\frac{V''(x)}{12M}$	0	0	0	0
β^3	0	$\frac{V'(x)^2}{24M}$	$-\frac{V^{(4)}(x)}{240M^2}$	0	0	0
β^4	0	0	$\frac{V''(x)^2}{160M^2}$ $+\frac{V'(x)V^{(3)}(x)}{120M^2}$	$-\frac{V^{(6)}(x)}{6720M^3}$	0	0
β^5	0	0	$-\frac{11V'(x)^2V''(x)}{1440M^2}$	$\frac{23V^{(3)}(x)^2}{40320M^3}$ $+\frac{19V''(x)V^{(4)}(x)}{20160M^3}$ $+\frac{V'(x)V^{(5)}(x)}{2240M^3}$	$-\frac{V^{(8)}(x)}{241920M^4}$	0
β^6	0	0	$\frac{V'(x)^4}{1152M^2}$	$-\frac{61V''(x)^3}{120960M^3}$ $-\frac{43V'(x)V^{(3)}(x)V''(x)}{20160M^3}$ $-\frac{5V'(x)^2V^{(4)}(x)}{8064M^3}$	$\frac{23V^{(4)}(x)^2}{483840M^4}$ $+\frac{19V^{(3)}(x)V^{(5)}(x)}{241920M^4}$ $+\frac{11V''(x)V^{(6)}(x)}{241920M^4}$ $+\frac{V'(x)V^{(7)}(x)}{60480M^4}$	$-\frac{V^{(10)}(x)}{10644480M^5}$

	$\hbar^6$	$\hbar^8$	$\hbar^{10}$	$\hbar^{12}$	$\hbar^{14}$
β^7	$\frac{V^{(3)}(x)V'(x)^3}{2016M^3}$ $+\frac{83V''(x)^2V'(x)^2}{80640M^3}$	$-\frac{V^{(6)}(x)V'(x)^2}{32256M^4}$ $-\frac{V^{(3)}(x)V^{(4)}(x)V'(x)}{480M^4}$ $-\frac{V''(x)V^{(5)}(x)V'(x)}{6720M^4}$ $-\frac{31V''(x)V^{(3)}(x)^2}{161280M^4}$ $-\frac{5V''(x)^2V^{(4)}(x)}{32256M^4}$	$\frac{71V^{(5)}(x)^2}{21288960M^5}$ $+\frac{61V^{(4)}(x)V^{(6)}(x)}{10644480M^5}$ $+\frac{19V^{(3)}(x)V^{(7)}(x)}{5322240M^5}$ $+\frac{17V''(x)V^{(8)}(x)}{10644480M^5}$ $+\frac{V'(x)V^{(9)}(x)}{2128896M^5}$	$-\frac{V^{(12)}(x)}{553512960M^6}$	0
β^8	$-\frac{17V'(x)^4V''(x)}{69120M^3}$	$\frac{1261V''(x)^4}{29030400M^4}$ $+\frac{227V'(x)V^{(3)}(x)V''(x)^2}{604800M^4}$ $+\frac{527V'(x)^2V^{(4)}(x)V''(x)}{2419200M^4}$ $+\frac{659V'(x)^2V^{(3)}(x)^2}{4838400M^4}$ $+\frac{17V'(x)^3V^{(5)}(x)}{483840M^4}$	$-\frac{71V^{(8)}(x)V'(x)^2}{63866880M^5}$ $-\frac{3067V^{(4)}(x)V^{(5)}(x)V'(x)}{159667200M^5}$ $-\frac{13V^{(3)}(x)V^{(6)}(x)V'(x)}{950400M^5}$ $-\frac{109V''(x)V^{(7)}(x)V'(x)}{15966720M^5}$ $-\frac{6353V''(x)V^{(4)}(x)^2}{319334400M^5}$ $-\frac{7939V^{(3)}(x)^2V^{(4)}(x)}{319334400M^5}$ $-\frac{13V''(x)V^{(3)}(x)V^{(5)}(x)}{394240M^5}$ $-\frac{3001V''(x)^2V^{(6)}(x)}{319334400M^5}$	$\frac{3433V^{(6)}(x)^2}{166053888800M^6}$ $+\frac{1501V^{(5)}(x)V^{(7)}(x)}{4151347200M^6}$ $+\frac{2003V^{(4)}(x)V^{(8)}(x)}{8302694400M^6}$ $+\frac{5V^{(3)}(x)V^{(9)}(x)}{41513472M^6}$ $+\frac{73V''(x)V^{(10)}(x)}{1660538880M^6}$ $+\frac{V'(x)V^{(11)}(x)}{92252160M^6}$	$-\frac{V^{(14)}(x)}{33210777600M^7}$

which, indeed, coincides with the corresponding expansion of the well-known analytic form of the Bloch density matrix for harmonic oscillator (see, e.g., Refs. [5, 6])

$$\langle x|\,e^{-\beta\hat{H}}\,|x\rangle_{g=0} \;=\; \frac{\exp\left(-\beta\frac{M}{2}\omega^2x^2\right)}{\sqrt{2\pi}\lambda}\sqrt{\frac{\beta\omega\hbar}{\sinh(\beta\omega\hbar)}}\exp\left[-\frac{Mx^2\omega}{\hbar}\left(\tanh\frac{\beta\omega\hbar}{2}-\frac{\beta\omega\hbar}{2}\right)\right]. \quad (31)$$

In passing we may note that the expansion of the single-particle partition function $Z(\beta)$ associated with (29) can be phrased in terms of the *parabolic cylindric function* and its derivatives

which, after re-expansion, give

$$\begin{aligned} Z(\beta) &= \frac{1}{\sqrt{2\pi}\lambda}\sqrt[4]{\frac{3}{2\beta g}}\left[\Gamma\left(\frac{1}{4}\right) + \frac{\sqrt{\frac{3}{2}}\sqrt{\beta}M\omega^2\Gamma\left(-\frac{1}{4}\right)}{2\sqrt{g}} + \frac{3\beta M^2\omega^4\Gamma\left(\frac{5}{4}\right)}{g}\right. \\ &- \frac{\beta^{3/2}\left(\Gamma\left(\frac{3}{4}\right)\left(g^2\hbar^2+18M^4\omega^6\right)\right)}{4\left(\sqrt{6}g^{3/2}M\right)} \\ &- \left.\frac{\beta^2\left(\Gamma\left(-\frac{3}{4}\right)\left(2g^2\omega^2\hbar^2+45M^4\omega^8\right)\right)}{128g^2} + \mathcal{O}\left(\beta^{5/2}\right)\right]. \end{aligned} \tag{32}$$

This, when combined with appropriate thermodynamic formulas, yields the following expressions for entropy S, the heat capacity C_V and internal energy U:

$$\begin{aligned} \frac{S}{k_B} &= -\frac{1}{k_B}\left(\frac{\partial F}{\partial T}\right)_V = \log Z(\beta) - \frac{\beta}{Z(\beta)}\left(\frac{\partial Z(\beta)}{\partial\beta}\right)_V \\ &= \frac{3}{4} + \log\left(\frac{2\Gamma\left(\frac{5}{4}\right)}{\lambda}\sqrt[4]{\frac{6}{\pi^2\beta g}}\right) - \frac{\sqrt{\frac{3}{2}}\sqrt{\beta}M\omega^2\Gamma\left(\frac{3}{4}\right)}{\sqrt{g}\Gamma\left(\frac{1}{4}\right)} \\ &+ \frac{\beta^{3/2}\left(\pi g^2\hbar^2\Gamma\left(\frac{5}{4}\right) + 3\sqrt{2}M^4\omega^6\Gamma\left(\frac{3}{4}\right)^3\right)}{\sqrt{3}g^{3/2}M\Gamma\left(\frac{1}{4}\right)^3} + \mathcal{O}\left(\beta^2\right), \\ \frac{C_V}{k_B} &= \frac{T}{k_B}\left(\frac{\partial S}{\partial T}\right)_V = -\frac{\beta}{k_B}\left(\frac{\partial S}{\partial\beta}\right)_V \\ &= \frac{3}{4} + \frac{\sqrt{\frac{3}{2}}\sqrt{\beta}M\omega^2\Gamma\left(\frac{3}{4}\right)}{2\sqrt{g}\Gamma\left(\frac{1}{4}\right)} \\ &- \frac{\beta^{3/2}\left(\sqrt{3}\pi g^2\hbar^2\Gamma\left(\frac{5}{4}\right) + 3\sqrt{6}M^4\omega^6\Gamma\left(\frac{3}{4}\right)^3\right)}{2g^{3/2}M\Gamma\left(\frac{1}{4}\right)^3} + \mathcal{O}\left(\beta^2\right), \\ U &= -T^2\left(\frac{\partial F/T}{\partial T}\right)_V = \left(\frac{\partial F\beta}{\partial\beta}\right)_V \\ &= \frac{3}{4\beta} + \frac{\sqrt{\frac{3}{2}}M\omega^2\Gamma\left(\frac{3}{4}\right)}{\sqrt{\beta}\sqrt{g}\Gamma\left(\frac{1}{4}\right)} - \frac{3M^2\omega^4\left(\Gamma\left(\frac{1}{4}\right)^2 - 4\Gamma\left(\frac{3}{4}\right)^2\right)}{4g\Gamma\left(\frac{1}{4}\right)^2} \\ &+ \frac{\sqrt{\beta}\left(2\sqrt{3}\pi g^2\hbar^2\Gamma\left(\frac{9}{4}\right) + 15\sqrt{6}M^4\omega^6\Gamma\left(\frac{3}{4}\right)^3\right)}{320g^{3/2}M\Gamma\left(\frac{5}{4}\right)^3} + \mathcal{O}\left(\beta\right). \end{aligned} \tag{33}$$

[$F = -k_B T \log Z(\beta)$ is the Helmholtz free energy]. These expansions are not only in excellent agreement with the classic (spectral-theorem based) expansions of Schwarz [14] and Gibson [37] but they also go beyond these expansions by providing explicit forms for higher-order terms not present in Refs. [14, 37].

Unfortunately when M in (28) is negative (i.e., we would have a double-well potential) the WK approach would fail. Indeed the WK expansion cannot accommodate non-perturbation effect such as multi-instanton contribution and ensuing tunneling, as by its very construction it is basically a perturbation expansion around a free solution. From this point of view a tunneling in a double well potential seems to be beyond reach in our expansion. Of course, tunneling could be included by considering some sort of a hybrid approach in which the "phase part" of the transition probability would be calculated via WKB (possibly including multi-istanton contribution), while the fluctuating factor would be evaluated perturbatively via WK method. One of the potential bonuses would be the fact that one could bypass the notorious problems with the Van Vleck determinant on caustics. Such a hybrid approach would, however, clearly go beyond the simple WK approach that is used in our paper. In our future investigation we will touch more upon this issue.

IV. OFF-DIAGONAL BLOCH DENSITY MATRIX ELEMENTS

So far, we have almost exclusively been dealing with the diagonal elements of the Bloch density matrix — Boltzmann density. This was well justified by expected applications in statistical physics, where typically only the partition function is required and hence only diagonal elements of the density matrix are relevant (of course, only as long as the Maxwell-Boltzmann statistics is considered). This is also the linchpin of the original Wigner–Kirkwood work.

Expansion and the formula for the Bloch density matrix (14) can be straightforwardly generalized beyond the original Wigner–Kirkwood analysis by considering the off-diagonal form of the density matrix (also called the heat kernel or euclidean Feynman amplitude). This would be particularly pertinent in cases, when one would like to incorporate the exchange effects that are a consequence of fermion or boson statistics or when the linear response theory would be in question. By following the same train of thought as in Sec. II we can phrase the path-integral representation of the full Bloch density matrix in terms sum over the Brownian bridge sample paths. The path transformation that transforms the Wiener process $\Omega_W = \{\boldsymbol{x}(\cdot)\}$ to the Brownian bridge process $\Omega_{BB} = \{\boldsymbol{\xi}(\cdot)\}$ is

$$\boldsymbol{x}(\tau) \;=\; \boldsymbol{x}_a(1-s) + \boldsymbol{x}_b s + \Lambda\boldsymbol{\xi}(s)\,. \tag{34}$$

Let us recall that the "Euclidean time" variable τ is connected with s via the relation $\tau = \beta\hbar s$.

The Brownian bridge sample paths fulfill the Dirichlet boundary conditions $\boldsymbol{\xi}(0) = \boldsymbol{\xi}(1) = \mathbf{0}$. With this the Feynman–Kac formula for the Bloch density matrix (3) acquires the form

$$\begin{aligned}\langle \boldsymbol{x}_b|\, e^{-\beta\hat{H}}\,|\boldsymbol{x}_a\rangle \;&=\; \frac{\exp\left\{-\frac{1}{2}[\Lambda^{-1}(\boldsymbol{x}_b-\boldsymbol{x}_a)]^2\right\}}{\det\Lambda} \\ &\times \int_{\boldsymbol{\xi}(0)=\mathbf{0}}^{\boldsymbol{\xi}(1)=\mathbf{0}} \mathcal{D}\boldsymbol{\xi}(s) \exp\left\{-\int_0^1 ds\left[\frac{1}{2}\,\dot{\boldsymbol{\xi}}^2(s) + \beta V(\boldsymbol{x}_a(1-s)+\boldsymbol{x}_b s + \Lambda\boldsymbol{\xi}(s))\right]\right\}\,,\end{aligned} \tag{35}$$

where the surface term in the action got canceled due to boundary conditions of the Brownian bridge. We can expand the potential $V(\ldots)$ around the free-particle classical solution as

$$V(\boldsymbol{x}_a(1-s)+\boldsymbol{x}_b s+\Lambda\boldsymbol{\xi}(s)) \;=\; V(\boldsymbol{x}_a(1-s)+\boldsymbol{x}_b s) + \sum_{\boldsymbol{m}\neq\mathbf{0}} \frac{V^{(\boldsymbol{m})}(\boldsymbol{x}_a(1-s)+\boldsymbol{x}_b s)}{\boldsymbol{m}!}\,(\Lambda\boldsymbol{\xi}(s))^{\boldsymbol{m}}\,, \tag{36}$$

and write the density matrix in the form

$$\langle \boldsymbol{x}_b |\, e^{-\beta \hat{H}}\, | \boldsymbol{x}_a \rangle = \frac{\exp\left\{ -\frac{1}{2}[\Lambda^{-1}(\boldsymbol{x}_b - \boldsymbol{x}_a)]^2 - \beta \tilde{V}(\boldsymbol{x}_b, \boldsymbol{x}_a) \right\}}{\det \Lambda}$$

$$\times \sum_{n=0}^{\infty} (-\beta)^n \sum_{\boldsymbol{m}_1, \ldots, \boldsymbol{m}_n \neq \boldsymbol{0}} \prod_{j=1}^{D} \lambda_j^{m_1^j + \ldots + m_n^j} \frac{(\tilde{V}_{s_1}^{(\boldsymbol{m}_1)}(\boldsymbol{x}_b, \boldsymbol{x}_a) \ldots \tilde{V}_{s_n}^{(\boldsymbol{m}_n)}(\boldsymbol{x}_b, \boldsymbol{x}_a) * \bar{Q}_{s_1 \cdots s_n})(\boldsymbol{t} = 1)}{\boldsymbol{m}_1! \ldots \boldsymbol{m}_n!} \,. \quad (37)$$

In the previous we have introduced the abbreviations

$$\begin{aligned} \tilde{V}(\boldsymbol{x}_b, \boldsymbol{x}_a) &= \int_0^1 ds\, V(\boldsymbol{x}_a(1-s) + \boldsymbol{x}_b s)\,, \\ \tilde{V}_{s_i}^{(\boldsymbol{m}_k)}(\boldsymbol{x}_b, \boldsymbol{x}_a) &= V^{(\boldsymbol{m}_k)}(\boldsymbol{x}_b - s_i(\boldsymbol{x}_b - \boldsymbol{x}_a))\,. \end{aligned} \quad (38)$$

The multi-dimensional convolution appearing in (37) is a straightforward extension of the one-dimensional convolution

$$(X(s_i) * Y(s_i))(t) = (Y(s_i) * X(s_i))(t) = \int_0^t ds_i\, X(t - s_i) Y(s_i)\,. \quad (39)$$

It is the above definition of the convolution which dictates the (seemingly strangely appearing) form of the right-hand-side of (38). Sub-indices s_i appearing in $\bar{Q}$ in (37) just indicate the integration variables in the convolution. We see again, that the key object is the coefficient function $\bar{Q}$ (cf. Eq. (8)) or better the ensuing $(|\boldsymbol{m}_1| + \ldots + |\boldsymbol{m}_n|)$-point correlator $\bar{Q}_{s_1 \cdots s_n}$

$$\begin{aligned} &\int_{\boldsymbol{\xi}(0)=\boldsymbol{0}}^{\boldsymbol{\xi}(1)=\boldsymbol{0}} \mathcal{D}\boldsymbol{\xi}(s)\, \boldsymbol{\xi}^{\boldsymbol{m}_1}(s_1) \ldots \boldsymbol{\xi}^{\boldsymbol{m}_n}(s_n) \exp\left[-\int_0^1 ds\, \frac{1}{2}\, \dot{\boldsymbol{\xi}}^2(s) \right] \\ &= \frac{\delta^{|\boldsymbol{m}_1| + \ldots + |\boldsymbol{m}_n|}}{\delta \boldsymbol{j}(s_1)^{\boldsymbol{m}_1} \ldots \delta \boldsymbol{j}(s_n)^{\boldsymbol{m}_n}} \int_{\boldsymbol{\xi}(0)=\boldsymbol{0}}^{\boldsymbol{\xi}(1)=\boldsymbol{0}} \mathcal{D}\boldsymbol{\xi}(s)\, \exp\left[-\int_0^1 ds\, \frac{1}{2}\, \dot{\boldsymbol{\xi}}^2(s) + \int_0^1 ds\, \boldsymbol{j}(s) \cdot \boldsymbol{\xi}(s) \right] \Bigg|_{\boldsymbol{j}=0} \\ &= \mathcal{N}\, \frac{\delta^{|\boldsymbol{m}_1| + \ldots + |\boldsymbol{m}_n|}}{\delta \boldsymbol{j}(s_1)^{\boldsymbol{m}_1} \ldots \delta \boldsymbol{j}(s_n)^{\boldsymbol{m}_n}}\, \exp\left[\frac{1}{2} \int_0^1 ds du\, j_i(s) \Delta_{ij}(s,u) j_j(u) \right] \Bigg|_{\boldsymbol{j}=0} . \end{aligned} \quad (40)$$

The normalization constant $\mathcal{N}$ denotes the path integral for a simple Brownian bridge. The summation convention is automatically utilized in the argument of the exponent on the last line. The Green function $\Delta_{ij}(s,u)$ is chosen so that it satisfies the equations

$$\begin{aligned} \frac{\partial^2}{\partial t^2} \Delta_{ij}(t,u) &= -\delta_{ij} \delta(t-u)\,, \\ \Delta_{ij}(0,u) &= \Delta_{ij}(1,u) = 0\,. \end{aligned} \quad (41)$$

The solution is the world-line Green function of Onofri and Zuk [40, 41]

$$\Delta_{ij}(s,u) = -\frac{1}{2} \delta_{ij} \left[|t-u| - (t + u - 2tu) \right]. \quad (42)$$

As a result, we can write $\bar{Q}(\boldsymbol{m}_1, \ldots, \boldsymbol{m}_n)$ in the form

$$\bar{Q} = \frac{\mathcal{N}}{n!} \int_0^1 ds_1 \ldots ds_n\, \frac{\delta^{|\boldsymbol{m}_1| + \ldots + |\boldsymbol{m}_n|}}{\delta \boldsymbol{j}(s_1)^{\boldsymbol{m}_1} \ldots \delta \boldsymbol{j}(s_n)^{\boldsymbol{m}_n}}\, \exp\left[\frac{1}{2} \int_0^1 dt du\, j_i(t) \Delta_{ij}(t,u) j_j(u) \right] \Bigg|_{\boldsymbol{j}=0} . \quad (43)$$

The former can be further simplified with the help of Coleman's identity:

$$F(-i\partial/\partial \boldsymbol{x})G(\boldsymbol{x}) \;=\; G(-i\partial/\partial \boldsymbol{y})F(\boldsymbol{y})e^{i\boldsymbol{y}\cdot\boldsymbol{x}}\big|_{\boldsymbol{y}=0}\,, \tag{44}$$

which is valid for any (sufficiently smooth) functions F and G. After some additional algebra one verifies that

$$\begin{aligned}\bar{Q} \;&=\; \frac{\mathcal{N}\, i^{|\boldsymbol{m}_1|+\ldots+|\boldsymbol{m}_n|}}{n!}\,\exp\left[-\frac{1}{2}\int_0^1 dtdu\,\frac{\delta}{\delta z_i(t)}\,\Delta_{ij}(t,u)\frac{\delta}{\delta z_j(u)}\right]\\ &\times\int_0^1 ds_1\ldots ds_n\,\boldsymbol{z}(s_1)^{\boldsymbol{m}_1}\ldots\boldsymbol{z}(s_n)^{\boldsymbol{m}_n}\Big|_{\boldsymbol{z}=0}\,.\end{aligned} \tag{45}$$

For similar reasons as in ordinary quantum field theory, i.e., namely for the Wick theorem application, it might be convenient to formulate the $\bar{Q}$-function in the Fourier picture. In this case the Fourier transform is discrete due to the Dirichlet boundary conditions for $\boldsymbol{\xi}$. In addition, when we periodically extend the shape of the potential V from the interval $s\in[0,1]$ to the whole $\mathbb{R}$ and take the Fourier transform the calculations of (37) will substantially simplify due to the convolution theorem [42].

Form (45) indicates that Q can be calculated via Wick's theorem with world-line Green's functions (42), cf. also Refs [5, 29, 48, 49]. In fact, it is not difficult to list the corresponding Feynman-like diagrammatic rules for $\bar{Q}(\boldsymbol{m}_1,\ldots,\boldsymbol{m}_n)$. On the other hand, the number of terms involved in evaluating $\bar{Q}$ via (45) grows as $(2\mathfrak{m}-1)!!=(2\mathfrak{m})!/2^{\mathfrak{m}}\mathfrak{m}!$ where $\mathfrak{m}=(|\boldsymbol{m}_1|+\ldots+|\boldsymbol{m}_n|)$ (see, for instance, Ref. [60]). This should be contrasted with (15) where the number of terms grows as (see Appendix B)

$$\prod_{j=1}^{D}\Big[(m_1^j+\ldots+m_n^j)/2+1\Big]\,. \tag{46}$$

Our prescription comprises substantially less terms and this is even more pronounced at high values of $\boldsymbol{m}_j$'s (i.e., at high derivative orders). In Appendix B we prove that the inequality

$$(2\mathfrak{m}-1)!!\;\geq\;\prod_{j=1}^{D}\Big[(m_1^j+\ldots+m_n^j)/2+1\Big]\,, \tag{47}$$

always holds whenever $\mathfrak{m}\geq 2$. There we also show that the number of terms is in our case exponentially lower than in Wick's theorem based approaches.

Note, also that the number of s-integrations in (45) matches the perturbation order, i.e., n, while the number of integrations in our formula (15) equals to the dimension of particles configuration space. In this respect, is the presented method less complex with the increasing perturbation order than other methods in use. As a matter of fact, with the method based on the world-line Green function, a complete calculation of all coefficients was achieved to order $\mathcal{O}(\beta^{12})$, see Ref. [50]. Closely related gradient expansion calculations (with the same order of precision) were performed in Ref. [51]

Finally, note that $\bar{Q}$ from (45) is non-zero only when $|\boldsymbol{m}_1|+\ldots+|\boldsymbol{m}_n|$ together with all partial sums $m_1^j+\ldots+m_n^j$ $(j=1,\ldots,D)$ is even. In fact, also all partial sums $m_1^j+\ldots+m_n^j$ $(j=1,\ldots,D)$ must be zero. This fact was already pointed out in Sect. II in connection with the coefficient Q. Again, the evenness is true only for smooth potentials. In the general case the space derivatives must be substituted with the generalized derivative of Schwartz [42] which can bring about also odd terms, i.e. odd powers of $\hbar$. Also other non-analytical behaviour can emerge — e.g., it was shown in [43] that exchange contributions to the free energy of the jellium vanish exponentially fast with $\hbar$ as a consequence of the Coulomb repulsion between identical charges which diverges at zero separation.

V. CONCLUSIONS AND PERSPECTIVES

In this paper we have presented a novel PI-based high-temperature expansions of the Boltzmann's density $\varrho(\boldsymbol{x},\beta)$ and partition function $Z(\beta)$. Ensuing generalizations to the full Bloch density matrix were also discussed and explicitly compared with the Onofri–Zuk world-line approach. It was found that our prescription comprises substantially less terms contributing to higher perturbation orders than the more conventional Wick's theorem based perturbation expansions. Also the algebraic complexity of the coefficient functions involved is markedly lower in our approach.

The expansions obtained are valid for arbitrary number of particles and provide an analytic control of the high-temperature behavior. In addition, the implementation is sufficiently general for any system described by smooth potential energy functions. Because of its analytic form, the presented high-temperature expansion can be further conveniently used, e.g., to analyze the breakdown of symmetry, generate a gradient expansion for the free energy for a wide class of potentials, calculate ground-state energies, set up the extended Thomas–Fermi approximations or serve as the starting point for a numerical evaluation of various thermodynamical quantities (e.g., virial coefficients, specific heat or entropy). As a demonstration, we have briefly discussed the high-temperature thermodynamics of the anharmonic oscillator.

We would like to remark that the compactness of our form for the coefficient function Q might be deceptive with regard to applications requiring the use of non-local potentials. In the genuine Wigner–Kirkwood method, the single-particle density is expressed as functional of the one-body potential $V(\boldsymbol{x})$. Though our treatment can accommodate also few-body potentials it is intrinsically formulated only for local potentials. Since non-local potentials are an integral part of statistical quantum theory, e.g. in cases when the exchange part of the Hartree–Fock self-consistent potential is considered, the corresponding generalization of Eqs. (15) and (37) to non-local potentials would be desirable. Situation is simple only for two-particle systems with potentials of the form $V(\boldsymbol{x}_1,\boldsymbol{x}_2)=V(\boldsymbol{x}_1-\boldsymbol{x}_2)$. There the transformation to the center of mass frame allows to reduce the problem to a single-particle in an external potential $V(\boldsymbol{x})$. For other cases, the formula (15) for the coefficient functions Q could be derived in the same spirit as in Section II but the appealing simplicity of Q would be clearly lost.

The versatility of the method developed in this paper together with a renewed interest in the study of the high-temperature asymptotic expansions of the Bloch density matrix suggest several extensions of this work. A pertinent extension could address spin-dependent potentials, like the spin-orbit interaction whose interest in nuclear physics is well known. Also the case of momentum dependent terms which are relevant in charged particle systems interacting with electromagnetic field or in Brueckner's theory used in nuclear physics, would be desirable to include. Important limitation of our method lies in the fact that our discussion was confined only to cases where Hamiltonians did not include fermionic degrees of freedom. Similarly as the original WK method also our approach is inherently formulated within the framework of Boltzmann statistics and so it does not incorporate the exchange effects (which are relevant, e.g., in a hot Fermionic plasma). There exist various generalizations of the WK formalism to include the effects of magnetic field [52], or exchange corrections (see, e.g., Refs. [53, 54]) and the corresponding extension of our approach in this direction would be also worth of pursuing particularly in view a naturalness with which PI's handle fermionic particle systems [5]. All these aforementioned issues are currently under active investigation.

It appears worthwhile to stressed that the WK expansion is not the WKB expansion. For instance, the leading asymptotic behaviors are different; while the WK expansion starts with $\exp(-\beta V(x))$, the WKB starts with $\exp(-\beta S[x_{\rm cl},x])$ (here the action functional S is evaluated along the classical solutions $x_{\rm cl}$ with the boundary conditions $x(0)=x(\hbar\beta)=x$). Even starting points for both these expansions were historically different. WK started with the Wigner transform approach to statistical physics [1, 2] while WKB (in PI's) started with the expansion

(in terms of moments of Gaussian fluctuations) around classical trajectory [5, 6]. It is also clear that in the WK one does not organize the expansion in terms of orders of fluctuations around classical solution (as the WKB does). Naturally, both approaches share many common features and there is a bulk of the literature comparing both methods and their respective pros and cons. The interested reader can see, e.g., Refs. [55, 56].

Let us finally make a few comments concerning the low-temperature regime. It is clear that when the temperature decreases, the de Broglie wavelength increases, and the Wigner–Kirkwood perturbation expansion becomes unwarranted. This happens whenever the involved thermal de Broglie wavelength is comparable with a typical length over which the potential varies. So the low temperature expansion is normally beyond reach of the WK method. Nevertheless, with the high-temperature expansion at one's disposal one can tackle also the low-temperature expansion (at least numerically) provided the sufficient number of the coefficient functions in the high-temperature series is available. To this end, one is free to employ some of the existent duality approaches. Among these, a particularly powerful is a nonperturbative approximation scheme called *variational* or *optimized perturbation theory* [5, 57–59]. There the basic idea is to combine the renormalization-group concept known as the *principle of minimal sensitivity* [59] with the techniques of perturbation theory and the variational principle to convert the divergent weak-coupling power series into a convergent strong-coupling power series (and vice versa).

Last but not least, recently Paulin *et al.* [28] employed the concept of the occupation time for Wiener processes to formulate the so-called *ergodic local-time approximation* to PI's. The ergodic approximation is particularly well suited for the low-temperature regime. In high-temperature domain it performs less satisfactory since the non-trivial correlations between occupation times must be taken into account [28]. Finding the dictionary that would allow a simple passage between our and Paulin *et al.* approach in the high and intermediate-temperature regimes would be particularly desirable in light of a similar mathematical structure (namely Eq. (4) that both approaches share. Work along these lines is presently in progress.

Acknowledgments

We would like to acknowledge helpful feedbacks from J. Klauder, H. Kleinert and C. Schubert. This work was supported by GAČR Grant No. P402/12/J077.

Appendix A: Simplification of coefficients $Q(\boldsymbol{m}_1, \ldots, \boldsymbol{m}_n)$

Here we employ a convenient trick that will allow us to can carry out the s-integrations in (11) explicitly. We first formally promote the upper limit of the s-integrations (i.e., 1) to a new variable s_{n+1}, and Laplace-transform Q with respect to s_{n+1}, i.e.

$$\begin{aligned}\widetilde{Q}(E) \;&=\; \int_0^\infty ds_{n+1} e^{-Es_{n+1}} \int_{0<s_1<\ldots<s_n<s_{n+1}} ds_1 \ldots ds_n \int_{\mathbb{R}^D} d\boldsymbol{y}_1 \ldots d\boldsymbol{y}_n \\ &\times \prod_{\nu=0}^{n} \langle \boldsymbol{y}_{\nu+1}| \exp\left[-(s_{\nu+1}-s_\nu)\frac{\hat{\boldsymbol{q}}^2}{2}\right] |\boldsymbol{y}_\nu\rangle\, \boldsymbol{y}_\nu^{\boldsymbol{m}_\nu} \,. \end{aligned} \tag{A1}$$

Change of variables $s'_\nu = s_{\nu+1} - s_\nu$, $\nu = 0, \ldots, n$, then leads to

$$\widetilde{Q}(E) \;=\; \int_0^\infty ds'_0 \ldots ds'_n \int_{\mathbb{R}^D} d\boldsymbol{y}_1 \ldots d\boldsymbol{y}_n \prod_{\nu=0}^{n} \langle \boldsymbol{y}_{\nu+1}| \exp\left[-s'_\nu\left(E + \frac{\hat{\boldsymbol{q}}^2}{2}\right)\right] |\boldsymbol{y}_\nu\rangle\, \boldsymbol{y}_\nu^{\boldsymbol{m}_\nu} \,. \tag{A2}$$

The s-integrations can now be done easily,

$$\widetilde{Q}(E) \;=\; \int_{\mathbb{R}^D} d\boldsymbol{y}_1 \ldots d\boldsymbol{y}_n \prod_{\nu=0}^{n} \langle \boldsymbol{y}_{\nu+1}| \, \frac{1}{E+\frac{\hat{\boldsymbol{q}}^2}{2}} \, |\boldsymbol{y}_\nu\rangle \, \boldsymbol{y}_\nu^{\boldsymbol{m}_\nu} \;. \tag{A3}$$

In order to further simplify (A3) we perform the re-scaling $\boldsymbol{y}_\nu \to \boldsymbol{y}_\nu/\sqrt{E}$, and use the fact that

$$\begin{aligned}\left\langle \frac{\boldsymbol{y}_{\nu+1}}{\sqrt{E}} \right| \frac{1}{E+\frac{\hat{\boldsymbol{q}}^2}{2}} \left| \frac{\boldsymbol{y}_\nu}{\sqrt{E}} \right\rangle \;&=\; \int_{\mathbb{R}^D} \frac{d\boldsymbol{q}}{(2\pi)^D} \frac{\exp\left(i\boldsymbol{q}\frac{\boldsymbol{y}_{\nu+1}-\boldsymbol{y}_\nu}{\sqrt{E}}\right)}{E+\frac{\hat{\boldsymbol{q}}^2}{2}} \\ &\overset{\boldsymbol{q}\to\sqrt{E}\boldsymbol{q}}{=} E^{D/2-1} \langle \boldsymbol{y}_{\nu+1}| \, \frac{1}{1+\frac{\hat{\boldsymbol{q}}^2}{2}} \, |\boldsymbol{y}_\nu\rangle \;.\end{aligned} \tag{A4}$$

This explicitly decouples E, giving rise to

$$\widetilde{Q}(E) \;=\; E^{D/2-n-1-(|\boldsymbol{m}_1|+\ldots+|\boldsymbol{m}_n|)/2} \int_{\mathbb{R}^D} d\boldsymbol{y}_1 \ldots d\boldsymbol{y}_n \prod_{\nu=0}^{n} \langle \boldsymbol{y}_{\nu+1}| \, \frac{1}{1+\frac{\hat{\boldsymbol{q}}^2}{2}} \, |\boldsymbol{y}_\nu\rangle \, \boldsymbol{y}_\nu^{\boldsymbol{m}_\nu} \;. \tag{A5}$$

Now the inverse Laplace transform can be performed and evaluated at $s_{n+1}=1$. With the help of the formula $\int_0^\infty ds\, s^\nu e^{-sE} = \Gamma(\nu+1)E^{-\nu-1}$, we obtain

$$Q \;=\; K \int_{\mathbb{R}^D} d\boldsymbol{y}_1 \ldots d\boldsymbol{y}_n \prod_{\nu=0}^{n} \langle \boldsymbol{y}_{\nu+1}| \, \frac{1}{1+\frac{\hat{\boldsymbol{q}}^2}{2}} \, |\boldsymbol{y}_\nu\rangle \, \boldsymbol{y}_\nu^{\boldsymbol{m}_\nu} \;, \tag{A6}$$

where the multiplicative factor

$$K \;=\; \frac{1}{\Gamma\left(n+1-\frac{D}{2}+\frac{|\boldsymbol{m}_1|+\ldots+|\boldsymbol{m}_n|}{2}\right)} \;. \tag{A7}$$

In the second step we invoke a resolutions of unity $\int_{\mathbb{R}^D} d\boldsymbol{y}_\nu \, |\boldsymbol{y}_\nu\rangle \langle \boldsymbol{y}_\nu| = \mathbb{I}$, which brings Q to the form

$$Q \;=\; K \langle \boldsymbol{y}_{n+1}| \, \frac{1}{1+\frac{\hat{\boldsymbol{q}}^2}{2}} \hat{\boldsymbol{y}}^{\boldsymbol{m}_n} \frac{1}{1+\frac{\hat{\boldsymbol{q}}^2}{2}} \hat{\boldsymbol{y}}^{\boldsymbol{m}_{n-1}} \cdots \frac{1}{1+\frac{\hat{\boldsymbol{q}}^2}{2}} \hat{\boldsymbol{y}}^{\boldsymbol{m}_1} \frac{1}{1+\frac{\hat{\boldsymbol{q}}^2}{2}} \, |\boldsymbol{y}_0\rangle \;. \tag{A8}$$

With the use of the algebraic identity

$$[\hat{y}_j, F(\hat{\boldsymbol{q}})] \;=\; i \left.\frac{\partial F(\boldsymbol{q})}{\partial q_j}\right|_{\boldsymbol{q}=\hat{\boldsymbol{q}}} \;, \tag{A9}$$

and the fact that $\hat{y}_j \, |\boldsymbol{y}_0\rangle = 0$, $(j=1,\ldots,D)$ we can bring (A8) to the form (recall the definition $\boldsymbol{y}_0 = \boldsymbol{y}_{n+1} = \boldsymbol{0}$)

$$Q \;=\; K \langle \boldsymbol{y}_{n+1}| \, G(\hat{\boldsymbol{q}}) \, |\boldsymbol{y}_0\rangle \;=\; K \int_{\mathbb{R}^D} \frac{d\boldsymbol{q}}{(2\pi)^D} \, G(\boldsymbol{q}) \;, \tag{A10}$$

with $G(\boldsymbol{q})$ defined as

$$G(\boldsymbol{q}) \;=\; \left(\frac{i^{|\boldsymbol{m}_n|}}{1+\frac{\boldsymbol{q}^2}{2}} \frac{\partial^{|\boldsymbol{m}_n|}}{\partial \boldsymbol{q}^{\boldsymbol{m}_n}}\right) \cdots \left(\frac{i^{|\boldsymbol{m}_1|}}{1+\frac{\boldsymbol{q}^2}{2}} \frac{\partial^{|\boldsymbol{m}_1|}}{\partial \boldsymbol{q}^{\boldsymbol{m}_1}}\right) \frac{1}{1+\frac{\boldsymbol{q}^2}{2}} \;. \tag{A11}$$

Note that we could arrive at the same conclusion by employing in (A6) the spectral expansion of the position operator (or better, its power) in both position and momentum representations, i.e.

$$\hat{\boldsymbol{y}}^{\boldsymbol{m}} \;=\; \int_{\mathbb{R}^D} d\boldsymbol{y}_\nu |\boldsymbol{y}_\nu\rangle \boldsymbol{y}_\nu^{\boldsymbol{m}} \langle \boldsymbol{y}_\nu| \;=\; \int_{\mathbb{R}^D} d\boldsymbol{q}_\nu |\boldsymbol{q}_\nu\rangle i^{|\boldsymbol{m}|} \frac{\partial^{|\boldsymbol{m}|}}{\partial \boldsymbol{q}_\nu^{\boldsymbol{m}}} \langle \boldsymbol{q}_\nu| \,. \tag{A12}$$

Ensuing lack of one δ-function then causes the residual $\boldsymbol{q}$-integration in (A10).

Appendix B: Structure of $Q(\boldsymbol{m}_1, \ldots, \boldsymbol{m}_n)$

In this appendix we show that the number of terms involved in evaluating $Q(\boldsymbol{m}_1, \ldots, \boldsymbol{m}_n)$ via (15) grows as (46). We start by observing that the function $G(\boldsymbol{q})$ in (A11) can be written as a sum

$$G(\boldsymbol{q}) \;=\; \sum_{\boldsymbol{r},s} a_{\boldsymbol{r},s} \frac{\boldsymbol{q}^{\boldsymbol{r}}}{\left(1+\frac{\boldsymbol{q}^2}{2}\right)^s} \,, \tag{B1}$$

with combinatorial factors $a_{\boldsymbol{r},s}$ whose explicit form is not not relevant for the arguments to follow. The components of multi-index $\boldsymbol{r}$ satisfy $0 \le r^j \le m_1^j + \ldots + m_n^j$ for all $j = 1, \ldots, D$ since each differentiation $\partial/\partial q_j$ can produce at most one power of q_j.

The summation index s in (B1) is not independent variable but it is fully specified once $\boldsymbol{r}$ is known. To see this, consider an elementary differentiation step

$$\frac{\partial}{\partial q^j} \frac{\boldsymbol{q}^{\boldsymbol{r}}}{\left(1+\frac{\boldsymbol{q}^2}{2}\right)^s} \;=\; \frac{r^j \boldsymbol{q}^{\boldsymbol{r}-\boldsymbol{e}_j}}{\left(1+\frac{\boldsymbol{q}^2}{2}\right)^s} - \frac{s\boldsymbol{q}^{\boldsymbol{r}+\boldsymbol{e}_j}}{\left(1+\frac{\boldsymbol{q}^2}{2}\right)^{s+1}} \,, \tag{B2}$$

where $e_j^i = \delta_{ij}$, and define Δ to be the difference between the degree of the polynomial in the denominator and the numerator. The derivative shifts Δ from $2s - |\boldsymbol{r}|$ to $2s - |\boldsymbol{r}| + 1$, and this is common to both terms on the right hand side. Hence, the nonzero terms in sum (B1) must satisfy the condition $2s - |\boldsymbol{r}| = |\boldsymbol{m}_1| + \ldots + |\boldsymbol{m}_n| + 2n + 2$. This is also evident on the dimensional ground.

We also note that due to (B2) r^j in (B1) has, for all j, the same even parity as the total degree of differentiation $m_1^j + \ldots + m_n^j$ because otherwise the integral in (A10) would vanish. Altogether, we see that there are only

$$\sum_{\boldsymbol{r},s} 1 \;=\; \prod_{j=1}^{D} \sum_{r^j=0}^{m_1^j+\ldots+m_n^j} 1 \;=\; \prod_{j=1}^{D} \Big[(m_1^j + \ldots + m_n^j)/2 + 1 \Big] \,, \tag{B3}$$

non-trivially contributing terms in (B1).

Let us close this appendix by proving the inequality (47). To this end we observe that one can write

$$\begin{aligned} (2\mathfrak{m}-1)!! \;&=\; \frac{2\mathfrak{m}!}{2^{\mathfrak{m}}\mathfrak{m}!} = \frac{1}{\sqrt{\pi}} \Gamma\Big[1/2 + \textstyle\sum_{j=1}^D (m_1^j + \ldots + m_n^j)\Big] \displaystyle\prod_{j=1}^{D} 2^{m_1^j+\ldots+m_n^j} \\ &\ge\; \prod_{j=1}^{D} 2^{m_1^j+\ldots+m_n^j} \;\ge\; \prod_{j=1}^{D} \Big[1 + (m_1^j + \ldots + m_n^j)/2\Big] \,. \end{aligned} \tag{B4}$$

On the first line we have used the duplication formula [46]: $\Gamma(z)\Gamma(z+1/2) = \sqrt{\pi}\,\Gamma(2z)2^{1-2z}$. On the second line the use was made of the inequality $\Gamma(1/2+z) \geq \sqrt{\pi}$ (valid for $z \geq 2$) and the convexity inequality $2^z - 1 \geq z\log 2 > z/2$ (valid for $z \geq 0$).

---

[1] E. Wigner, Phys. Rev. **40**, 749 (1932).
[2] J.G. Kirkwood, Phys. Rev. **44**, 31 (1933).
[3] B. Simon, *Functional Integration and Quantum Physics*, (Academic, New York, 1979).
[4] Z. Haba, *Feynman Integral and Random Dynamics in Quantum Physics; A Probabilistic Approach to Quantum Dynamics*, (Kluwer, London, 1999).
[5] H. Kleinert, *Path Integrals in Quantum Mechanics, Statistics, Polymer Physics, and Financial Markets*, 5-th edition, (World Scientific, London, 2009).
[6] J. Zinn-Justin, *Path Integrals in Quantum Mechanics*, (Oxford University Press, Oxford, 2005).
[7] W. Fischer, H. Leschke and P. Müller, J. Phys. A: Math. Gen. **25**, 3835 (1992) 3835.
[8] E.W. Brown, B.K. Clark, J.L. DuBois and D.M. Ceperley, Phys. Rev. Lett. **110**, 146405 (2013).
[9] W. Krauth, *Statistical Mechanics: Algorithms and Computations*, (Oxford University Press, Oxford, 2006)
[10] F.T. Hioe and E.W. Montroll, J. Math. Phys. **16**, 1945 (19750.
[11] F.T. Hioe, D. Machlillen and E.W. Montroll, Phys. Rep. **43**, 305 (1978).
[12] K. Banerjee, P. Bhatnager, V. Choudry and S.S. Kanwal, Proc. Roy. Soc. (London) A**360**, 575 (1978).
[13] W. Witschel, Chem. Phys. **56**, 265 (1980).
[14] M. Schwartz,Jr., J. Stat. Phys. **15**, 255 (1976).
[15] W.H. Miller, J. Chem. Phys. **55**, 3146 (1971).
[16] V.S. Jorish, V.Yu. Zitserman, Chem. Phys. Lett. **34**, 378 (1975).
[17] H.J. Korsch, J. Phys A: Math. Gen. **12**, 1521 (1979).
[18] P. Brantut, et al., Science **337**, 1069 (2012).
[19] Ch. Grenier, C. Kollath and A. Georges, [ArXiv preprint 1209.3942].
[20] G. Chabrier, D. Saumon and A. Potekhin, J. Phys. A **39**, 4411 (2006).
[21] A. Alastuey and Ph.A. Martin, Phys. Rev. A**40**, 6485 (1989); B. Jancovici, Mol Phys. **32**, 1177 (1976); M.M. Gombert and D. Léger, Phys. Rev. E**57**, 3962 (1998).
[22] M.E. Boyd, S.Y. Larsen and J.E. Kilpatrick, J. Chem. Phys. **50**, 4034 (1969).
[23] J. Cao and G.A. Voth, J. Chem. Phys. **101**, 6168 (1994).
[24] B. Militzer and D.M. Ceperley, Phys. Rev. E **63**, 066404 (2001).
[25] C. Predescu, D. Sabo and J.D. Doll, J. Chem. Phys. **119**, 4641 (2003).
[26] R. Feynman and H. Kleinert, Phys. Rev. A **34**, 5080 (1986).
[27] R. Giachetti and V. Tognetti, Phys. Rev. Lett. **55**, 912 (1985).
[28] S. Paulin, A. Alastuey and T. Dauxois, J. Stat. Phys. **128**, 1391 (2007).
[29] C. Schubert, Physics Report **355**, 73 (2001).
[30] D. Fliegner, M.G. Schmidt and C. Schubert, Z. Phys. C **64**, 11 (1994).
[31] D. Fliegner, P. Haberl, M.G. Schmidt and C. Schubert, Ann. Phys. (N.Y.) **264**, 51 (1998).
[32] A.A. Belkov, D. Ebert, A.V. Lanyov and A. Schaale, Int. J. Mod. Phys. A **8**, 1313 (1993).
[33] L. Carson, Phys. Rev. D **42**, 2853 (1990).
[34] K. Kikkawa, Prog. Theor. Phys. **56**, 947 (1976).
[35] R. MacKenzie, F. Wilczek and A. Zee, Phys. Rev. Lett. **53**, 2203 (1984).
[36] C.M. Fraser, Z. Phys. C **28**, 101 (1985).
[37] W.G. Gibson, J. Phys. A: Math. Gen. **17**, 1891 (1984).
[38] R.P. Feynman and A.R. Hibbs, *Quantum Mechanics and Path Integrals*, (McGraw-Hill, New York, 1965)
[39] B. Simon, *Functional Integration and Quantum Physics*, (Academic Press, New York, 1979).
[40] E. Onofri, Am. J. Phys. **46**, 379 (1978).
[41] J.A. Zuk, J. Phys. A **18**, 1795 (1985).
[42] see, e.g., V.S. Vladimirov, *Equations of Mathematical Physics*, (Marcel Dekker, Inc, New York,

1971).
[43] B. Jancovici, Physica A, **91** , 152 (1978).
[44] T. Kihara, Y. Midzuno and T. Shizume, J. Phys. Soc. Jpn. **10**, 249 (1955).
[45] L.D. Landau, and E. Lifschitz, *Statistical Physics*, (Pergamon, Elmsford, 1980).
[46] I.S. Gradshteyn and I.M. Ryzhik, *Table of Integrals, Series, and Products*, 7-th edition, (Elsevier, New York, 2007).
[47] See supplementary material at [...] for WOLFRAM MATHEMATICA notebook `expansion1D.nb` that implements the formulas (26) and (27), and allows to insert a specific (smooth) potential $V(x)$. The expansion up to order β^{18} is available in the file `expansion1D18orders.m`, and is imported automatically into the `.nb` notebook.
[48] Z. Bern and D.A. Kosower, Phys. Rev. Lett. **66**, 1669 (1991); Nucl. Phys. B **379**, 451 (1992).
[49] M.J. Strassler, Nucl. Phys. B **385**, 145 (1992).
[50] D. Fliegner, P. Haberl, M.G. Schmidt, C. Schubert, Ann. Phys. (N.Y.) **264**, 51 (1998).
[51] D. Fliegner, M.G. Schmidt and C. Schubert, Z. Phys. C **64**, 111 (1994).
[52] A. Alastuey and B. Jancovici, Physica A: Stat. Mech. **97**, 349 (1979).
[53] L. Wang, Plasma Phys. Control. Fusion **29**, 395 (1987).
[54] J. Caro, E. Ruiz Arriola and L.L. Salcedo, J. Phys. G **22**, 981 (1996).
[55] T.A. Osborn and F.H. Molzahn, Phys. Rev. A**34**, 1696 (1986).
[56] M. Durand, P. Schuck and X. Viñas, Phys. Rev. A**36**, 1824 (1987).
[57] H. Kleinert, Phys. Lett. A **173**, 332 (1993).
[58] C.M. Bender, K.A. Milton, M. Moshe, S.S. Pinsky and L.M. Simmons Jr., Phys. Rev. Lett. **58**, 2615 (1987).
[59] P.M. Stevenson, Phys. Rev. D**23**, 2916 (1981).
[60] M. Blasone, P. Jizba and G. Vitiello, *Quantum Field Theory and its Macroscopic Manifestations* (Imperial College Press, London, 2011).

B Full article: Local-time representation of path integrals

Journal reference:
P. Jizba and V. Zatloukal, *Local-time representation of path integrals*, Phys. Rev. E **92**, 062137 (2015) [arXiv:1506.00888].

The origins of this work date back to my two-month stay at ENS Lyon in the year 2012, where I was supervised by Prof. Angel Alastuey. Indeed, many of his inspiring ideas are engraved into this article.

Local-time representation of path integrals

Petr Jizba[1,*] and Václav Zatloukal[2,†]

[1,2] *FNSPE, Czech Technical University in Prague, Břehová 7, 115 19 Praha 1, Czech Republic*

[1] *ITP, Freie Universität in Berlin, Arnimallee 14, D-14195 Berlin, Germany*

[2] *Max Planck Institute for the History of Science, Boltzmannstrasse 22, D-14195 Berlin, Germany*

Abstract

We derive a local-time path-integral representation for a generic one-dimensional time-independent system. In particular, we show how to rephrase the matrix elements of the Bloch density matrix as a path integral over x-dependent local-time profiles. The latter quantify the time that the sample paths $x(t)$ in the Feynman path integral spend in the vicinity of an arbitrary point x. Generalization of the local-time representation that includes arbitrary functionals of the local time is also provided. We argue that the results obtained represent a powerful alternative to the traditional Feynman–Kac formula, particularly in the high and low temperature regimes. To illustrate this point, we apply our local-time representation to analyze the asymptotic behavior of the Bloch density matrix at low temperatures. Further salient issues, such as connections with the Sturm–Liouville theory and the Rayleigh–Ritz variational principle are also discussed.

I. INTRODUCTION

The path integral (PI) has been used in quantum physics since the revolutionary work of Feynman [1], although the basic observation goes back to Dirac [2, 3] who appreciated the rôle of the Lagrangian in short-time evolution of the wave function, and even suggested the time-slicing procedure for finite, i.e., non-infinitesimal, time lags. Since then the PI approach yielded invaluable insights into the structure of quantum theory [4] and provided a viable alternative to the traditional operator-formalism-based canonical quantization. During the second half of the 20th century, the PI became a standard tool in quantum field theory [5] and statistical physics [6], often providing the easiest route to derivation of perturbative expansions and serving as an excellent framework for (both numerical and analytical) non-perturbative analysis [7].

Feynman PI has its counterpart in pure mathematics, namely, in the theory of continuous-time stochastic processes [8]. There the concept of integration over a space of continuous functions (so-called fluctuating paths or sample paths) had been introduced by Wiener [9] already in 1920's in order to represent and quantify the Brownian motion. Interestingly enough, this so-called

*Electronic address: p.jizba@fjfi.cvut.cz
†Electronic address: zatlovac@fjfi.cvut.cz

Wiener integral (or integral with respect to Wiener measure) was formulated 2 years before the discovery of the Schrödinger equation and 25 years before Feynman's PI formulation.

The *local time* for a Brownian particle (in some literature also called *sojourn time*) has been of interest to physicists and mathematicians, since the seminal work of Paul Lévy in 1930's [11]. In its essence, the local time characterizes the time that a sample trajectory $x(t)$ of a given stochastic process spends in the vicinity of an arbitrary point X. This in turn defines a sample trajectory L^X of a new stochastic process. A rich theory has been developed for local-time processes that stem from diffusion processes (see, e.g., Ref. [12] and citations therein). For later convenience, we should particularly highlight the Ray–Knight theorem which states that the local time of the Wiener process can be expressed in terms of the squared Bessel process [13–15]. In contrast to mathematics, the concept of the local time is not uniquely settled in physics literature. Various authors define essentially the same quantity under different names (local time, occupation time, traversal time, etc.), and with different applications in mind. For example, in Ref. [16] the *traversal time* is used to study quantum scattering and tunneling processes, in [17] the small-temperature behavior of the equilibrium density matrix is analyzed with a help of the *occupation time*, while in Ref. [18] the large-time behavior of path integrals that contain functionals of the *local time* is discussed.

The aim of this paper is to derive a local-time PI representation of the Bloch density matrix, i.e., the matrix elements $\langle x_b|\, e^{-\beta\hat{H}}\, |x_a\rangle$ of the Gibbs operator. This can serve not only as a viable alternative to the commonly used Feynman–Kac representation but also as a powerful tool for extracting both large and small-temperature behavior. Apart from the general theoretical outline, our primary focus here will be on the low-temperature behavior which is technically more challenging than the large-temperature regime. In fact, the large-temperature expansion was already treated in some detail in our previous paper [21]. Last but not least, we also wish to promote the concept of the local time which is not yet sufficiently well known among the path-integral practitioners.

The structure of the paper is as follows. To set the stage we recall in the next section some fundamentals from the Feynman PI which will be needed in later sections. In Section III we provide motivation for the introduction of a local time, and construct a heuristic version of the local-time representation of PI's. The key technical part of the article is contained in Section IV, where we derive by means of the replica trick the local-time representation of the Bloch density matrix. Relation to the Sturm–Liouville theory is also highlighted in this context. A local-time analog of the Feynman–Matthews–Salam formula [19, 20] is presented in Section V and its usage is illustrated with a computation of the one-point distribution of the local time. Since a natural arena for local-time PI's is in thermally extremal regimes, we confine our attention in Section VI on large- and small-β asymptotic behavior of the Bloch density matrix. There we also derive an explicit leading-order behavior in large-β (i.e., low-temperature) expansion. The analysis is substantially streamlined by using the Laplace asymptotic formula and the Rayleigh–Ritz variational principle. Finally, Section VII summarizes our results and discusses possible extensions, applications, and future developments of the present work. For the reader's convenience the paper is supplemented with two appendices which clarify some finer technical details.

II. PATH-INTEGRAL REPRESENTATION OF THE BLOCH DENSITY MATRIX

Consider a non-relativistic one-dimensional quantum-mechanical system described by a time-independent Hamiltonian $\hat{H} = \frac{\hat{p}^2}{2M} + V(\hat{x})$ where $\hat{p}\,|x\rangle = -i\hbar\partial_x\,|x\rangle$. Throughout this paper we will study the matrix elements

$$\rho(x_a, x_b, \beta) \;\equiv\; \langle x_b|\, e^{-\beta\hat{H}}\, |x_a\rangle \;, \tag{1}$$

of the Gibbs operator $e^{-\beta\hat{H}}$, where $\beta = 1/(k_B T)$ is the inverse temperature and k_B is the Boltzmann constant. The matrix $\rho(x_a, x_b, \beta)$, known also as the Bloch density matrix, is a fundamental object in quantum statistical physics, as the expectation value of an operator $\hat{O}$ at the temperature T can be written in the form

$$\langle \hat{O} \rangle \;=\; \frac{1}{Z} \int_{\mathbb{R}} \int_{\mathbb{R}} dx_a dx_b \; \rho(x_a, x_b, \beta) \, \langle x_b | \hat{O} | x_a \rangle \,, \tag{2}$$

where $Z = \int_{\mathbb{R}} dx \; \rho(x, x, \beta)$ is the partition function of the system. In case of need, ensuing quantum mechanical transition amplitudes can be obtained from (1) via a Wick rotation which formally amounts to the substitution $\beta \to it/\hbar$, converting thus the Gibbs operator $e^{-\beta\hat{H}}$ to the quantum evolution operator $e^{-it\hat{H}/\hbar}$.

The matrix elements in Eq.(1) can be represented via the path integral as [4, 7]

$$\rho(x_a, x_b, \beta) \;=\; \int_{x(0)=x_a}^{x(\beta\hbar)=x_b} \mathcal{D}x(\tau) \exp\left\{ -\frac{1}{\hbar} \int_0^{\beta\hbar} d\tau \left[\frac{M}{2} \dot{x}^2 + V(x) \right] \right\} . \tag{3}$$

This represents a "sum" over all continuous trajectories $x(\tau)$, $\tau \in [0, \beta\hbar]$, connecting the initial point $x(0) = x_a$ with the final point $x(\beta\hbar) = x_b$. It should be noted that the integral $\int_0^{\beta\hbar} d\tau \left[\frac{M}{2} \dot{x}^2 + V(x) \right]$ is the classical Euclidean action integral along the path $x(\tau)$ with $0 < \tau \leq \beta\hbar$. In the following we will denote the Euclidean action as $\mathcal{A}$. The integrand in $\mathcal{A}$, i.e., $(M/2)\dot{x}^2(\tau) + V(x(\tau))$, can be identified with the classical Hamiltonian function, in which the momentum p is substituted for $M\dot{x}$. One can also regard (3) as an expectation value of the functional $\exp[-\int_0^{\beta\hbar} d\tau \, V(x(\tau))/\hbar]$ over the (driftless) Brownian motion with the diffusion coefficient $M/2\hbar$, and duration $\beta\hbar$, that starts at point x_a, and terminates at x_b. The latter stochastic process is also known as Brownian bridge.

III. LOCAL-TIME REPRESENTATION OF PATH INTEGRALS: HEURISTIC APPROACH

The purpose of this section is twofold. Firstly, we would like to motivate a need for reformulation of PI's in the language of local-time stochastic process. In particular, we point out when such a reformulation can be more pertinent than the conventional "sum over histories" prescription. Secondly, we wish to outline a heuristic construction of the local-time representation of PI's. More rigorous and explicit (but less intuitive) formulation of PI's over ensemble of local times will be presented in the subsequent Section.

To provide a physically sound motivation for the local-time representation of PI's we follow exposition of Paulin *et al.* in Ref. [17]. To this end we first consider the diagonal elements of the Bloch density matrix, i.e., $\rho(x_a, x_a, \beta)$ (often referred to as the Boltzmann density). Upon shifting $x \to x + x_a$, and setting $x = \lambda\xi$, $\tau = s\beta\hbar$ ($\lambda \equiv \sqrt{\beta\hbar^2/M}$ is the thermal de Broglie wavelength), the PI (3) can be reformulated in terms of dimensionless quantities s and $\xi(s)$ as

$$\rho(x_a, x_a, \beta) \;=\; \frac{1}{\lambda} \int_{x(0)=0}^{x(1)=0} \mathcal{D}\xi(s) \, \exp\left\{ -\int_0^1 ds \left[\frac{1}{2} \dot{\xi}^2 + \beta V(x_a + \lambda\xi) \right] \right\} . \tag{4}$$

Note in particular, that in contrast to $\mathcal{D}x(\tau)$ the measure $\mathcal{D}\xi(s)$ does not explicitly depend on β, and thus β-dependent parts in the PI are under better control. Such a rescaled representation is particularly useful when discussing large- and/or small-β behavior of the path integral in question. Path fluctuations in the potential are controlled by $\lambda \propto \sqrt{\beta}$, and the factor β quantifies the significance of the potential V with respect to the kinetic term.

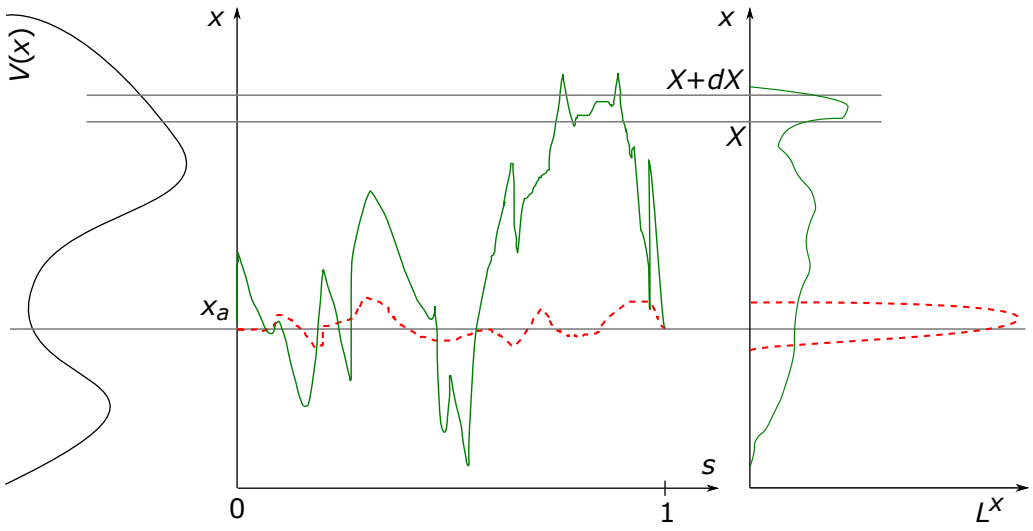

FIG. 1: In the middle, two typical paths $x(s\beta\hbar) = x_a + \lambda\xi(s)$ are plotted as functions of the dimensionless time s. The solid green path, representing a typical trajectory with a high value of β, exhibits large fluctuations, whereas the dashed red path, corresponding to small β, stays in the vicinity of the initial and final point x_a. On the right, two local-time profiles $L(x)$ are shown. The broad one (solid green) arises from the violently fluctuating path $x(s\beta\hbar)$, whereas the narrow one (dashed red) corresponds to the path with small fluctuations. On the left, we depict a generic potential $V(x)$.

For small β (i.e., high temperature), typical paths $x(s\beta\hbar) = x_a + \lambda\xi(s)$ stay in the vicinity of the point x_a, as depicted in Fig. 1, and therefore a systematic Wigner–Kirkwood expansion can be readily developed by Taylor-expanding the potential part of the action [21].

When β is large (i.e., low temperature), the trajectories $x(s\beta\hbar)$ fluctuate heavily around the value x_a, and the potential term V dominates over the kinetic one. From the statistical physics point of view, the most important contribution to the low temperature behavior of the path integral (4) should come from those paths that spend a sizable amount of time near the *global* minimum of the potential $V(x)$. For this reason, it is important to be able to keep track of the time which a given path spends in an infinitesimal neighborhood of an arbitrary point x.

Let us define, for each Wiener trajectory $x(\tau)$ present in the Feynman path integral (3) the ensuing *local time* as

$$L^X(\tau) \;=\; \int_0^\tau d\tau'\, \delta(X - x(\tau'))\;. \tag{5}$$

Since the local time $L^X(\tau)$ is a functional of the random trajectory $x(\tau')$ for $0 < \tau' < \tau$, it represents a random variable. From the definition (5) we can immediately see that $L^X \geq 0$ for all $X \in \mathbb{R}$, $\int_{\mathbb{R}} dX\, L^X(\tau) = \tau$ and that L^X has a compact support. In addition, it can be proved [8, 12] that local-time trajectories L^X are, with probability one, continuous curves which (similarly as trajectories in the underlying Wiener process) are nowhere differentiable. In Fig. 1 we depict two examples of representative local-time trajectories. An extensive mathematical discussion of properties of the local time can be found, e.g. in Refs. [12, 13].

With the definition (5) the potential part of the Euclidean action can be recast into form $\int_{\mathbb{R}} dX\, L^X(\beta\hbar)V(X)$. A local-time representation of the Bloch density matrix $\rho(x_a, x_b, \beta)$ is then

given by

$$\rho(x_a, x_b, \beta) \;=\; \int \mathcal{D}L^x\, \mathcal{W}[L; \beta, x_a, x_b]\, \delta\Bigg(\int_{\mathbb{R}} dX\, L^X - \beta\hbar\Bigg) \exp\left[-\frac{1}{\hbar}\int_{\mathbb{R}} dX\, L^X V(X)\right], \qquad (6)$$

where the PI "sum" is taken over all local-time trajectories L^x, with x being the independent variable (not to be mistaken with the Wiener trajectory $x(\tau)$). The δ-function enforces the normalization constraint mentioned above. Basically, transition to the local-time description represents a change (or a functional substitution) of stochastic variables $x(\tau) \to L^x(\beta\hbar)$. The weight factor $\mathcal{W}$ appearing in (6) can be formally written in the form

$$\mathcal{W}[L; \beta, x_a, x_b] \;=\; \exp\left[-\frac{1}{\hbar}\int_0^{\beta\hbar} d\tau\, \frac{M}{2}\dot{x}^2\right] \det\left(\frac{\delta L^x(\beta\hbar)}{\delta x(\tau)}\right)^{-1}. \qquad (7)$$

It is a function of x_a, x_b (which are implicitly present in $L^x(\beta\hbar)$) and β, and a functional of the local time L^x. Of course, these cavalier manipulations do not have more than a heuristic nature, and it is, indeed, a non-trivial task to determine $\mathcal{W}$ directly from (7). For this reason, we will in the following Section tackle this problem indirectly.

IV. LOCAL-TIME REPRESENTATION OF PATH INTEGRALS: DERIVATION

In this Section, we present a derivation of the local-time representation of the Bloch density matrix (1). Initially, we limit ourselves to considering the case of the diagonal part, $x_b = x_a$, and arrive at the key result (16), which expresses the matrix elements in the ensuing Laplace picture with respect to β. This intermediate outcome is shown to agree with the Sturm–Liouville theory. In the next step, we generalize the latter result to the off-diagonal elements ($x_b \neq x_a$). The inverse Laplace transform will then yield the sought local-time representation of PI [cf. Eq. (28)].

A. Field-theoretic representation

It follows from the definition (1) that the function $\rho(x_a, x_b, \beta)$ satisfies the heat equation

$$\left[\frac{\partial}{\partial\beta} - \frac{\hbar^2}{2M}\frac{\partial^2}{\partial x_b^2} + V(x_b)\right]\rho(x_a, x_b, \beta) \;=\; 0\,, \qquad (8)$$

with the initial condition $\rho(x_a, x_b, 0_+) = \delta(x_a - x_b)$. This is merely a Wick-rotated ($t \to -i\hbar\beta$) analogue of the Schrödinger equation. The Feynman–Kac formula [1, 10, 34] then ensures that the PI (3) can be calculated by solving corresponding parabolic differential equation (8).

In the Laplace picture Eq. (8) takes the form

$$\left[E - \frac{\hbar^2}{2M}\frac{\partial^2}{\partial x_b^2} + V(x_b)\right]\widetilde{\rho}(x_a, x_b, E) \;=\; \delta(x_a - x_b)\,, \qquad (9)$$

with $\widetilde{\rho}(x_a, x_b, E) \;=\; \int_0^\infty d\beta e^{-\beta E}\rho(x_a, x_b, \beta)$. Eq. (9) implies that $\widetilde{\rho}$ is nothing but the Green function of the operator $E + \hat{H}$. With the benefit of hindsight, we represent the Green function $\widetilde{\rho}$ as a path integral over fluctuating fields — so-called functional integral [5]. This is rather standard strategy in Quantum Field Theory [6, 20], and in our case it yields

$$\widetilde{\rho}(x_a, x_b, E) \;=\; \frac{\int_{\psi(X_-)=0}^{\psi(X_+)=0} \mathcal{D}\psi(x)\, \psi(x_a)\psi(x_b)\, e^{-\frac{1}{2}\mathcal{A}^E[\psi]}}{\int_{\psi(X_-)=0}^{\psi(X_+)=0} \mathcal{D}\psi(x)\, e^{-\frac{1}{2}\mathcal{A}^E[\psi]}}\,, \qquad (10)$$

where

$$\mathcal{A}^E[\psi] \;\equiv\; \int_{X_-}^{X_+} dx\,\psi(x)\left[-\frac{\hbar^2}{2M}\frac{d^2}{dx^2}+V(x)+E\right]\psi(x)$$

$$=\; \int_{X_-}^{X_+} dx\left[\frac{\hbar^2}{2M}\psi'(x)^2+(V(x)+E)\psi(x)^2\right], \tag{11}$$

is the Euclidean action functional of the field-theoretic path integral. The super-index "E" in $\mathcal{A}$ indicates the shift in the potential $V(x)$ by the amount E. Here, we have confined our quantum-mechanical system within a finite box $[X_-, X_+]$, with $X_- \ll \min\{x_a, x_b\}$ and $X_+ \gg \max\{x_a, x_b\}$. A real scalar field $\psi(x)$ satisfies Dirichlet boundary conditions $\psi(X_-) = \psi(X_+) = 0$ so as to ensure the validity of the operations being performed.

B. Replica trick

Since we will ultimately want to invert the Laplace transform to regain from $\widetilde{\rho}(x_a, x_b, E)$ the original Bloch density matrix $\rho(x_a, x_b, \beta)$, we cannot treat the denominator in (10) as an irrelevant normalization constant (which is the usual practice in Quantum Field Theory) but we have to take care of its E-dependence. To this end we take advantage of the formula

$$\frac{a}{b} \;=\; \lim_{D\to 0} ab^{D-1}\,, \tag{12}$$

which is a simple version of the so-called *replica trick*. [The usual replica-trick formula (cf. e.g., Ref. [35]) can be obtained from (12) by integrating both sides with respect to b and subsequently dividing by a.] With the help of (12) we can rewrite (10) as a multidimensional functional integral

$$\widetilde{\rho}(x_a, x_b, E) \;=\; \lim_{D\to 0}\frac{2}{D}\int_{\boldsymbol{\psi}(X_-)=\mathbf{0}}^{\boldsymbol{\psi}(X_+)=\mathbf{0}} \mathcal{D}\boldsymbol{\psi}(x)\,\boldsymbol{\psi}(x_a)\cdot\boldsymbol{\psi}(x_b)\,e^{-\sum_{\sigma=1}^{D}\mathcal{A}^E[\psi_\sigma]}\,, \tag{13}$$

where the multiplet $\boldsymbol{\psi} = (\psi_1, \ldots, \psi_D)$ is a D-component "replica" field in $1+0$ dimensions, $\boldsymbol{\psi}(x_a)\cdot\boldsymbol{\psi}(x_b)$ denotes the scalar product $\sum_{\sigma=1}^{D}\psi_\sigma(x_a)\psi_\sigma(x_b)$, and we have rescaled the fields by a factor of $\sqrt{2}$ in passing. The factor $1/D$ results from a PI generalization of the well know mean-value identity $\langle x_i\, y_i\rangle = \langle \mathbf{x}\cdot\mathbf{y}\rangle/D$ valid for any two vectors in D-dimensional statistically isotropic environments.

As a side remark, note that we may now invert the Laplace transform, using the trivial identity

$$\int_0^\infty d\beta\, e^{-\beta E}\delta(\beta - c) \;=\; e^{-cE} \qquad \text{for} \quad c \;>\; 0\,, \tag{14}$$

to obtain the representation

$$\rho(x_a, x_b, \beta) \;=\; \lim_{D\to 0}\frac{2}{D}\int_{\boldsymbol{\psi}(X_-)=\mathbf{0}}^{\boldsymbol{\psi}(X_+)=\mathbf{0}} \mathcal{D}\boldsymbol{\psi}\,\boldsymbol{\psi}(x_a)\cdot\boldsymbol{\psi}(x_b)\,\delta\left(\int_{X_-}^{X_+}\boldsymbol{\psi}(x)^2 dx - \beta\right) e^{-\sum_{\sigma=1}^{D}\mathcal{A}^{E=0}[\psi_\sigma]}\,. \tag{15}$$

Upon scaling $\boldsymbol{\psi} \to \sqrt{\beta}\boldsymbol{\psi}$, this agrees with the formula (2.9) in Ref. [18]. Though the result (15) generalizes to arbitrary number of dimensions of the x-space, i.e., $x \in \mathbb{R}^d$, our further development will be illustrated (for simplicity's sake) only on the one-dimensional case.

C. Connection with radial harmonic oscillator

In order to derive the weight factor $\mathcal{W}$ (cf. Eq. (7)) we have arrived at the representation (15) with D replica fields. This form is still not very transparent, and a further simplification step is needed to get rid of an explicit dependence of the measure on D. To this end, we note that $\sum_{\sigma=1}^{D} \mathcal{A}^E[\psi]$ is in fact the action of a D-dimensional harmonic oscillator with the "time" variable x, "position" variable ψ, mass $\hbar^2/M$, and time-dependent "frequency" $V(x)+E$. Considering for a moment only diagonal matrix elements, $x_b = x_a$, spherical symmetry in the replica field space allows to reduce the path integral (13) to its radial part. Due to the boundary conditions, $\boldsymbol{\psi}(X_-) = \boldsymbol{\psi}(X_+) = \mathbf{0}$, only the zero-angular-momentum (s-wave) contribution is non-vanishing (generally a weighted sum over radial PI's with different angular momenta would be required). This will be rigorously justified at the end of this Section. The corresponding *radial* PI representation for (13) reads [6, 7, 24]

$$\widetilde{\rho}(x_a, x_a, E) \;=\; \lim_{D\to 0} \frac{2}{D\Omega(D)} \lim_{\eta_\pm \to 0} (\eta_- \eta_+)^{\frac{1-D}{2}} \int_{\eta(X_-)=\eta_-}^{\eta(X_+)=\eta_+} \mathcal{D}\eta(x)\, \eta^2(x_a)\, e^{-A_D^E[\eta]}\,. \tag{16}$$

Here, the radial part $\eta \equiv \sqrt{\boldsymbol{\psi}^2}$ of the D-dimensional replica field $\boldsymbol{\psi}$ is always non-negative, i.e., $\eta(x) \geq 0$; the area of a unit sphere in D dimensions, $\Omega(D) = 2\pi^{D/2}/\Gamma(D/2)$, may be replaced by its small-D asymptotic form $\Omega(D) \sim D$; and $\eta_\pm$ have been introduced to regularize the origin of the $\boldsymbol{\psi}$-space. The new action functional

$$\mathcal{A}_D^E[\eta] \;\equiv\; \mathcal{A}^E[\eta] \;+\; \int_{X_-}^{X_+} dx\, \frac{M}{\hbar^2} \frac{(D-1)(D-3)}{8\eta^2(x)}\,, \tag{17}$$

is the Euclidean action functional of the *radial harmonic oscillator* [7, 24, 36]. It contains an additional centrifugal potential term (Edwards–Gulyaev or Langer term [7, 25, 37]), which emerges from Bessel function $I_{D/2-1}$ present in the finite sliced form of the radial PI (16). At this point we should stress that in contrast to the quantum-mechanical radial PI, one can use safely the asymptotic expansion for the Bessel function $I_{D/2-1}$ (see, e.g. Ref. [33]):

$$\begin{aligned} I_\mu(y_j) \;&\sim\; \frac{1}{\sqrt{2\pi y_j}}\, e^{y_j - (\mu^2-1/4)/2y_j}\,, \qquad (|y_j| \gg 1,\ \mathrm{Re}[y_j] > 0)\,, \\ y_j \;&=\; (M/\varepsilon\hbar) r_j r_{j-1}\,, \end{aligned} \tag{18}$$

in the Euclidean PI sliced form. Here the infinitesimal "time" slice ε is related to the number of slices N via the relation $\varepsilon = \hbar\beta/N$. In quantum mechanic this is a problematic step because (18) requires $\mathrm{Re}[y_j] > 0$ while there $\mathrm{Re}[y_j] = \mathrm{Re}[(M/i\varepsilon\hbar) r_j r_{j-1}] = 0$.

Fortunately, the PI for radial harmonic oscillator is exactly solvable even in the case of x-dependent oscillator frequency. The solution reads [24]

$$\begin{aligned} (\eta_2 x_2 | \eta_1 x_1)_D \;&\equiv\; \int_{\eta(x_1)=\eta_1}^{\eta(x_2)=\eta_2} \mathcal{D}\eta(x) \exp\left\{ -\int_{x_1}^{x_2} dx \left[\frac{\hbar^2}{2M}\eta'^2 + (V(x)+E)\eta^2 + \frac{M}{\hbar^2}\frac{(D-1)(D-3)}{8\eta^2} \right] \right\} \\ &=\; \frac{\hbar^2}{M} \frac{\sqrt{\eta_1\eta_2}}{G(x_1)} I_{D/2-1}\left(\frac{\hbar^2}{M} \frac{\eta_1\eta_2}{G(x_1)} \right) \exp\left[-\frac{\hbar^2}{2M} \left(\frac{F'(x_2)}{F(x_2)}\eta_2^2 - \frac{G'(x_1)}{G(x_1)}\eta_1^2 \right) \right]. \end{aligned} \tag{19}$$

The functions $F(x)$ and $G(x)$ are two independent solutions of the differential equation

$$\left[\hat{H} + E\right] y(x) \;=\; \left[-\frac{\hbar^2}{2M}\frac{d^2}{dx^2} + V(x) + E \right] y(x) \;=\; 0\,, \tag{20}$$

with the initial conditions $F(x_1) = 0$ and $F'(x_1) = 1$, and $G(x_2) = 0$ and $G'(x_2) = -1$. In addition, the Wronskian $W(F,G) \equiv F(x)G'(x) - F'(x)G(x)$ is independent of x, as can be proved by differentiation and by using the fact that F and G both satisfy Eq. (20). By equating the values of $W(F,G)$ at points x_1 and x_2, and taking into account the initial conditions for F and G, we find a useful identity $F(x_2) = G(x_1)$.

Now, the PI in (16) can be sliced at point x_a, and expressed as

$$\widetilde{\rho}(x_a, x_a, E) \;=\; \int_0^\infty d\eta_a \, (\eta_+ X_+ | \eta_a x_a)_D \, \eta_a^2 \, (\eta_a x_a | \eta_- X_-)_D \, . \tag{21}$$

The limits in Eq. (16) are readily carried out with the help of the asymptotic formulas $I_{D/2-1}(z) \sim (z/2)^{D/2-1}/\Gamma(D/2)$, and $\Gamma(z) \sim 1/z$, valid for $z \to 0_+$. Subsequent integration over η_a brings (16) to form

$$\widetilde{\rho}(x_a, x_a, E) \;=\; -\frac{2M}{\hbar^2} \frac{F_1(x_a) G_2(x_a)}{F_1(x_a) G_2'(x_a) - F_1'(x_a) G_2(x_a)} \, , \tag{22}$$

where $F_1(x)$ solves Eq. (20) with initial conditions $F_1(X_-) = 0$ and $F_1'(X_-) = 1$, and $G_2(x)$ solves the same equation with $G_2(X_+) = 0$ and $G_2'(X_+) = -1$. The denominator in (22) is the Wronskian $W(F_1, G_2)$. The full derivation is given in Appendix A.

Although rather explicit, Eq. (22) is not well suited for the Laplace transform inversion, since functions $F(x)$ and $G(x)$ contain E in a non-trivial way, which, in addition, significantly hinges on the actual form of $V(x)$. For formal manipulations it is still better the employ the PI representation (16). For instance, using Eq. (14) we can easily invert the Laplace transform to return from E back to the β-variable, namely

$$\rho(x_a, x_a, \beta) = \lim_{D\to 0} \frac{2}{D^2} \lim_{\eta_\pm \to 0} (\eta_- \eta_+)^{\frac{1-D}{2}} \int_{\eta(X_-)=\eta_-}^{\eta(X_+)=\eta_+} \mathcal{D}\eta(x) \, \eta^2(x_a) \, \delta\!\left(\int_{X_-}^{X_+} \eta^2 dx - \beta \right) e^{-A_D^{E=0}[\eta]} \, . \tag{23}$$

Note that we have utilized the asymptotic form $\Omega(D) \sim D$ which holds for $D \ll 1$. We shall see shortly that (23) can be straightforwardly related to the local-time PI representation of the Boltzmann density matrix.

Let us finally comment on the higher-angular-momentum terms which, as claimed, should not contribute to the expression (16). For arbitrary angular momentum $\ell \geq 0$, we employ formula (19) with a slight modification $D \to D + 2\ell$. Now, for example, in the limit $\eta_- \to 0$, this goes like $(\eta_a x_a | \eta_- X_-)_{D+2\ell} \propto \eta_-^{\ell + D/2 - 1/2}$, which, multiplied by the prefactor $\eta_-^{1/2-D/2}$, implies the behavior $\sim \eta_-^\ell$. That is, only the $(\ell = 0)$-term can give a non-vanishing contribution.

D. Connection with the Sturm–Liouville problem

Consider again Eq. (9) and a finite interval $x \in [X_-, X_+]$. The corresponding Green function of the operator $\hat{H} + E$ can be easily constructed (at least formally) with the help of the Sturm–Liouville theory [22, 23]. An immediate consequence of the latter is that for $x_a < x_b$ the Green function has the form

$$\widetilde{\rho}(x_a, x_b, E) \;=\; -\frac{2M}{\hbar^2} \frac{F(x_a) G(x_b)}{W(F,G)} \, , \tag{24}$$

where the functions $F(x)$ and $G(x)$ satisfy Eq. (20) with the initial conditions $F(X_-) = 0$ and $F'(X_-) = 1$, and $G(X_+) = 0$ and $G'(X_+) = -1$, respectively. In addition, the above Green function should be symmetric due to the Hermitian nature of $\hat{H}$.

The Sturm–Liouville theory ensures that the solution to the second-order differential equation (20) is unique, when specifying the values of $y(x_0)$ and $y'(x_0)$ at some point x_0. Therefore, the functions F and G must coincide with F_1 and G_2 of Eq. (22), and the diagonal part of (24), i.e., $\widetilde{\rho}(x_a, x_a, E)$, reduces to expression (22). This is an important consistency check of our representation (16).

E. Extension to off-diagonal matrix elements

Let us now generalize the PI representation (16) to the full Bloch density matrix, i.e., we wish to include also the off-diagonal matrix elements, $x_b \neq x_a$. If we go back to the replica representation (13), we realize that the requirement $x_b \neq x_a$ spoils rotational symmetry in the replica field space, and thus precludes straightforward reduction to a radial path integral. Instead of refining the reduction procedure, we simply make a guess, which, as we prove in Appendix A, coincides with the well-established Sturm–Liouville formula (24). Our guess is based on mathematical results presented in [13]. In particular, we claim that the extension of the representation (16) to off-diagonal matrix elements should read

$$\widetilde{\rho}(x_a, x_b, E) = \lim_{D\to 0} \frac{2}{D^2} \lim_{\eta_\pm \to 0} (\eta_- \eta_+)^{\frac{1-D}{2}} \int_{\eta(X_-)=\eta_-}^{\eta(X_+)=\eta_+} \mathcal{D}\eta(x)\, \eta(x_a)\eta(x_b)\, e^{-\mathcal{A}^E_\Delta[\eta]}\,, \tag{25}$$

with the action functional

$$\mathcal{A}^E_\Delta[\eta] \;\equiv\; \mathcal{A}^E[\eta] \;+\; \int_{X_-}^{X_+} dx\, \frac{M}{\hbar^2} \frac{\Delta(x)}{8\eta^2(x)}\,, \tag{26}$$

where $\mathcal{A}^E[\eta]$ is defined in Eq. (11), and $\Delta(x)$ is a piecewise constant function

$$\Delta(x) = \begin{cases} -1 & \text{for } x \in [x_a, x_b] \\ (D-1)(D-3) & \text{otherwise.} \end{cases} \tag{27}$$

At this point we can invert the Laplace transform with the help of Eq. (14). As a result, we obtain the sought local-time PI representation of the Bloch density matrix (1), namely

$$\rho(x_a, x_b, \beta) = \lim_{D\to 0} \frac{2}{D^2} \lim_{\eta_\pm \to 0} (\eta_- \eta_+)^{\frac{1-D}{2}} \int_{\eta(X_-)=\eta_-}^{\eta(X_+)=\eta_+} \mathcal{D}\eta\; \eta(x_a)\eta(x_b)\, \delta\!\left(\int_{X_-}^{X_+} \eta^2 dx - \beta\right) e^{-\mathcal{A}^{E=0}_\Delta[\eta]}\,. \tag{28}$$

Here, integrations over $\eta(x)$ run from 0 to $+\infty$, i.e., the paths $\eta(x)$ are non-negative. Comparing this result with the anticipated heuristic form (6), we can identify $\eta^2(x) = L^X(\beta\hbar)/\hbar$. Representation (28) allows us to identify the weight factor (7) with

$$\mathcal{W}_D[\eta; \beta, x_a, x_b] \;=\; \frac{2}{D^2} (\eta_- \eta_+)^{\frac{1-D}{2}} \eta(x_a)\eta(x_b) \exp\left\{ -\int_{X_-}^{X_+} dx \left[\frac{\hbar^2}{2M} \eta'^2 + \frac{M}{\hbar^2} \frac{\Delta(x)}{8\eta^2} \right] \right\}. \tag{29}$$

Contrary to expectation, the right-hand-side of this expression does not depend on β. Sub-index D in $\mathcal{W}_D$ indicates that the weight factor must be regularized when we pull it out of the PI (28). By analogy with quantum mechanics one can represent (28) in the discretized time-sliced form. In such a case the weight $\mathcal{W}_D$ would be a product of terms involving the Bessel functions $I_{D/2-1}$, if $\Delta(x) = (D-1)(D-3)$, or I_0, if $\Delta(x) = -1$ (see Ref. [24]).

Last but not least, expressions (28)-(29) indicate that the square root of L^X is (at least from a physicist's point of view) more convenient variable to describe local-time trajectories than L^X alone. From a mathematical standpoint, the local-time representation of the density matrix (28) can be regarded as a PI variant of the Ray–Knight theorem [13–15] which plays a prominent rôle in the theory of stochastic processes.

V. FUNCTIONALS OF THE LOCAL TIME

Formula (28) provides a way of rewriting the PI (3) in terms of the local time. In this Section, we consider more general scenario, in which the initial path integral is of the form

$$\bar{F}(x_a, x_b, \beta) \;\equiv\; \int_{x(0)=x_a}^{x(\beta\hbar)=x_b} \mathcal{D}x(\tau)\, F[L]\, \exp\left\{-\frac{1}{\hbar}\int_0^{\beta\hbar} d\tau \left[\frac{M}{2}\dot{x}^2 + V(x)\right]\right\}, \tag{30}$$

where F is an arbitrary functional of the local time $L^X(\beta\hbar)$, which itself is (as seen in Section III) a functional of the paths $x(\tau)$. Relation (30) represents a local-time analog of the Feynman–Matthews–Salam formula [19, 20].

To bring it into more manageable form, we may observe that for any X, the action of L^X in the PI (30) can be taken over by the functional derivative $-\hbar\delta/\delta V(X)$, acting on the exponential. This becomes transparent after rewriting the potential part as $\int_0^{\beta\hbar} d\tau\; V(x(\tau)) = \int_{\mathbb{R}} dX\, V(X) L(X)$. The entire functional $F[L]$ can be therefore pulled out of the path integral, which then allows to write

$$\bar{F}(x_a, x_b, \beta) \;=\; F\left[-\hbar\frac{\delta}{\delta V}\right] \rho(x_a, x_b, \beta)\,. \tag{31}$$

When we employ the local-time representation of PI for $\rho(x_a, x_b, \beta)$ (cf. Eq. (28)), each functional derivative $-\hbar\delta/\delta V(x)$ will produce the term $\hbar\eta^2(x)$. In such a way $\bar{F}$ can be written as

$$\begin{aligned}
&\bar{F}(x_a, x_b, \beta) \\
&= \lim_{D\to 0} \frac{2}{D^2} \lim_{\eta_\pm \to 0} (\eta_- \eta_+)^{\frac{1-D}{2}} \int_{\eta(X_-)=\eta_-}^{\eta(X_+)=\eta_+} \mathcal{D}\eta\; \eta(x_a)\eta(x_b)\, \delta\left(\int_{X_-}^{X_+} \eta^2 dx - \beta\right) F[\hbar\eta^2] e^{-\mathcal{A}_\Delta^{E=0}[\eta]}\,,
\end{aligned} \tag{32}$$

where, strictly speaking, the functional $F[\cdots]$ is regularized in such a way that it depends on L^X only for $X \in [X_-, X_+]$, and $X_\pm$ are sent to $\pm\infty$ only at the end of the calculation.

First, let us make the simple observation that the formula (32) reduces to (28) for the choice $F[L] = 1$. One of the most important mean values of a local-time functional, as evaluated with Eq. (32), is the mean of $\exp(-\int_{\mathbb{R}} dX L^X j(X))$ which gives the moment-generating functional. The local-time moment structure is particularly pertinent in various perturbative expansions, including low- and high-temperature expansions (see Section VI). Another important example, namely the case of a one-point distribution function will be discussed in the following subsection.

In passing we should note, that should we have started from (15) and repeated the above procedure, an analog of Eq. (32) for higher-dimensional spaces, $x \in \mathbb{R}^d$, could be easily obtained. This would include the D-dimensional replica field $\boldsymbol{\psi}$ in the d-dimensional Euclidean configuration space.

A. Example: One-point distribution function at the origin

Simple, though quite important consequence of Eq. (32) is that it readily provides the N-point distribution functions of the local time. This is achieved when we set $F[L] = \prod_{n=1}^N \delta(L^{X_n} - L_n)$. In order to see what is involved let us now illustrate the calculation for $N = 1$ (with $L_1 \equiv L$). Our discussion will be greatly simplified by considering only a free particle (i.e., $V(x) = 0$) that starts and ends at the origin, i.e., $x_a = x_b = 0$. This corresponds to a stochastic process known as Brownian bridge. Our goal is to derive the one-point distribution function, denoted $p(L;\beta)$, of the local time at $X = 0$. We define $p(L;\beta)$ by Eq. (30) with $F[L] = \delta(L^0 - L)$, and calculate it from the representation (32) as follows.

In the Laplace picture, $\widetilde{p}(L;E)=\int_0^\infty d\beta e^{-\beta E}p(L;\beta)$, the path integral (32) can be sliced at $x_a=x_b=0$ so that

$$\widetilde{p}(L;E)=\lim_{D\to 0}\frac{2}{D^2}\lim_{\eta_\pm\to 0}(\eta_-\eta_+)^{\frac{1-D}{2}}\int_0^\infty d\eta_0\,\eta_0^2\,\delta(\hbar\eta_0^2-L)(\eta_+X_+|\eta_0\;0)_D(\eta_0\;0|\eta_-X_-)_D\,. \tag{33}$$

The η_0-integration can be done easily by realizing that $\delta(\hbar\eta_0^2-L)=\delta(\eta_0-\sqrt{L/\hbar})/2\sqrt{\hbar L}$. Furthermore, the limits in $\eta_\pm$ and D can be carried out with the help of formulas (A2) and (A3) from Appendix A. Consequently, we obtain

$$\widetilde{p}(L;E)=\exp\left[-\frac{L\hbar^2}{2M}\left(\frac{F_1'(0)}{F_1(0)}-\frac{G_3'(0)}{G_3(0)}\right)\right], \tag{34}$$

where, for the free-particle case, $F_1(x)=\sinh[\sqrt{2ME/\hbar^2}(x-X_-)]/\sqrt{2ME/\hbar^2}$, and $G_3(x)=\sinh[\sqrt{2ME/\hbar^2}(X_+-x)]/\sqrt{2ME/\hbar^2}$, as one can straightforwardly verify. In the limit $X_\pm\to\pm\infty$, Eq. (34) reduces to

$$\widetilde{p}(L;E)=e^{-\sqrt{2\hbar^2E/M}L}, \tag{35}$$

and its inverse-Laplace transform yields

$$p(L;\beta)=\frac{L\exp\left(-\frac{L^2\hbar^2}{2\beta M}\right)}{\sqrt{2\pi M\beta^3/\hbar^2}}\,. \tag{36}$$

We stress that $p(L;\beta)$ thus obtained is, in fact, the (unnormalized) *joint* probability density for stochastic events "$x(0)=0\rightsquigarrow x(\beta\hbar)=0$" and "$L^0=L$". By Bayes' theorem of the probability calculus, the desired conditional probability density $p[L^0=L|x(0)=0\rightsquigarrow x(\beta\hbar)=0]$ is obtained from (36) by dividing $p(L;\beta)$ by the Brownian-bridge probability density $p[x(0)=0\rightsquigarrow x(\beta\hbar)=0]$, which is (omitting again normalization) $(2\pi\beta\hbar^2/M)^{-1/2}$ (see, e.g., Ref. [4]). Normalization factors mutually cancel in the fraction and we arrive at

$$p[L^0=L|x(0)=0\rightsquigarrow x(\beta\hbar)=0]\;=\;\frac{\hbar^2L\exp\left(-\frac{L^2\hbar^2}{2\beta M}\right)}{\beta M}\,, \tag{37}$$

which is clearly normalized to 1. One can proceed along the same lines also in more complicated higher-dimensional ($N>1$) cases. Our result agrees with the one found through other means in Ref. [13].

VI. ASYMPTOTIC BEHAVIOR OF THE BLOCH DENSITY MATRIX

A compelling feature of the local-time representation (28) is that it naturally captures both small- and large-β asymptotic regimes. This should be compared with the Feynman–Kac PI representation (3), which is typically suitable only for the small-β (i.e., large-temperature) analysis. The latter is epitomized either by WKB approximation [6, 7] or Wigner–Kirkwood expansion [21]. In the large-β (small-temperature) limit, the spectral representation of the Gibbs operator, $e^{-\beta\hat{H}}=\sum_n e^{-\beta E_n}\,|\phi_n\rangle\,\langle\phi_n|$, reduces the Bloch density matrix to the ground-state contribution

$$\rho(x_a,x_b,\beta)\;\overset{\beta\to\infty}{\sim}\;e^{-\beta E_0}\,\psi^*_{gs}(x_a)\psi_{gs}(x_b)\,, \tag{38}$$

that is not evident from the Feynman–Kac PI representation [27]. In connection with Eq. (38) it is useful to remind that in $d = 1$ the discrete bound states can all be chosen to be real [29], so that the Bloch density matrix is real and symmetric and can be written in the form

$$\rho(x_a, x_b, \beta) \;=\; \sum_{n=0} e^{-\beta E_n} \psi_n(x_a)\psi_n(x_b) \;\stackrel{\beta\to\infty}{\sim}\; e^{-\beta E_0}\, \psi_{gs}(x_a)\psi_{gs}(x_b)\,. \tag{39}$$

Let us first comment on the small-β regime of the local-time representation, assuming $x_b = x_a$ for simplicity. This case was discussed in detail in our previous article [21]. There one should first Taylor-expand the potential $V(x)$ around the point x_a, and then expand the exponential part containing the structure $\int \eta^2(x) O(x - x_a)dx$, where

$$O(x - x_a) \;=\; \beta \sum_{m\neq 0} \frac{V^{(m)}(x_a)}{m!} [\lambda(x - x_a)]^m\,. \tag{40}$$

After the term $e^{-\beta V(x_a)}/\lambda$ is factored out of the integral, the individual summands of the ensuing series are of the form (32) with the potential $V(x) = 0$, and functional $F[L] \propto \prod_n L^{x_n}/\hbar$. The latter can be related to the power expansion in β presented in [21] through the equality of representations (30) and (32). The whole Bloch density matrix (containing also off-diagonal elements) can be treated similarly in a full analogy with Ref. [21].

Let us now turn to the second and more interesting situation, namely to the large-β regime. In doing so, we will also highlight some pertinent technical issues related to the radial PI involved. The large-β expansion of Eq. (28) can be conveniently studied after rescaling $\eta \to \sqrt{\beta}\eta$, in which case we can write

$$\begin{aligned}
\rho(x_a, x_b, \beta) \;&=\; \lim_{D\to 0} \frac{2}{D^2} \lim_{\eta_\pm\to 0} (\eta_-\eta_+)^{\frac{1-D}{2}} \int_{\eta(X_-)=\eta_-}^{\eta(X_+)=\eta_+} \mathcal{D}\eta(x)\; \eta(x_a)\eta(x_b) \\
&\times\; \delta\!\left(\int_{X_-}^{X_+} \eta^2 dx - 1\right) \exp\left\{ - \int_{X_-}^{X_+} dx \left[\frac{\beta\hbar^2}{2M} \eta'^2 + \beta V(x)\eta^2 + \frac{M}{\beta\hbar^2} \frac{\Delta(x)}{8\eta^2} \right] \right\} \\
&=\; \lim_{D\to 0} \frac{2}{D^2} \lim_{\eta_\pm\to 0} (\eta_-\eta_+)^{\frac{1-D}{2}} \frac{\beta\delta^2}{\delta J(x_a)\delta J(x_b)} \int_{c-i\infty}^{c+i\infty} \frac{d\kappa}{2\pi i} \int_{\eta(X_-)=\eta_-}^{\eta(X_+)=\eta_+} \mathcal{D}\eta(x) \\
&\times\; \exp\left\{ -\beta \left[\int_{X_-}^{X_+} dx \left(\frac{\hbar^2}{2M} \eta'^2 + V(x)\eta^2 - \kappa\eta^2 \right) + \kappa \right] \right\} \\
&\times\; \exp\left\{ - \int_{X_-}^{X_+} dx \left[\frac{M}{\beta\hbar^2} \frac{\Delta(x)}{8\eta^2} + J\eta \right] \right\} \Bigg|_{J=0}\,,
\end{aligned} \tag{41}$$

where c is an arbitrary real number. With the *method of images* [7, 24, 38] we can rewrite the

radial PI involved as a superposition of two genuine one-dimensional PI's [36]

$$\int_{\eta(X_-)=\eta_-}^{\eta(X_+)=\eta_+} \mathcal{D}^R\eta(x) \exp\left\{-\beta\left[\langle\eta|\hat{H}|\eta\rangle - \kappa\left(\langle\eta|\eta\rangle - 1\right)\right] - \langle J|\eta\rangle\right\} \exp\left[-\int_{X_-}^{X_+} dx\, \frac{M}{\beta\hbar^2}\frac{\Delta(x)}{8\eta^2}\right]_R$$

$$= \int_{\eta(X_-)=\eta_-}^{\eta(X_+)=\eta_+} \mathcal{D}\eta(x) \exp\left\{-\beta\left[\langle\eta|\hat{H}|\eta\rangle - \kappa\left(\langle\eta|\eta\rangle - 1\right)\right] - \langle J||\eta|\rangle\right\}$$
$$\times \exp\left[-\int_{X_-}^{X_+} dx\, \frac{M}{\beta\hbar^2}\frac{\Delta(x)}{8\eta^2}\right]$$
$$+ \sin(\pi D/2) \int_{\eta(X_-)=-\eta_-}^{\eta(X_+)=\eta_+} \mathcal{D}\eta(x) \exp\left\{-\beta\left[\langle\eta|\hat{H}|\eta\rangle - \kappa\left(\langle\eta|\eta\rangle - 1\right)\right] - \langle J||\eta|\rangle\right\}$$
$$\times \exp\left[-\int_{X_-}^{X_+} dx\, \frac{M}{\beta\hbar^2}\frac{\Delta(x)}{8\eta^2}\right], \tag{42}$$

where Dirac's notation was employed [47]. A few comments are in order about the right-hand-side of the above relation. First, it should be noticed the presence of the parity-even terms $\langle J||\eta|\rangle$ in PI's. Second, PI's differ by their respective Dirichlet boundary conditions. Third, the super-script "R" was used to stress the restricted nature of the fluctuations in the radial PI measure while the measure without "R" represents a usual one-dimensional PI measure, i.e.

$$\mathcal{D}^R\eta(x) \doteq \lim_{N\to\infty}\left(\frac{\beta\hbar^2}{2\pi\varepsilon M}\right)^{N/2}\prod_{k=1}^{N-1}\int_0^\infty d\eta_k, \quad \mathcal{D}\eta(x) \doteq \lim_{N\to\infty}\left(\frac{\beta\hbar^2}{2\pi\varepsilon M}\right)^{N/2}\prod_{k=1}^{N-1}\int_{-\infty}^\infty d\eta_k\,. \tag{43}$$

Here "$\doteq$" denotes De Witt's "equivalence" symbol [39]. Finally, the correct time-sliced form of the exponential with the centrifugal potential is (cf. e.g., Refs. [7, 36])

$$\exp\left[-\int_{X_-}^{X_+} dx\, \frac{M}{\beta\hbar^2}\frac{\Delta(x)}{8\eta^2}\right]_R \doteq \lim_{N\to\infty}\prod_{k=1}^{N}\sqrt{2\pi\frac{\beta\hbar^2}{M}\frac{\eta_k\eta_{k-1}}{\varepsilon}\tilde{\Delta}_k}\exp\left(-\frac{\beta\hbar^2}{M}\frac{\eta_k\eta_{k-1}}{\varepsilon}\tilde{\Delta}_k\right)$$
$$\times I_{\frac{D-2}{2}}\left(\frac{\beta\hbar^2}{M}\frac{\eta_k\eta_{k-1}}{\varepsilon}\tilde{\Delta}_k\right),$$

$$\exp\left[-\int_{X_-}^{X_+} dx\, \frac{M}{\beta\hbar^2}\frac{\Delta(x)}{8\eta^2}\right] \doteq \lim_{N\to\infty}\prod_{k=1}^{N}\psi_{\frac{D-2}{2}}\left(-\frac{\beta\hbar^2}{M}\frac{\eta_k\eta_{k-1}}{\varepsilon}\tilde{\Delta}_k\right), \tag{44}$$

with

$$\tilde{\Delta}_k \equiv \tilde{\Delta}(x_k) = \begin{cases} -(D-1)(D-3) & \text{for } x_k \in [x_a, x_b] \\ 1 & \text{otherwise,} \end{cases} \tag{45}$$

and (see, e.g., Refs. [36, 42])

$$\psi_p(-x) = e^{-x}\sqrt{\frac{\pi x}{2}}\left[I_{-p}(x) + I_p(x)\right],$$

$$\psi_p(x) = \frac{e^x}{\sin(\pi p)}\sqrt{\frac{\pi x}{2}}\left[I_{-p}(x) - I_p(x)\right] = e^x\sqrt{\frac{2x}{\pi}}K_p(x)\,. \tag{46}$$

[I_p and K_p are the modified Bessel functions of the first and the second kind, respectively.] In cases when $x \gg 1$ meaning that $|\eta_k \eta_{k-1}| \gg \varepsilon$ (e.g., "typical situation" for very fine time slicings) the asymptotic form of $\psi_p(\pm x) \sim 1 \mp (1-4p^2)/8x + \mathcal{O}(1/x^2)$ holds. With help of the preceding asymptotic behavior one obtains

$$\begin{aligned}\prod_{k=1}^{N} \psi_{\frac{D-2}{2}}\left(-\frac{\beta\hbar^2}{M}\frac{\eta_k\eta_{k-1}}{\varepsilon}\tilde{\Delta}_k\right) &\sim \prod_{k=1}^{N}\left[1-\frac{M}{\beta\hbar^2}\frac{(D-3)(D-1)}{8\eta_k\eta_{k-1}\tilde{\Delta}_k}\,\varepsilon+\mathcal{O}(\varepsilon^2)\right]\\ &\sim \prod_{k=1}^{N}\exp\left[-\frac{M}{\beta\hbar^2}\frac{\Delta_k}{8\eta_k\eta_{k-1}}\,\varepsilon+\mathcal{O}(\varepsilon^2)\right]\\ &\sim \exp\left[-\int_{X_-}^{X_+} dx\,\frac{M}{\beta\hbar^2}\frac{\Delta(x)}{8\eta^2}\right]. \qquad (47)\end{aligned}$$

Potential singularities of the integral at $\eta = 0$ can be regularized, e.g., by a principal value prescription. Unfortunately, the formula (47) cannot be directly used in our case because the boundary values η_- and η_+ are arbitrarily close to zero, and hence the assumed asymptotic behavior for ψ_p is not fulfilled. This situation can be rectified by factorizing out the problematic boundary points as

$$\begin{aligned}&\prod_{k=1}^{N} \psi_{\frac{D-2}{2}}\left(-\frac{\beta\hbar^2}{M}\frac{\eta_k\eta_{k-1}}{\varepsilon}\tilde{\Delta}_k\right)\\ &\sim \frac{\sin^2(\pi D/2)}{\pi}\left(\frac{\beta\hbar^2}{2M\varepsilon}\right)^{D-1}\left[(\eta_--\eta_1)(\eta_+-\eta_{N-1})\right]^{(D-1)/2}\prod_{k=2}^{N-1}\exp\left[-\frac{M}{\beta\hbar^2}\frac{\Delta_k}{8\eta_k\eta_{k-1}}\,\varepsilon+\mathcal{O}(\varepsilon^2)\right]. \qquad (48)\end{aligned}$$

Here we have utilized the asymptotic form $\psi_p(-x) \sim -(x/2)^{p+1/2}\,\sin(\pi p)/(\sqrt{\pi}\;\Gamma(-p)) + \mathcal{O}(x^{p+3/2})$ valid for $0 < x \ll 1$ and $p < 0$ ($p \notin \mathbb{Z}^-$). For the second PI in (42) — which has negative lower Dirichlet boundary condition (namely $\eta_- \mapsto -\eta_-$), we need to employ the asymptotic expansion $\psi_p(x) \sim (x/2)^{p+1/2}\,\Gamma(-p)/\sqrt{\pi} + \mathcal{O}(x^{p+3/2})$ (again $0 < x \ll 1$) instead. This implies that in the second PI we get in contrast to (48) only "$\sin(\pi D/2)$" rather than "$\sin^2(\pi D/2)$".

The passage from the radial PI (41) to the ordinary (1-dimensional) PI brings about an important advantage, namely, one can perform the WKB approximation. In particular, one can use Laplace's formula of the asymptotic calculus [40, 41]

$$\int_{-\infty}^{\infty} dt\, f(t,\beta)\exp\left[-\beta g(t)\right] \;=\; \sqrt{\frac{2\pi}{\beta g''(t_0)}}\, f(t_0,\beta)\,\exp\left[-\beta g(t_0)\right] \;+\; \mathcal{O}\left(\frac{\exp\left[-\beta g(t_0)\right]}{\beta^{3/2}}\right), \quad (49)$$

with t_0 being a solution of $g'(t) = 0$ (provided $g(t)$ has a smooth absolute minimum at the interior point $t = t_0$ ($\neq \pm\infty$)). The function $f(t,\beta)$ is assumed to be bounded as $\beta \to \infty$. In case of need, the full asymptotic expansion can be systematically generated via conventional Laplace's method, see e.g. Ref. [41]. In Appendix B we show that

$$\sqrt{\frac{2\pi}{\beta g''(t_0)}} \;\mapsto\; \left(\frac{\hbar^2}{2\pi M}\right)\left\{\det{}'\left[-\frac{d^2}{dx^2}+\frac{2M}{\hbar^2}(V(x)-E_0)\right]\right\}^{-1/2}. \qquad (50)$$

Here E_0 is the ground state energy and the prime in $\det'[\cdots]$ indicates that the zero mode is factored out from the determinant. In fact, there is a quick way to compute $\det'\,[\cdots]$, by using

either the Wronski construction [44, 45] or the contour integration method [46]. In both these approaches one arrives at the result

$$\begin{aligned}\det{}'\left[-\frac{d^2}{dx^2}+\frac{2M}{\hbar^2}(V(x)-E_0)\right] &= -\frac{1}{\dot\eta_0(X_+)\dot\eta_0(X_-)}\\ &= -\frac{\varepsilon^2}{[\eta_+-(\eta_0)_{N-1}][(\eta_0)_1-\eta_-]} \sim \frac{\varepsilon^2}{(\eta_0)_{N-1}(\eta_0)_1}\,.\end{aligned} \tag{51}$$

Here η_0 is the (normalized) ground-state wavefunction of the Hamiltonian $\hat H$ [or equivalently the zero-mode eigenvector of $(\hat H - E_0)$] with the Dirichlet conditions $\eta_0(X_-)=\eta_-\sim 0$ and $\eta_0(X_+)=\eta_+\sim 0$. A similar result would hold also in the second PI in (42) where $\eta_-\mapsto-\eta_-$. The only difference in this case would be the presence of a minus sign in front of the last three expressions in (51).

To complete the WKB approximation, we substitute for $f(t_0,\beta)$ in (49) the functional expression

$$\beta\exp\left[-\langle J||\eta_0|\rangle-\int_{X_-}^{X_+}dx\,\frac{M}{\beta\hbar^2}\,\frac{\Delta(x)}{8\eta_0^2}\right], \tag{52}$$

in its explicit time-sliced form (48). Note that such $f(t_0,\beta)$ is bounded for $\beta\to\infty$ as required by Laplace's formula. In (52) we have denoted the WKB solution that minimizes the functional $\langle\eta|\hat H|\eta\rangle-\kappa\,(\langle\eta|\eta\rangle-1)$ as η_0, i.e., with the same symbol as in (51). This is because according to the Rayleigh–Ritz variation principle (see, e.g., Refs. [29, 31]), such a WKB function $\eta(x)$ is the ground-state wavefunction of the Hamiltonian $\hat H$, i.e., $\eta_0(x)=\psi_{gs}(x)$ with $\kappa_0=E_0$. Notice also that the stationary point in κ is real but the integration contour in κ is parallel to the imaginary axis. Both reality and positivity of $\eta(x)$ pose no restriction in the Rayleigh–Ritz principle, because the ground state can always be chosen real and positive [32]. By substituting for $g(t_0)$ the expression $\langle\eta_0|\hat H|\eta_0\rangle-\kappa_0\,(\langle\eta_0|\eta_0\rangle-1)=E_0$ and using the Laplace asymptotic formula (49), it is easy to see that for the first PI in (42) we get (cf. also Appendix B)

$$\frac{\sin^2(\pi D/2)}{\pi^2}\,(\eta_-\eta_+)^{\frac{D-1}{2}}\exp\left(-\langle J|\eta_0\rangle-\beta E_0\right), \tag{53}$$

while for the second PI we have

$$\frac{\sin(\pi D/2)}{\pi^2}\,(\eta_-\eta_+)^{\frac{D-1}{2}}\exp\left(-\langle J|\eta_0\rangle-\beta E_0\right). \tag{54}$$

By plugging this into (41) and performing the $\eta_\pm\to 0$ and $D\to 0$ limits, respectively, we get the leading large-β behavior of the Bloch density matrix in the form

$$\rho(x_a,x_b,\beta) \;=\; e^{-\beta E_0}\,\psi_{gs}(x_a)\psi_{gs}(x_b)\,, \tag{55}$$

as expected from the spectral expansion, cf. also Eq. (39).

We conclude the discussion of the low-temperature expansion by noting that the Rayleigh–Ritz variation principle states that *all* eigenvalues and (normalized) eigenvectors of $\hat H$ come from stationary solutions of $\langle\eta|\hat H|\eta\rangle-\kappa\,(\langle\eta|\eta\rangle-1)$, and conversely [29]. In the spirit of the WKB approximation one should sum over all path integrals evaluated about *all* stationary solutions. It is, however, only the ground state configuration $\{\psi_{gs}(x),E_0\}$ that acquires the global minimum and which gives the largest contribution to the WKB approximation. This fact was implicitly used in our preceding reasonings. Should we have included also other stationary solutions we would recover higher-order terms in the spectral expansion of the Bloch density matrix (39).

So what we have just demonstrated is that the WKB expansion of the local-time PI (in contrast to the Feynman–Kac PI) representation picks up the correct asymptotic behavior known from spectral theory. As mentioned in Section III, this should be expected because the most important contribution to the low-temperature behavior of $\rho(x_a, x_a, \beta)$ stems from those paths that spend a sizable amount of time near the global minimum, and the WKB expansion of local-time PI's is organized precisely in terms of the local time of a stationary configuration and ensuing fluctuations. Of course, the usefulness of the local-time PI approach lies in the situations where neither energy spectrum nor associated eigenvalues are explicitly known and various direct PI techniques can be conveniently employed to probe the low-temperature regime.

VII. CONCLUSION AND OUTLOOK

In this paper, we have derived the local-time PI representation of the Bloch density matrix. We have shown that the result obtained, apart from being of interest in pure mathematics (stochastic theory, Sturm–Liouville theory, etc), can serve as a useful alternative to the traditional Feynman–Kac PI representation of Green functions of Fokker–Planck equations. Furthermore, by analytically continuing the result back to the real time via the inverse Wick rotation, $\beta \to it/\hbar$, one obtains the local-time PI representation of quantum-mechanical transition amplitudes, i.e., matrix elements of the evolution operator $e^{-it\hat{H}/\hbar}$. From a physics point of view, perhaps the most important application of local-time PI's lies in statistical physics, and namely in the low and high temperature treatments of the Bloch density matrix. This is because in conventional PI's only a very tiny subset of paths gives a relevant contribution in these asymptotic regimes. In particular, the high-temperature regime of the Boltzmann density function $\rho(x, x, \beta)$ is dominated by paths that spend a sizable amount of time in the vicinity of the point x. Similarly, the low-temperature regime is controlled by paths with a large local time near the global minimum of the potential. Here we have exemplified the conceptual convenience of the local-time formulation by providing a generic analysis of the low-temperature behavior of the Bloch density matrix. Our formulation proved to be particularly instrumental in obtaining the correct asymptotic behavior (known from the spectral theory) which is otherwise notoriously difficult to obtain within the Feynman–Kac PI framework [4, 17]. As a byproduct we have uncovered an interesting connection between a low-temperature PI expansion, the Laplace asymptotic formula and the Rayleigh–Ritz variational principle.

In order to further reinforce our analysis, we formulated a local-time analog of the Feynman–Matthews–Salam formula which is (similarly as its QFT counterpart) expedient in number of statistical-physics contexts. The prescription obtained was substantiated by an explicit calculation of a one-point distribution function of the local time. In addition, the obtained relationship between the local-time representation of PI and the radial PI provides a practical illustration of the Ray–Knight theorem of the stochastic calculus.

It appears worthwhile to stress that our local-time representation (with its build-in replica field trick) is in its present form applicable only to one-dimensional quantum mechanical systems. With a hindsight we reflected this fact already in our choice of the incipient PI (3) where we assumed $\tau \in \mathbb{R}$ and $x \in \mathbb{R}$. Though one may easily proceed up to Eq. (15) without any restriction on the value of d (in fact, Eq. (15) is valid for any $x \in \mathbb{R}^d$ with $d \geq 1$), a further progress in this direction is hindered by the fact that the replica fields depend on a d-dimensional argument x, and thus the PI in (15) can no longer be regarded as a quantum mechanical PI (i.e., PI over fluctuating paths). In effect, we cannot use existing mathematical techniques of the PI calculus (e.g., transformation of PI's to polar coordinates), that we have employed to get the radial PI (16). The issue of the extension of our local-time PI representation to higher-dimensional configuration space is currently under active investigation.

Acknowledgements

The authors acknowledge A. Alastuey, H. Kleinert, Z. Haba and D.S. Grebenkov for fruitful discussions. The work has been supported by the GAČR Grant No. GA14-07983S. V.Z. was also partially supported by the CTU in Prague Grant No. SGS13/217/OHK4/3T/14 and by the DFG Grant: KL 256/54-1.

Appendix A: Off-diagonal matrix elements

In this appendix we show that the representation (25) reduces to the well established result (24) of the Sturm–Liouville theory. Since $\widetilde{\rho}(x_a, x_b, E)$ is symmetric in x_a and x_b, we will assume, without loss of generality, that $x_a < x_b$.

The path integral in (25) can be expressed via Eq. (19) as

$$\int_0^\infty d\eta_a d\eta_b \; (\eta_+ X_+|\eta_b x_b)_D \eta_b (\eta_b x_b|\eta_a x_a)_2 \eta_a (\eta_a x_a|\eta_- X_-)_D \,. \tag{A1}$$

The limits in Eq. (25) can be carried with the help of the asymptotic formulas $I_{D/2-1}(z) \approx (z/2)^{D/2-1}/\Gamma(D/2)$, and $\Gamma(z) \approx 1/z$, valid for $z \to 0$. We obtain

$$\begin{aligned} \frac{1}{D}\eta_-^{\frac{1-D}{2}} (\eta_a x_a|\eta_- X_-)_D \quad &\xrightarrow{\eta_- \to 0} \quad \left(\frac{\hbar^2 \eta_a}{2M F_1(x_a)}\right)^{D/2} \frac{\exp\left(-\frac{\hbar^2}{2M}\frac{F_1'(x_a)}{F_1(x_a)}\eta_a^2\right)}{\frac{D}{2}\Gamma(\frac{D}{2})\sqrt{\eta_a}} \\ &\xrightarrow{D\to 0} \quad \frac{1}{\sqrt{\eta_a}} \exp\left(-\frac{\hbar^2}{2M}\frac{F_1'(x_a)}{F_1(x_a)}\eta_a^2\right), \end{aligned} \tag{A2}$$

where $F_1(x)$ satisfies Eq. (20) with initial conditions $F_1(X_-) = 0$ and $F_1'(X_-) = 1$, and similarly, we find

$$\frac{1}{D}\eta_+^{\frac{1-D}{2}} (\eta_+ X_+|\eta_b x_b)_D \quad \xrightarrow{\eta_+ \to 0, D \to 0} \quad \frac{1}{\sqrt{\eta_b}} \exp\left(\frac{\hbar^2}{2M}\frac{G_3'(x_b)}{G_3(x_b)}\eta_b^2\right), \tag{A3}$$

where $G_3(x)$ satisfies Eq. (20) with initial conditions $G_3(X_+) = 0$ and $G_3'(X_+) = -1$. Formula (25) then reduces to

$$\begin{aligned} \widetilde{\rho}(x_a, x_b, E) \;=\; & \frac{2\hbar^2}{M}\int_0^\infty d\eta_a d\eta_b \, \frac{\eta_a \eta_b}{G_2(x_a)} \, I_0\!\left(\frac{\hbar^2}{M}\frac{\eta_a\eta_b}{G_2(x_a)}\right) \\ & \times \exp\left[-\frac{\hbar^2}{2M}\left(\frac{W(G_2,F_1)\eta_a^2}{F_1(x_a)G_2(x_a)} + \frac{W(G_3,F_2)\eta_b^2}{F_2(x_b)G_3(x_b)}\right)\right], \end{aligned} \tag{A4}$$

where $F_2(x)$ and $G_2(x)$ satisfy Eq. (20) with initial conditions $F_2(x_a) = 0$ and $F_2'(x_a) = 1$, and $G_2(x_b) = 0$ and $G_2'(x_b) = -1$, respectively. The Wronskian $W(F,G) \equiv F(x)G'(x) - F'(x)G(x)$ is independent of x, as discussed in Section IV C, and antisymmetric, i.e., $W(F,G) = -W(G,F)$.

Wronskians $W(G_2, F_1)$ and $W(G_3, F_2)$ assume a particularly simple form when evaluated at points x_b and x_a, respectively, due to the initial conditions satisfied by G_2 and F_2. We find $W(G_2, F_1) = F_1(x_b)$ and $W(G_3, F_2) = G_3(x_a)$. Rescaling $\eta_a \to \sqrt{G_2(x_a)M/\hbar^2}\eta_a$, $\eta_b \to \sqrt{F_2(x_b)M/\hbar^2}\eta_b$, and using the relation $F_2(x_b) = G_2(x_a)$ we obtain

$$\widetilde{\rho}(x_a, x_b, E) \;=\; \frac{2M}{\hbar^2} G_2(x_a) \int_0^\infty d\eta_a d\eta_b \, \eta_a \eta_b \, I_0(\eta_a\eta_b) \exp\left(-\frac{F_1(x_b)}{2F_1(x_a)}\eta_a^2 - \frac{G_3(x_a)}{2G_3(x_b)}\eta_b^2\right). \tag{A5}$$

The integrations are readily performed using the formula [33]

$$\int_0^\infty dz\, I_0(bz) \exp\left(-\frac{a}{2}z^2\right) \;=\; \frac{1}{a}\exp\left(\frac{b^2}{2a}\right), \tag{A6}$$

yielding

$$\widetilde{\rho}(x_a, x_b, E) \;=\; \frac{2M}{\hbar^2}\frac{F_1(x_a)G_3(x_b)G_2(x_a)}{F_1(x_b)G_3(x_a) - F_1(x_a)G_3(x_b)}\,. \tag{A7}$$

To prove equality with (24), we only have to show that

$$F_1(x_a)G_3(x_b) - F_1(x_b)G_3(x_a) \;=\; G_2(x_a)W(F_1, G_3)\,. \tag{A8}$$

This is done by realizing that $G_2(x)$, being a solution of the second-order linear differential equation (20), can be uniquely composed as a linear combination of two other solutions $F_1(x)$ and $G_3(x)$,

$$G_2(x) \;=\; \frac{F_1(x)G_3(x_b) - F_1(x_b)G_3(x)}{W(F_1, G_3)}\,. \tag{A9}$$

Indeed, thus defined G_2 satisfies the initial conditions $G_2(x_b) = 0$ and $G_2'(x_b) = -1$.

We conclude that

$$\widetilde{\rho}(x_a, x_b, E) \;=\; -\frac{2M}{\hbar^2}\frac{F_1(x_a)G_3(x_b)}{W(F_1, G_3)}\,, \tag{A10}$$

which coincides with the Sturm–Liouville result (24).

Appendix B: Proof of identity (50)

In this appendix we derive the identity (B6). According to Laplace's formula (49) we may assume that the dominant contribution to the PI (42) comes from the extremization of

$$g(t) \;\mapsto\; \langle\eta|\hat{H}|\eta\rangle - \kappa\left(\langle\eta|\eta\rangle - 1\right) \;\equiv\; s[\eta, \kappa]\,, \tag{B1}$$

while the role of $f(t, \beta)$ is played by the functional expression

$$\exp\left[-\langle J||\eta|\rangle - \int_{X_-}^{X_+} dx\, \frac{M}{\beta\hbar^2}\frac{\Delta(x)}{8\eta^2}\right]. \tag{B2}$$

Let η_0 and k_0 are corresponding extremizers of $s[\eta, \kappa]$ and let $\delta\eta$ and $\delta\kappa$ describe fluctuations around η_0 and k_0. Then the expansion of $s[\eta, \kappa]$ reads as

$$s[\eta, \kappa] \;=\; s[\eta_0, \kappa_0] \;+\; \langle\delta\eta|\hat{H} - \kappa_0|\delta\eta\rangle - \delta\kappa\left(\langle\delta\eta|\eta_0\rangle \;+\; \langle\eta_0|\delta\eta\rangle\right) \;+\; \cdots\,, \tag{B3}$$

(recall that the linear terms are absent due to the extremalization condition $\delta s = 0$). Notice that according to the Rayleigh–Ritz variation principle (see, e.g., Refs. [29, 31]), η_0 and κ_0 must correspond to the (normalized) ground-state wavefunction of the Hamiltonian $\hat{H}$ and to the

ground-state energy E_0, respectively. For the case at hand the leading WKB approximation (i.e., if we include only quadratic terms in the expansion (B3)) becomes, cf. Laplace's formula (49)

$$\begin{aligned}
&\int_{\eta(X_-)}^{\eta(X_+)} \mathcal{D}\eta \exp\{-\beta s[\eta,\kappa]\} \exp\left[-\langle J||\eta|\rangle - \int_{X_-}^{X_+} dx\, \frac{M}{\beta\hbar^2}\frac{\Delta(x)}{8\eta^2}\right] \\
&\quad = \exp[-\beta E_0] \exp\left[-\langle J||\eta_0|\rangle - \int_{X_-}^{X_+} dx\, \frac{M}{\beta\hbar^2}\frac{\Delta(x)}{8\eta_0^2}\right] \\
&\quad \times \frac{1}{2\pi}\int_{-\infty}^{\infty} d\delta\kappa \int_{\delta\eta(X_-)=0}^{\delta\eta(X_+)=0} \mathcal{D}\delta\eta \exp\left[-\beta(\langle\delta\eta|,\delta\kappa)\left\|\begin{matrix}\hat{H}-E_0, & i|\eta_0\rangle \\ i\langle\eta_0|, & 0\end{matrix}\right\|\begin{pmatrix}|\delta\eta\rangle \\ \delta\kappa\end{pmatrix}\right] \\
&\quad = \exp[-\beta E_0] \exp\left[-\langle J||\eta_0|\rangle - \int_{X_-}^{X_+} dx\, \frac{M}{\beta\hbar^2}\frac{\Delta(x)}{8\eta_0^2}\right] \left\{\det \hat{H}_0^{-1} \det\left\|\begin{matrix}\hat{H}-E_0, & i\eta_0 \\ i\eta_0^{\intercal}, & 0\end{matrix}\right\|\right\}^{-1/2}.
\end{aligned} \tag{B4}$$

Here we have used that $s[\eta_0,\kappa_0] = E_0$. We have also set $c = E_0$ in the κ-integration and subsequently rotated the integration contour so that the $\delta\kappa$-integration would run along the real axis. The (formal) expression inside of curly parentheses is a customary short-hand notation for the correct time-sliced form

$$\{\cdots\} \;=\; (2\pi)^2 \det\left\|\begin{matrix}-\varepsilon^2\nabla\overline{\nabla} + \varepsilon^2 2M(V(x)-E_0)/\hbar^2, & i2M\eta_0\varepsilon^2/\hbar^2 \\ i2M\eta_0^{\intercal}\varepsilon^2/\hbar^2, & 0\end{matrix}\right\|, \tag{B5}$$

where the difference operators (lattice derivatives) ∇ and $\overline{\nabla}$ are defined as [7]

$$\nabla\eta(x) \;=\; \frac{1}{\varepsilon}\left[\eta(x+\varepsilon) \;-\; \eta(x)\right], \qquad \overline{\nabla}\eta(x) \;=\; \frac{1}{\varepsilon}\left[\eta(x) \;-\; \eta(x-\varepsilon)\right], \tag{B6}$$

with $\nabla\overline{\nabla} = \overline{\nabla}\nabla$ being the Hermitian operator on the space of "time-sliced" functions with vanishing end points, i.e., $\eta(x_N) = \eta(x_0) = 0$. Eq. (B5) can be further simplified by using the *Schur complement* technique for calculation of determinants of partitioned matrices [43]. In particular, we have

$$\{\cdots\} \;=\; \left(\frac{2\pi M\varepsilon^2}{\hbar^2}\right)^2 \det\left[-\varepsilon^2\nabla\overline{\nabla} + \varepsilon^2\frac{2M}{\hbar^2}(V(x)-E_0)\right] \eta_0^{\intercal}\left\|-\varepsilon^2\nabla\overline{\nabla} + \varepsilon^2\tfrac{2M}{\hbar^2}(V(x)-E_0)\right\|^{-1}\eta_0, \tag{B7}$$

In order to find a finite expression for the indeterminate form $0/0$ (caused by the presence of the *zero mode*) we must properly regularize the numerator and denominator in (B7). This can be done by introducing a small parameter k^2 which moves the zero mode away from zero. In

this way we can write

$$\begin{aligned}
\{\cdots\} &= \lim_{k\to 0}\varepsilon\left(\frac{2\pi M}{\hbar^2}\right)^2 \frac{\det\left[-\varepsilon^2\nabla\overline{\nabla}+\varepsilon^2\frac{2M}{\hbar^2}(V(x)-E_0)+\varepsilon^2k^2\right]}{k^2} \\
&= \lim_{k\to 0}\varepsilon\left(\frac{2\pi M}{\hbar^2}\right)^2 \frac{\det\left[-\varepsilon^2\nabla\overline{\nabla}+\varepsilon^2\frac{2M}{\hbar^2}(V(x)-E_0)+\varepsilon^2k^2\right]}{k^2\det\left[-\varepsilon^2\nabla\overline{\nabla}\right]}\det\left[-\varepsilon^2\nabla\overline{\nabla}\right] \\
&= \varepsilon\left(\frac{2\pi M}{\hbar^2}\right)^2 \frac{\det'\left[-d^2/dx^2+\frac{2M}{\hbar^2}(V(x)-E_0)\right]}{\det\left[-d^2/dx^2\right]}\det\left[-\varepsilon^2\nabla\overline{\nabla}\right] \\
&= \left(\frac{2\pi M}{\hbar^2}\right)^2 \det'\left[-\frac{d^2}{dx^2}+\frac{2M}{\hbar^2}(V(x)-E_0)\right]. \qquad \text{(B8)}
\end{aligned}$$

The prime in $\det'[\cdots]$ indicates that the zero mode is divided out from the determinant. On the first line of (B8) we have used the fact that in the continuum limit

$$\eta_0^{\intercal}\left\|-\varepsilon^2\nabla\overline{\nabla}+\varepsilon^2\tfrac{2M}{\hbar^2}(V(x)-E_0)+\varepsilon^2k^2\right\|^{-1}\eta_0 \;\sim\; \frac{1}{\varepsilon^3}\int_{\mathbb{R}^2}dxdy\,\eta_0(x)G^k(x,y)\eta_0(y) \;=\; \frac{1}{\varepsilon^3k^2} \qquad \text{(B9)}$$

where $G^k(x,y)$ is the Green's function satisfying the equation

$$\left[-\frac{d^2}{dx^2}+\frac{2M}{\hbar^2}(V(x)-E_0)+k^2\right]G^k(x,y) \;=\; \delta(x-y)\,. \qquad \text{(B10)}$$

On the last line of (B8) we have employed the well-known formulas [7, 45]:

$$\begin{aligned}
\det\left[-\varepsilon^2\nabla\overline{\nabla}\right] &= N \;=\; (X_+-X_-)/\varepsilon\,, \\
\det\left[-d^2/dx^2\right] &= X_+-X_-\,. \qquad \text{(B11)}
\end{aligned}$$

Comparison of (B4) and (B8) with (49) yields the result (50).

---

[1] R.P. Feynman, Rev. Mod. Phys. **20**, 367 (1948).
[2] P.A.M. Dirac, Physikalische Zeitschrift der Sowjetunion **3**, 64 (1933).
[3] P.A.M. Dirac, *The Principles of Quantum Mechanics*, 2nd edition, (Clarendon, Oxford, 1935).
[4] R.P. Feynman and A.R. Hibbs, *Quantum Mechanics and Path Integrals*, (McGraw-Hill, New York, 1965).
[5] P. Ramond, *Field Theory: A Modern Primer*, 2nd edition, (Westview Press, New York, 2001).
[6] J. Zinn-Justin, *Quantum Field Theory and Critical Phenomena*, 4th edition, (Oxford University Press, Oxford, 2002).
[7] H. Kleinert, *Path Integrals in Quantum Mechanics, Statistics, Polymer Physics, and Financial Markets*, 5th edition, (World Scientific, London, 2009).
[8] D. Revuz and M. Yor, *Continuous Martingales and Brownian Motion*, (Springer, Berlin, 1999).
[9] N. Wiener, J. Math. & Phys. **2**, 132 (1923).
[10] M. Kac, Trans. Am. Math. Soc. **65**, 1 (1949).
[11] P. Lévy, Compositio Mathematica **7**, 283 (1939).
[12] M. Marcus and J. Rosen, *Markov Processes, Gaussian Processes, and Local Times*, 1st edition, (Cambridge University Press, Cambridge, 2006).
[13] A.N. Borodin, Russ. Math. Surv. **44**, 1 (1989).
[14] D. Ray, Illinois J. Math. **7**, 615 (1963).

[15] F.B. Knight, Trans. Amer. Math. Soc. **109** 56 (1963).
[16] D. Sokolovski and L.M. Baskin, Phys. Rev. A **36**, 4604 (1987).
[17] S. Paulin, A. Alastuey and T. Dauxois, J. Stat. Phys. **128**, 1391 (2007).
[18] J.M. Luttinger, J. Math. Phys. **23**, 1011 (1982).
[19] N.P. Landsman and Ch.G. van Weert, Phys. Rep. **145**, 141 (1987)
[20] M. Blasone, P. Jizba and G. Vitiello, *Quantum Field Theory and its Macroscopic Manifestations*, (Imperial College Press, London, 2011).
[21] P. Jizba and V. Zatloukal, Phys. Rev. E **89**, 012135 (2014).
[22] V.S. Vladimirov, *Equations of Mathematical Physics*, (Marcel Dekker, New York, 1971).
[23] A. Zettl, *Sturm–Liouville Theory*, (American Mathematical Society, New York, 2010).
[24] C. Grosche and F. Steiner, *Handbook of Feynman Path Integrals*, (Springer, Berlin, 1998).
[25] S.F. Edwards and Y.V.Gulyaev, Proc. Roy. Soc. A **279**, 229 (1964).
[26] J.M. Luttinger, J. Math. Phys. **24**, 2070 (1983).
[27] The low temperature expansion is typically obtained indirectly via duality approaches. Among these, a particularly powerful non-perturbative approximation scheme is the so-called *variational* or *optimized* perturbation theory [7, 28, 30].
[28] C.M. Bender, K.A. Milton, M. Moshe, S.S. Pinsky and L.M. Simmons Jr., Phys. Rev. Lett. **58**, 2615 (1987).
[29] A. Messiah, *Quantum Mechanics, Two Volumes Bound as One*, (Dover Publications, Inc., New York, 1999).
[30] P.M. Stevenson, Phys. Rev. D **23**, 2916 (1981).
[31] D.J. Griffiths, *Introduction to Quantum Mechanics*, 2nd edition, (Pearson Prentice Hall, New York, 2004).
[32] J. Mur-Petit, A. Polls and F. Mazzanti, Am. J. Phys. **70**, 808 (2002).
[33] I.S. Gradshteyn and I.M. Ryzhik, *Table of Integrals, Series, and Products*, 7th edition, (Elsevier, New York, 2007).
[34] M. Friedlin, *Functional integration and partial differential equations*, (Princeton University Press, Princeton, NJ, 1985).
[35] M. Mezard, G. Parisi G. and M. Virasoro, *Spin Glass Theory and Beyond*, (World Scientific, Berlin, 1987).
[36] F. Steiner, *Path Integrals in Polar Coordinates from eV to GeV*, in *Path Integrals from meV to MeV, Bielefeld, 1985*, Edited by M.C. Gutzwiller et al. (World Scientific, Singapore, 1986) pp. 335-359.
[37] D. Peak and A. Inomata, J. Math. Phys. **10**, 1422 (1969).
[38] A. Auerbach and L. S. Schulman,J. Phys. A: Math. Gen. **30**, 5993 (1997).
[39] B.S. De Witt, Rev. Mod. Phys. **29**, 377 (1957).
[40] N. Bleistein and R.A. Handelsman, *Asymptotic Expansions of Integrals*, (Dover Publications, New York, 1986).
[41] A. Erdélyi, *Asymptotic Expansions*, (Dover Publications, New York, 1956).
[42] R.B. Dinge, *Asymptotic expansions: Their Derivation and Interpretation*, (Academic Press, New York, 1973).
[43] E. Wasserstrom, SIAM Review **15**, 89 (1973).
[44] A.J. McKane and M.B. Tarlie, J. Phys. A: Math. Gen. **28**, 693 (1995).
[45] H. Kleinert and A. Chervyakov, Phys. Lett. A **245**, 345 (1998).
[46] K. Kirsten and A.J. McKane, Annals of Physics **308**, 502 (2003).
[47] The prefactor "$\sin(\pi D/2)$" guarantees the correct behavior at the origin and for our radial PI with the angular momentum ℓ it should read "$-\sin(\pi(\ell+1/2))$", cf. Refs. [36, 42]. Since in our case $\ell=(D-3)/2$, we have $-\sin(\pi(\ell+1/2))=\sin(\pi D/2)$.

C Full article: Green function of the double-fractional Fokker-Planck equation: Path integral and stochastic differential equations

Journal reference:

H. Kleinert and V. Zatloukal, *Green function of the double-fractional Fokker-Planck equation: Path integral and stochastic differential equations*, Phys. Rev. E **88**, 052106 (2013) [arXiv:1503.01667].

This work was done during my research stay at FU Berlin in the year 2013, under a kind supervision of Prof. Hagen Kleinert.

Co-authorship statement

I confirm that Vaclav Zatloukal contributed by at least 40% to the article

H. Kleinert and V. Zatloukal, *Green function of the double-fractional Fokker-Planck equation: Path integral and stochastic differential equations*, Phys. Rev. E **88**, 052106 (2013) [arXiv:1503.01667],

with his main contribution consisting in the analytical manipulations with the single and double fractional distribution functions, and in numerical simulations of the stochastic differential equation.

Hagen Kleinert

February 2016

Prof. Hagen Kleinert, Freie Universität Berlin

Green function of the double fractional Fokker-Planck equation – Path integral and stochastic differential equations

H. Kleinert*
Institut für Theoretische Physik, Freie Universität Berlin, 14195 Berlin, Germany and ICRANeT Piazzale della Repubblica, 10 -65122, Pescara, Italy

V. Zatloukal
Faculty of Nuclear Sciences and Physical Engineering, Czech Technical University in Prague, Břehová 7, 115 19 Praha 1, Czech Republic and Max Planck Institute for the History of Science, Boltzmannstrasse 22, 14195 Berlin, Germany

The statistics of rare events, the so-called *Black-Swan Events*, is goverened by non-Gaussian distributions with heavy power-like tails. We calculate the Green functions of the associated Fokker-Planck equations and solve the related stochastic differential equations. We also discuss the subject in the framework of path integration.

I. INTRODUCTION

Gaussian random walks prove to be a natural and rather universal starting point for many stochastic processes. In fact, the famous *central-limit theorem* shows that many independent random movements of finite variance $\sigma^2 = \langle x^2 \rangle$ always pile up to display a Gaussian distribution [1]. In particular, Gaussian random walks constitute the basis of the most important tool in the theory of financial markets, the Black-Scholes option price theory [2] (Nobel Prize 1997), by which a portfolio of assets is hoped to remain steadily growing through hedging [3].

However, since the last stock market crash and the still ongoing financial crisis it has become clear that distributions which describe realistically the behaviour of financial markets belong to a more general universality class, the so-called Lévy stable distribution [5–7]. They result from a sum of random movements of infinite variance [8], and account for the fact that rare events, the so-called Black-Swan Events [9], which initiate crashes, are much more frequent than in Gaussian distributions. These are events in the so-called Lévy tails $\propto 1/|x|^{1+\lambda}$ of the distributions, whose description is based on a generalized Hamiltonian [10]:

$$H(p) = \text{const}\,(p^2)^{\lambda/2}. \tag{1}$$

Such tail-events are present in many physical situations, e.g., in velocity distributions of many body systems with long-range forces [11], in the self-similar distribution of matter in the universe [12–14], and in the distributions of windgusts [15] and earthquakes [16], with often catastrophic consequences.

Distributions with Lévy tails are a consequence of rather general maximal entropy assumptions [17]. In the limit $\lambda \to 2$, the Lévy distributions reduce to Gaussian distributions.

The simplest Lévy-type random walk is described by the stochastic differetial equation of the Langevin type

$$\frac{d}{ds}x(s) \equiv \dot{x}(s) = \eta(s), \tag{2}$$

*Electronic address: h.k@fu-berlin.de

where $\eta(s)$ is a noise variable as a function of a pseudotime s with zero expectation value and a probability distribution characterized by a parameter λ [18]:

$$P[\eta] \equiv e^{-\int ds \tilde{H}(\eta)} = \int \mathcal{D}p \exp\left\{\int ds \left[ip\eta - (p^2)^{\lambda/2}\right]\right\}. \tag{3}$$

Using this we may solve the stochastic differential equation (2) in which the noise $\eta(s)$ has nonzero correlation functions for even $n = 2, 4, 6, \ldots$:

$$\langle \eta(s_1) \ldots \eta(s_n) \rangle \equiv \int \mathcal{D}\eta \, \eta(s_1) \ldots \eta(s_n) P[\eta]. \tag{4}$$

For $\lambda = 2$, the distribution is Gaussian and $\eta(s)$ is a standard white noise variable. If we solve (2) in D dimensions with an initial condition $\mathbf{x}(0) = \mathbf{0}$, the variable $\mathbf{x}(s)$ has a distribution

$$P_{\rm G}(\mathbf{x}, s) = (4\pi s)^{-D/2} e^{-\mathbf{x}^2/4s}. \tag{5}$$

This distribution is the Green function of the Fokker-Planck equation

$$(\partial_s + \hat{\mathbf{p}}^2) P_G(\mathbf{x}, s) = \delta(s)\delta^{(D)}(\mathbf{x}), \tag{6}$$

where $\hat{\mathbf{p}} \equiv i\partial_{\mathbf{x}} \equiv i\boldsymbol{\nabla}$. For $\lambda \neq 2$, the distribution is non-Gaussian and it solves the *fractional Fokker-Planck equation*

$$[\partial_s + (\hat{\mathbf{p}}^2)^{\lambda/2}] P(\mathbf{x}, s) = \delta(s)\delta^{(D)}(\mathbf{x}). \tag{7}$$

A solution of this equation that evolves from the δ-function is

$$P(\mathbf{x}, s) = e^{-s(\hat{\mathbf{p}}^2)^{\lambda/2}} \delta^{(D)}(\mathbf{x}), \tag{8}$$

and for $s = 1$ it coincides with the noise probability,

$$P(\mathbf{x}, 1)|_{\mathbf{x}=\boldsymbol{\eta}} = P(\boldsymbol{\eta}) = \int \frac{d^D p}{(2\pi)^D} e^{i\mathbf{p}\boldsymbol{\eta} - (\mathbf{p}^2)^{\lambda/2}}. \tag{9}$$

Applications of the fractional Fokker-Planck equation are numerous in non-Brownian diffusion processes. These are observed in chaotic systems and in the fluid dynamics of rheology and biology. See [19, 20] for an overview. The mathematics of Eq. (7) with variable diffusion coefficient is in [21].

The fractional Fokker-Planck equation (7) can be generalized further to the *double fractional Fokker-Planck equation*

$$[\hat{p}_4^{1-\gamma} + D_\lambda (\hat{\mathbf{p}}^2)^{\lambda/2}] P(\mathbf{x}, t) = \delta(t)\delta^{(D)}(\mathbf{x}), \tag{10}$$

where $\hat{p}_4 \equiv \partial_t$, $\hat{\mathbf{p}} \equiv i\partial_{\mathbf{x}} \equiv i\boldsymbol{\nabla}$ and a parameter has been allowed for that is the analogue of the diffusion constant D in the ordinary diffusion process [22].

We should explain the physical origin of the fractional powers in the space and time derivatives of the above equation. Such powers occur naturally in many-particle systems if the interaction strength or the range becomes very large. As long as the interaction strength is small and the range is short, such systems are described by a second-quantized field theory with a free-particle action

$$\mathcal{A}_0 = \int dt d^3x \psi^\dagger(\mathbf{x}, t)(i\partial_t + \hbar^2\nabla^2/2m - V(\mathbf{x}))\psi(\mathbf{x}, t), \tag{11}$$

and an interaction of the type

$$\mathcal{A}_{\rm int} = \frac{g}{4!}\int dt d^3x (\psi^\dagger\psi)^2 \ . \tag{12}$$

The partition function can be calculated from the functional integral

$$Z = \oint \mathcal{D}\psi\mathcal{D}\psi^\dagger e^{i(\mathcal{A}_0+\mathcal{A}_{\rm int})/\hbar}. \tag{13}$$

A perturbation expansion leads to an effective action in the form of a power series of $g\Psi^\dagger\Psi$, where $\Psi = \langle\psi\rangle$ are the expectation values of the field. This series is divergent and must be resummed. For large interaction strength g, this produces anomalous power behaviors in the field strength as well as in the momenta [23, 24]. The free-field part of the effective action leads to a field equation of the fractional Fokker-Planck or Schrödinger type, in which momentum and energy appear with powers different from $\lambda = 2$ and $\gamma = 0$, respectively.

In addition, equations of the type (10) are known to govern various different phenomena. In chaotic systems, for example, they describe anomalous diffusion processes with memory (time non-locality) [25, 26]. In fact, the fractional time derivatives also arise as the infinitesimal generators of coarse grained time evolutions [27], or they can be derived from a random walk model when the mean waiting time of the walker diverges [28].

It is the purpose of this note to calculate the Green functions of general fractional Fokker-Planck equation (10) and specify the path integrals solved by them [4, 29].

II. DOUBLE FRACTIONAL FOKKER-PLANCK EQUATION

A convenient definition of the fractional derivatives uses the same formula as in the dimensional continuation of Feynman diagrams [30, 31],

$$(\hat{\mathbf{p}}^2)^{\lambda/2} = \Gamma[-\lambda/2]^{-1}\int d\sigma\sigma^{-\lambda/2-1}e^{\sigma\hat{\mathbf{p}}^2}. \tag{14}$$

The solution of (10) can be written formally as

$$P(\mathbf{x},t) = [(\hat{p}_4+\epsilon)^{1-\gamma} + D_\lambda(\hat{\mathbf{p}}^2)^{\lambda/2}]^{-1}\delta(t)\delta^{(D)}(\mathbf{x}), \tag{15}$$

where infinitesimal $\epsilon > 0$ ensures forward-in-time nature of the Green function, and its explicit appearance will be suppressed from now on. Using the representation $\delta(t) = \int_{-\infty}^{+\infty}\frac{dE}{2\pi}e^{-iEt}$, we arrive at

$$P(\mathbf{x},t) = \int\frac{dE}{2\pi}\frac{e^{-iEt}}{(-iE)^{1-\gamma}+D_\lambda(\hat{\mathbf{p}}^2)^{\lambda/2}}\delta^{(D)}(\mathbf{x}). \tag{16}$$

Now we expand the fraction into a geometric series, and integrate term by term using the formula [32]

$$\int_{-\infty}^{+\infty}\frac{dE}{2\pi}\frac{e^{-iEt}}{(-iE+\epsilon)^{(1-\gamma)(n+1)}} = \frac{\theta(t)t^{n(1-\gamma)-\gamma}}{\Gamma[(1-\gamma)(n+1)]}, \tag{17}$$

where $\theta(t)$ is the Heaviside step function. The result can be cast as

$$P(\mathbf{x},t) = \theta(t)t^{-\gamma}E_{1-\gamma,1-\gamma}[-t^{1-\gamma}D_\lambda(\hat{\mathbf{p}}^2)^{\lambda/2}]\delta^{(D)}(\mathbf{x}), \tag{18}$$

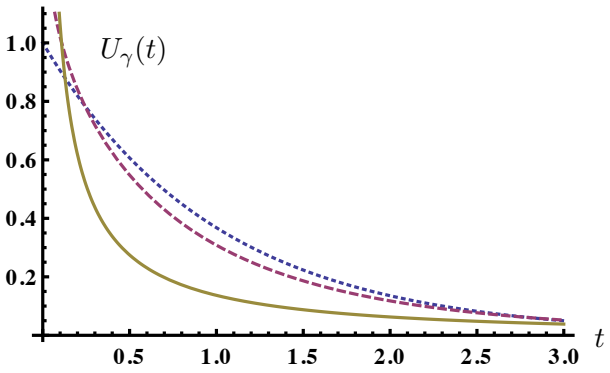

Figure 1: (Color online) The function $U_\gamma(t)$ for $\hat{H} = 1$, and various values of γ. Dotted (blue) curve: $\gamma = 0$, standard exponential function; Dashed (red) curve: $\gamma = 0.1$; Solid (yellow) curve: $\gamma = 0.5$.

where $E_{\alpha,\beta}(z) = \sum_{n=0}^{\infty} \frac{z^n}{\Gamma(\alpha n+\beta)}$ is the *Mittag-Leffler* function [33, 34]. This can be interpreted by writing

$$P(\mathbf{x}, t) = \langle \mathbf{x}| \, \hat{U}_\gamma(t) \, |\mathbf{0}\rangle \, , \tag{19}$$

with the γ-deformed evolution $\hat{U}_\gamma$ defined by

$$\hat{U}_\gamma(t) = \theta(t) t^{-\gamma} E_{1-\gamma,1-\gamma}(-t^{1-\gamma}\hat{H}), \tag{20}$$

with $\hat{H} \equiv D_\lambda(\hat{\mathbf{p}}^2)^{\lambda/2}$ [35] (See Fig. 1.). The occurrence of the Mittag-Leffler function in solutions of the time-fractional Fokker-Planck equation has been noted previously, for example, in the review article [22].

For $\gamma = 0$, the equation (10) reduces to a single (space) fractional Fokker-Planck equation

$$[\hat{p}_4 + D_\lambda(\hat{\mathbf{p}}^2)^{\lambda/2}]P(\mathbf{x}, t) = \delta^{(D)}(\mathbf{x})\delta(t), \tag{21}$$

the Mittag-Leffler function reduces to $E_{1,1}(z) = \exp(z)$, and the evolution operator recovers its standard form $\hat{U}_0(t) = \theta(t)\exp(-t\hat{H})$. The solution, which we shall denote by $P_X(\mathbf{x}, t)$ for a more specific reference, is the *multivariate Lévy stable distribution* [36]:

$$P_X(\mathbf{x}, t) = \int \frac{d^D p}{(2\pi)^D} e^{-tD_\lambda(\mathbf{p}^2)^{\lambda/2}} e^{-i\mathbf{px}}. \tag{22}$$

For $\lambda = 2$, it reduces to the standard quantum mechanical Gaussian expression (5). For $\lambda = 1$, the result is

$$P_X(\mathbf{x}, t) = \frac{[\Gamma(D/2 + 1/2)/\pi^{(D+1)/2}]D_\lambda t}{[(D_\lambda t)^2 + |\mathbf{x}|^2]^{D/2+1/2}}, \tag{23}$$

which is the Cauchy-Lorentz distribution function. In Fig. 2, we plot P_X in $D = 1$ dimension for $\lambda = 1, 1.5, 2$.

In the Appendix we provide various useful representations of $P_X(\mathbf{x}, t)$. At this place it is worth mentioning that this probability can be written as a superposition of Gaussian distributions $P_{\rm G}(\sigma, \mathbf{x}) = (4\pi\sigma)^{-D/2} e^{-\mathbf{x}^2/4\sigma}$ to be specified in Eq. (55).

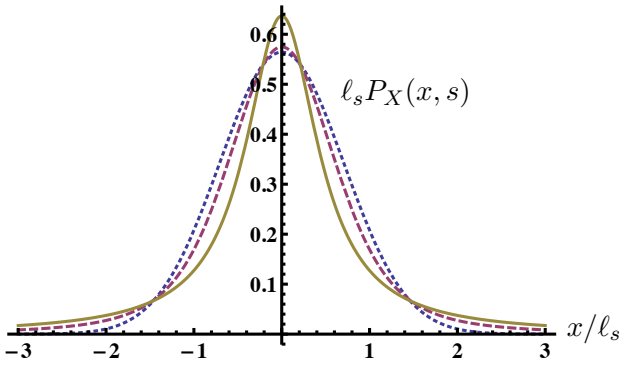

Figure 2: (Color online) Dotted (blue) curve: $\lambda = 2$, standard Gaussian distribution; Dashed (red) curve: $\lambda = 1.5$; Solid (yellow) curve: $\lambda = 1$, Cauchy-Lorenz distribution. The length scale is $\ell_s = 2(D_\lambda s)^{1/\lambda}$.

A. Smeared-time representation, and relation between physical time t and pseudotime s

If we use in (16) the Schwinger's formula $1/A = \int_0^\infty ds\ e^{-sA}$, we can express $P(\mathbf{x},t)$ as an integral

$$P(\mathbf{x},t) = \int_0^\infty ds P_X(\mathbf{x},s) P_T(t,s), \tag{24}$$

where P_X solves the *space-fractional* diffusion equation (21), with $t \equiv s$, and P_T solves the *time-fractional* equation

$$[\partial_s + \hat{p}_4^{1-\gamma}] P_T(t,s) = \delta(t)\delta(s), \tag{25}$$

which encodes the relation between the *pseudotime* s and the physical time t. The factorized ansatz (24) has been used previously in [37] to solve the time-fractional Fokker-Planck equation.

For $\gamma = 0$, $P_T(t,s) = \delta(t-s)$, and (24) reduces to $P(\mathbf{x},t) = P_X(\mathbf{x},t)$.

For $\gamma > 0$, we obtain an *asymmetric Lévy stable distribution* [38]

$$P_T(t,s) = \int_{-\infty}^{\infty} \frac{dE}{2\pi} e^{-s(-iE)^{1-\gamma}} e^{-iEt}. \tag{26}$$

An important feature is that $P_T(t,s)$ vanishes for $t < 0$. This can be seen by placing the branch cut of a multivalued function $z^{1-\gamma}$ along the negative real axis, and calculating (26) as a complex integral with contour that follows the real axis, and closes in the upper half-plane. See Fig. 3 (a) where P_T is plotted as a function of t for the case $\gamma = 0.03$, and various values of s.

It is illustrative to view formula (24) as a smearing of the distribution $P_X(\mathbf{x},s)$ around the time position t, defined by the probability density function $P_T(t,s)$. For this purpose we plot in Fig. 3 (b) $P_T(t,s)$ as a function of s, with parameter t describing the position of the peak in the probability distribution.

The two plots in Fig. (3) are related through the formula

$$P_T(t,s) = (C/t) P_T(C, C^{1-\gamma} t^{\gamma-1} s), \tag{27}$$

which can be deduced from (26) by a simple change of the integration variable $E \to (C/t)E$. Here C is an arbitrary constant. The function $P_T(t,s)$ as a function of two variables is shown in Figure (4).

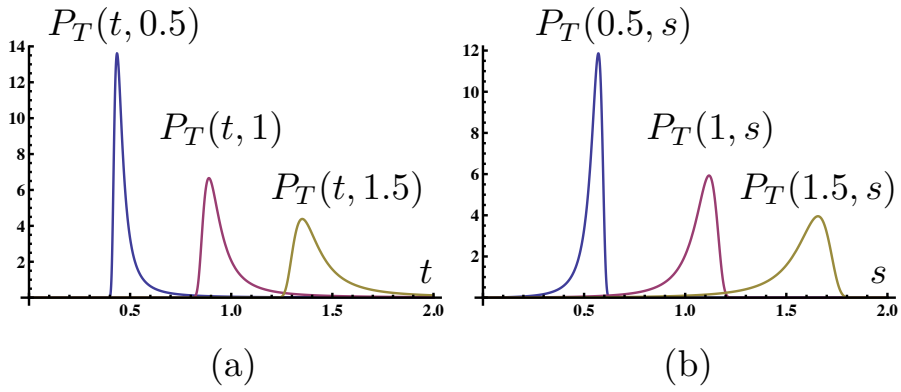

Figure 3: (Color online) (a) $P_T(t, s)$ as a distribution of t with increasing values of the pseudotime $s = 0.5, 1, 1.5$. (b) $P_T(t, s)$ as a distribution of s with increasing values of the real time $t = 0.5, 1, 1.5$. In both cases $\gamma = 0.03$.

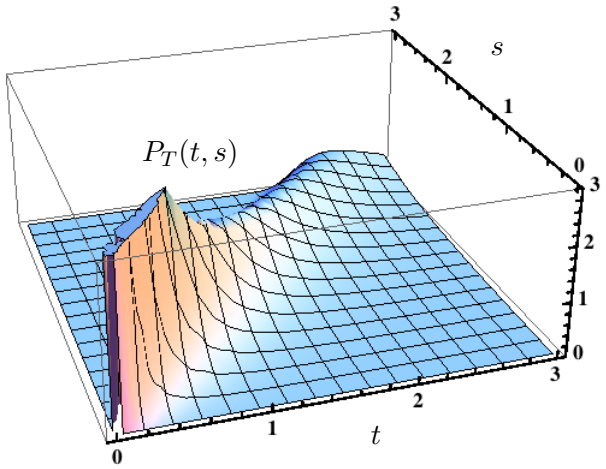

Figure 4: (Color online) $P_T(t, s)$ as a function of both t and s. Here $\gamma = 0.1$.

When $\gamma = 0$, $P_T(t, s) = \delta(t - s)$ is concentrated at the point t, i.e., there is no smearing. For increasing γ the peak around t broadens, which can be accounted for by derivatives of the δ-function. The action of P_T on a test function $f(s)$ is

$$\int_0^\infty ds\ P_T(t, s) f(s) = \sum_{n=0}^{\infty} \frac{f^{(n)}(t)}{n!} \int_0^\infty ds\ P_T(t, s)(s - t)^n. \tag{28}$$

We represent $f^{(n)}(t) = (-1)^n \int d\tau \delta^{(n)}(\tau - t) f(\tau)$, and calculate

$$\int_0^\infty ds P_T(t, s) s^k = \int \frac{dE}{2\pi} \frac{e^{-iEt} k!}{(-iE)^{(1-\gamma)(k+1)}} = \frac{k! \theta(t) t^{(1-\gamma)k-\gamma}}{\Gamma[(1-\gamma)(k+1)]} \tag{29}$$

to find that

$$P_T(t,s) = \sum_{n=0}^{\infty} \frac{t^n}{n!} c_n(t) \delta^{(n)}(s-t), \tag{30}$$

where

$$c_n(t) = \sum_{k=0}^{n} \binom{n}{k} (-1)^k \frac{k! \theta(t) t^{-\gamma(k+1)}}{\Gamma[(1-\gamma)(k+1)]}. \tag{31}$$

In view of these relations, the equation (24) translates into

$$P(\mathbf{x},t) = \sum_{n=0}^{\infty} \frac{(-t)^n}{n!} c_n(t) \partial_t^n P_X(\mathbf{x},t). \tag{32}$$

One can easily verify that for $\gamma = 0$, $c_n = \delta_{n0}$, and $P(\mathbf{x},t) = P_X(\mathbf{x},t)$.

B. Fox H-function representation of the Green function

Solution of the double fractional equation (10) has been obtained previously in terms of the *Fox H-function* [39]. We derive the same result starting from formula (24), where we consider the representation (58) of $P_X(\mathbf{x},s)$. Integration over the pseudotime s can be performed, followed by the E integration, that yields

$$P(\mathbf{x},t) = \frac{t^{-\gamma}}{\pi^{D/2}|\mathbf{x}|^D} H_{2,3}^{2,1}\left(\left[\frac{|\mathbf{x}|}{\ell_t}\right]^{\lambda} \Bigg|^{(1,1);(1-\gamma,1-\gamma)}_{(1,1),(D/2,\lambda/2);(1,\lambda/2)} \right). \tag{33}$$

Here $\ell_t \equiv 2(D_\lambda t^{1-\gamma})^{1/\lambda}$ is a t-dependent length scale, and $H_{2,3}^{2,1}$ is the Fox H-function [40, 41], defined by the contour integral

$$\frac{P(\mathbf{x},t)|\mathbf{x}|^D}{t^{-\gamma}\pi^{-D/2}} = \int_{\mathcal{C}} \frac{dz}{2\pi i} \frac{\Gamma(1+z)\Gamma(\frac{D}{2}+\frac{\lambda}{2}z)\Gamma(-z)}{\Gamma(-\frac{\lambda}{2}z)\Gamma(1-\gamma+(1-\gamma)z)} \left[\frac{|\mathbf{x}|^\lambda}{\ell_t^\lambda}\right]^{-z}, \tag{34}$$

where the contour $\mathcal{C}$ runs from $-i\infty$ to $+i\infty$. In Fig. 5 we show how values of $\gamma > 0$ modify the Gaussian distribution (for which $\lambda = 2$, $\gamma = 0$).

The large-$|\mathbf{x}|$ asymptotics of (33) is governed by the pole of the integrand at $z = 1$:

$$t^\gamma |\mathbf{x}|^D P(\mathbf{x},t) \overset{|\mathbf{x}|\to\infty}{\approx} \frac{\ell_t^\lambda}{|\mathbf{x}|^\lambda} \frac{-\Gamma(\frac{D+\lambda}{2})}{\pi^{D/2}\Gamma(2-2\gamma)\Gamma(-\frac{\lambda}{2})}. \tag{35}$$

Analysis of the small-$|\mathbf{x}|$ behavior is more subtle due to a richer pole structure of the integrand in (34) (see [42]). If we assume only simple poles, we can extract the leading behavior

$$t^\gamma P(\mathbf{x},t) \overset{|\mathbf{x}|\to 0}{\approx} \begin{cases} A(t) + B(t)|\mathbf{x}|^{2\lambda - D}, & 2\lambda - D < 2 \\ A(t) + \mathcal{O}[|\mathbf{x}|^2](t), & 2\lambda - D > 2 \end{cases}, \tag{36}$$

with

$$A(t) = \frac{\pi^{1-D/2}\ell_t^{-D} 2/\lambda}{\sin(\pi\frac{D}{\lambda})\Gamma(\frac{D}{2})\Gamma[\frac{(1-\gamma)(\lambda-D)}{\lambda}]}, \tag{37}$$

$$B(t) = -\frac{\pi^{-D/2}\Gamma(\frac{D}{2}-\lambda)}{\Gamma(\lambda)\Gamma(\gamma-1)\ell_t^{2\lambda}}. \tag{38}$$

In particular, for $2\lambda < D$ the value of $P(\mathbf{x},t)$ tends to either $+\infty$ or $-\infty$ as $|\mathbf{x}| \to 0$. See Fig. 6.

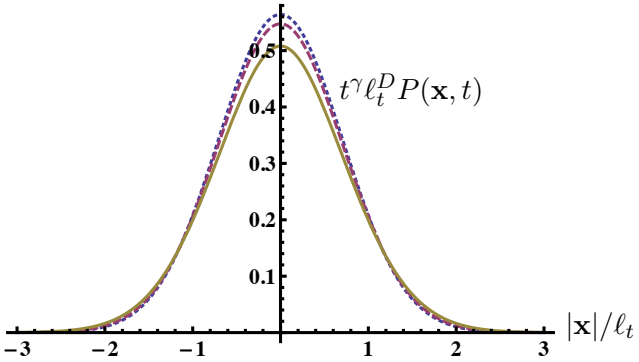

Figure 5: (Color online) In all cases $\lambda = 2$. Dotted (blue) curve: $\gamma = 0$, standard Gaussian distribution; Dashed (red) curve: $\gamma = 0.03$; Solid (yellow) curve: $\gamma = 0.1$.

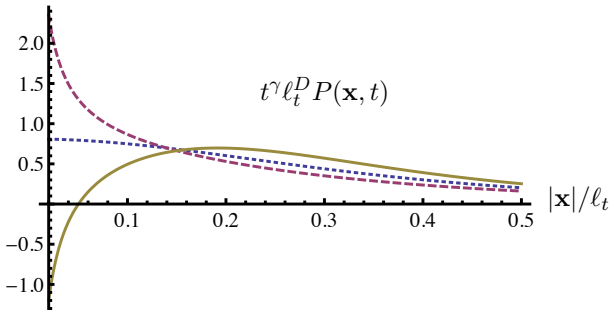

Figure 6: (Color online) Dotted (blue) curve: $\gamma = 0, \lambda = 1$, Cauchy-Lorentz distribution; Dashed (red) curve: $\gamma = 0.1, \lambda = 1$; Solid (yellow) curve: $\gamma = -0.1, \lambda = 1$, assumes negative values. Here D=3.

III. PATH-INTEGRAL FORMULATION

We note that the probability (15) may be calculated from the *doubly fractional canonical path integral* over fluctuating orbits $t(s), \mathbf{x}(s)$ $p_4(s), \mathbf{p}(s)$ viewed as functions of some pseudotime s [43]:

$$\{\mathbf{x}_b t_b s_b | \mathbf{x}_a t_s s_a\} = \int \mathcal{D}\mathbf{x}\mathcal{D}t\mathcal{D}\mathbf{p}\mathcal{D}p_4 e^{\mathcal{A}}, \tag{39}$$

with $\mathcal{A}$ being the euclidean action of the paths $t(s), \mathbf{x}(s)$:

$$\mathcal{A} = \int ds[i(\mathbf{p}\mathbf{x}' - ip_4 t') - \mathcal{H}(\mathbf{p}, p_4)]. \tag{40}$$

Here $t'(s) \equiv dt(s)/ds$, $\mathbf{x}'(s) \equiv d\mathbf{x}(s)/ds$, and $\mathcal{H}(\mathbf{p}, p_4) = p_4^{1-\gamma} + D_\lambda(\hat{\mathbf{p}}^2)^{\lambda/2}$. At each s, the integrals over the components of $\mathbf{p}(s)$ run from $-\infty$ to ∞, whereas those over $p_4(s)$ run from $-i\infty$ to $i\infty$. To obtain the distribution $P(\mathbf{x}, t)$, we finally form the integral

$$P(\mathbf{x}, t) = \int_0^\infty ds\{\mathbf{x}\, t\, s | \mathbf{0}\, 0\, 0\}. \tag{41}$$

This is analogous to prescription (24) which links solutions of the space- and time-fractional diffusion equations (21) and (25).

If $\gamma = 0$, the path integral over $p_4(s)$ yields the functional $\delta[t'(s) - 1]$, which ensures that dt and ds increments are equal. This brings (39) to the canonical path integral

$$(\mathbf{x}_b t_b | \mathbf{x}_a t_a) = \int \mathcal{D}\mathbf{x}\mathcal{D}\mathbf{p} e^{\mathcal{A}'}, \tag{42}$$

with

$$\mathcal{A}' = \int d\tau [i\mathbf{p}\dot{\mathbf{x}} - D_\lambda (\hat{\mathbf{p}}^2)^{\lambda/2}]. \tag{43}$$

Now $P(\mathbf{x}, t) = (\mathbf{x}t|\mathbf{0}\,0)$ satisfies the ordinary fractional Fokker-Planck equation

$$[\hat{p}_4 + D_\lambda (\hat{\mathbf{p}}^2)^{\lambda/2}] P(\mathbf{x}, t) = \delta(t)\delta^{(D)}(\mathbf{x}), \tag{44}$$

which has been discussed at length in recent literature [44].

IV. LANGEVIN EQUATIONS AND COMPUTER SIMULATIONS

In the past, many nontrivial Schrödinger equations (for instance that of the $1/r$-potential) have been solved with path integral methods by re-formulating them on the pseudotime axis s, that is related to the time t via a *space-dependent differential equation* $t'(s) = f(x(t))$. This method was invented by Duru and Kleinert [45] to solve the path integral of the hydrogen atom, and has recently been applied successfully to various Fokker-Planck equations [46, 47]. The stochastic differential equation (47), that connects pseudotime s and the physical time t, may be seen as a stochastic version of the Duru-Kleinert transformation that promises to be a useful tool to study non-Markovian systems.

Certainly, the solutions of Eq. (44) can also be obtained from a stochastic differential equation

$$\dot{\mathbf{x}} = \boldsymbol{\eta}, \tag{45}$$

whose noise is distributed with a fractional probability

$$P[\boldsymbol{\eta}] = \int \mathcal{D}^D p e^{\int dt (i\mathbf{p}\cdot\boldsymbol{\eta} - D_\lambda (\mathbf{p}^2)^{\lambda/2})}. \tag{46}$$

Simulating this stochastic differential equation on a computer, we confirm the analytic form (22) of $P_X(\mathbf{x}, s) = P(\mathbf{x}, t)$ for $\gamma = 0$. See Fig. 7 (a).

Analogously, the solution of Eq. (25) can also be obtained from a SDE

$$t'(s) = \eta_T(s), \tag{47}$$

with noise distribution

$$P[\eta_T] = \int \mathcal{D}p_4 e^{\int ds (p_4 \eta_T - (p_4)^{1-\gamma})}, \tag{48}$$

and compared with the result (26) for $P_T(t, s)$. See Fig. 7 (b).

Solution of the double fractional Fokker-Planck equation (10) can be obtained, in view of the relation (41) (or (24)), by simulating (45) for $t \equiv s$ and (47), and letting the final value of the pseudotime s be random. This yields a probability distribution $P(\mathbf{x}, t)$. In Fig. 8 we compare

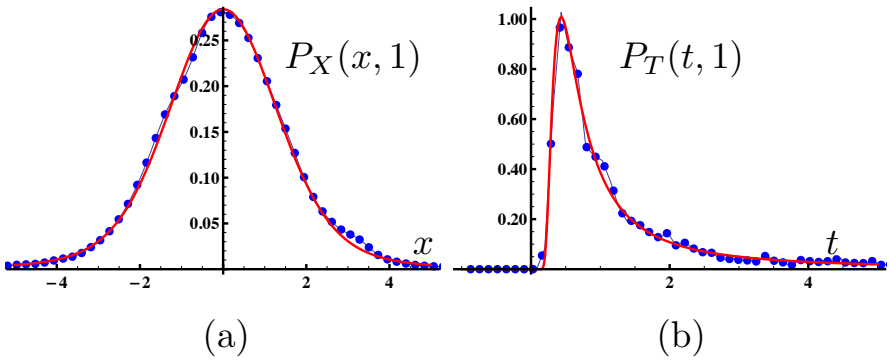

Figure 7: (Color online) Comparison of analytic (solid red curve) and numerical (blue circles) results for the distribution function $P_X(x, s{=}1)$ in $D = 1$ dimension (a), and $P_T(t, s{=}1)$ for $\gamma = 0.3$ (b). In each case an average has been taken over 5000 representative trajectories of stochastic differential equations (45) and (47), with 10 time steps $\Delta s = 0.1$.

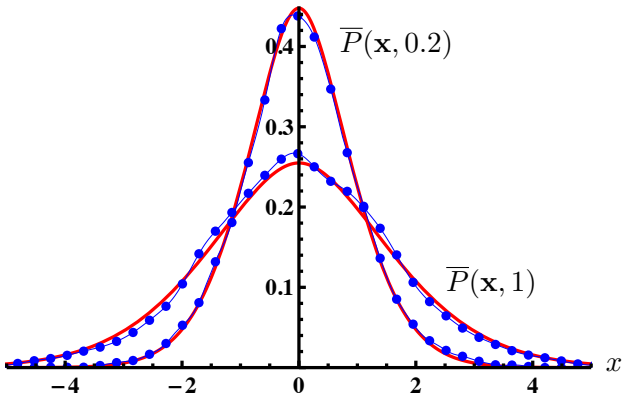

Figure 8: (Color online) Comparison of computer simulation and the renormalized exact solution $\overline{P}(\mathbf{x}, t)$ for t=0.2,1.

the results of a computer simulation with the analytic form (34) by plotting $P(\mathbf{x}, t)$ as a function of $\mathbf{x}$ for various values of time t. Since the distribution $P(\mathbf{x}, t)$ itself is not normalized, but rather

$$\int d^D x P(\mathbf{x}, t) = \int_0^\infty ds P_T(t, s) = \frac{\theta(t) t^{-\gamma}}{\Gamma(1-\gamma)}, \tag{49}$$

we define a renormalized version $\overline{P}(\mathbf{x}, t) = P(\mathbf{x}, t) / \int d^D x P(\mathbf{x}, t)$.

V. SUMMARY

Summarizing, we have seen that a many-body system with strong couplings between the constituents satisfies a more general form of the Schrödinger equation, in which the momentum and the energy appear with a power different from $\lambda = 2$ and $\gamma = 0$, respectively. We have calculated the associated Green functions and discussed their properties and their representations.

We pointed out that these Green functions can be written as path integrals over fluctuating time and space orbits that are functions of some pseudotime s. This is a Markovian object, but non-Markovian in the physical time t. The non-Markovian character is caused by the fact that function $t(s)$ follows a stochastic differential equation of the Langevin type.

The particle distributions can also be obtained by solving a Langevin type of equation in which the noise has correlation functions whose probability distribution is specified by an equation like (46).

The Green functions whose theory was presented here will play an important role in the development of an interacting theory of fields whose worldlines contain non-Gaussian random walks displaying extremely large deviations from their avarages.

Acknowledgment: We are grateful to P. Jizba, and A. Pelster for useful comments. One of the authors (V.Z.) is grateful for the financial support from the Deutsche Forschungsgemeinschaft, Grant KL 256/54-1, and the Czech Science Foundation (GAČR), Grant No. P402/12/J077.

Appendix 1: Fractional differential operators that enter the general fractional Fokker-Planck equation (7) are defined through formula (14). Using $e^{-\sigma\hat{\mathbf{p}}^2}\delta(\mathbf{x}) = (4\pi\sigma)^{-D/2}e^{-\mathbf{x}^2/(4\sigma)}$, and $e^{-\sigma\hat{p}_4}\delta(t) = \delta(t-\sigma)$, we derive the following relations,

$$|\mathbf{x}|^\lambda = \frac{\pi^{D/2}\Gamma(\frac{\lambda+D}{2})}{2^{-\lambda-D}\Gamma(-\frac{\lambda}{2})}(\hat{\mathbf{p}}^2)^{-(\lambda+D)/2}\delta^{(D)}(\mathbf{x}), \tag{50}$$

$$\theta(t)t^\alpha = \Gamma(\alpha+1)(\hat{p}_4)^{-\alpha-1}\delta(t), \tag{51}$$

which we can substitute into (33), (34) in order to verify that these satisfy the equation (10). We first obtain

$$P(\mathbf{x},t) = \int_{\mathcal{C}}\frac{dz}{2\pi i}\Gamma(1+z)\Gamma(-z)D_\lambda^z(\hat{\mathbf{p}}^2)^{\lambda z/2} \times(\hat{p}_4)^{(\gamma-1)(z+1)}\delta^{(D)}(\mathbf{x})\delta(t), \tag{52}$$

which can be pole-expanded to yield

$$\sum_{n=0}^{\infty}(-D_\lambda)^n(\hat{\mathbf{p}}^2)^{\lambda n/2}(\hat{p}_4)^{(\gamma-1)(n+1)}\delta^{(D)}(\mathbf{x})\delta(t). \tag{53}$$

Summing up this geometric series, we arrive at

$$P(\mathbf{x},t) = [\hat{p}_4^{1-\gamma} + D_\lambda(\hat{\mathbf{p}}^2)^{\lambda/2}]^{-1}\delta^{(D)}(\mathbf{x})\delta(t). \tag{54}$$

Appendix 2: We derive several expressions for the solution $P_X(\mathbf{x},s)$ of (21), starting from the representation (22).

On expanding the exponential, and representing the powers as $(\mathbf{p}^2)^{\lambda n/2} = \Gamma[-\lambda n/2]^{-1}\int_0^\infty\frac{d\sigma}{\sigma}\sigma^{-\lambda n/2}e^{-\sigma\mathbf{p}^2}$, the momentum integration yields the superposition of Gaussian expression

$$P_X(\mathbf{x},s) = \int_0^\infty\frac{d\sigma}{\sigma}f_\lambda(\sigma)P_G(\mathbf{x},D_\lambda^{2/\lambda}s^{2/\lambda}\sigma), \tag{55}$$

with weight

$$f_\lambda(\sigma) = \sum_{n=0}^{\infty}\frac{(-1)^n\sigma^{-\lambda n/2}}{n!\Gamma(-\lambda n/2)}. \tag{56}$$

To prove this, we perform the σ-integration term by term, using the formula $\int_0^\infty \frac{d\sigma}{\sigma}\sigma^{-\nu}e^{-a/\sigma} = \Gamma(\nu)/a^\nu$, and obtain the large-$|\mathbf{x}|$ expansion

$$P_X(\mathbf{x},s) = \frac{1}{\pi^{D/2}|\mathbf{x}|^D}\sum_{n=0}^{\infty}\frac{(-1)^n\Gamma(\frac{\lambda n+D}{2})}{n!\Gamma(-\lambda n/2)}\left[\frac{\ell_s^\lambda}{|\mathbf{x}|^\lambda}\right]^n, \tag{57}$$

where $\ell_s = 2(D_\lambda s)^{1/\lambda}$. The series can also be viewed as a pole expansion of the contour integral, and hence

$$P_X(\mathbf{x},s) = \frac{1}{\pi^{D/2}|\mathbf{x}|^D}\int_{\mathcal{C}}\frac{dz}{2\pi i}\frac{\Gamma(\frac{\lambda z+D}{2})\Gamma(-z)}{\Gamma(-\lambda z/2)}\left[\frac{|\mathbf{x}|^\lambda}{\ell_s^\lambda}\right]^{-z}, \tag{58}$$

with the contour $\mathcal{C}$ running from $-i\infty$ to $+i\infty$. From this, the expansion (57) arises by enclosing the right complex half-plane and calculating the residua of the integrand, using $\mathrm{Res}(\Gamma(az+b),-(n+b)/a) = (-1)^n/(n!a)$. A small-$|\mathbf{x}|$ expansion of (58) is obtained by closing the integration contour in the left half-plane, leading to

$$P_X(\mathbf{x},s) = \sum_{n=0}^{\infty}\frac{(-1)^n 2/\lambda}{\pi^{D/2}\ell_s^D}\frac{\Gamma(\frac{2n+D}{\lambda})}{n!\Gamma(\frac{D}{2}+n)}\left[\frac{|\mathbf{x}|^2}{\ell_s^2}\right]^n. \tag{59}$$

The series (57) and (59) are convergent, or asymptotic, or even trivially zero, depending on the parameter λ.

---

[1] W. Feller *An Introduction to Probability Theory and Its Applications* vol. 2, Wiley, New York, 1991; J.-P. Bouchaud and M. Potters, *Theory of Financial Risks*, *From Statistical Physics to Risk Management*, Cambridge U. Press, 2000. See also Ch. 20 in [4].

[2] F. Black and M. Scholes, J. Pol. Economy **81**, 637 (1973).

[3] The theory has been reviewed in many detailed publications, our notation follows the textbook [4].

[4] H. Kleinert, *Path Integrals in Quantum Mechanics, Statistics, Polymer Physics, and Financial Markets*, World Scientific, Singapore, 2006.

[5] T. Preis, *Econophysics in a Nutshell*, Science & Culture 76, 333-337 (2010)

[6] R. N. Mantegna, H. E. Stanley, *Introduction to Econophysics: Correlations and Complexity in Finance*, Cambridge University Press (2000)

[7] B. Podobnik, P. Ch. Ivanov, Y. Lee, A. Chessa and H. E. Stanley, Europhys. Lett. **50** 711 (2000) (arXiv:cond-mat/9910433)

[8] A travelling pedestrian salesman is a Gaussian random walker, as a jetsetter he becomes a Lévy random walker.

[9] See `http://en.wikipedia.org/wiki/Black_swan_theory`

[10] The concept of a Hamiltonian in the theory of statistical distributions was introduced in the textbook [4]. It has its root in the path integral formulation of quantum mechanics and emphasizes the fact that in this formulation particles run along fluctuating world lines in spacetime, where they perform random walks with distributions that may be Gaussian or nongaussian depending on the form of the Hamiltonian as functions of the momentum p. The distributions solve a Fokker-Planck equation of the type (7), driven by differential operator that is obtained by replacing the momentum in the Hamiltonian $H(p)$ by the differential operator $-i\partial_x$.

[11] C. Nardini, S. Gupta, S. Ruffo, T. Dauxois, and F. Bouchet, J. Stat. Mech. (2012) L01002 (http://arxiv.org/pdf/1111.6833.pdf)

[12] R. E. Angulo, V. Springel, S. D. M. White, A. Jenkins, C. M. Baugh, C. S. Frenk, Monthly Notices of the Royal Astronomical Society 426: 20462062 (2012) (arXiv:1203.3216).

[13] Du Jiulin, 2004 Europhys. Lett. **67**, 893 (2004), Phys. Lett. A **329**, 262(2004).

[14] J. Einasto, (arXiv:1109.5580).

[15] F. Boettcher, C. Renner, H.P. Waldl, J. Peinke, Boundary-Layer Meteorology (2003) Volume 108, Issue 1, pp 163-173 (arXiv:physics/0112063).

[16] P. Bhattacharyya, A. Chatterjee, B.K. Chakrabarti, Physica A **381**, 377 (2007) (arXiv:physics/0510038) .

[17] S. Umarov, C. Tsallis, M. Gell-Mann, and S. Steinberg, J. Math. Phys. 51, 033502 (2010) (http://arxiv.org/abs/cond-mat/0606040).

[18] Note that the function $\tilde{H}(\eta)$ is the functional Fourier transform of the Hamiltonian (1) that drives the Fokker-Planck equation (7). See Eq. (20.153) in Ref. [4].

[19] M.F. Shlesinger, G.M. Zaslavsky, U. Frish (Eds.), *Lévy Flights and Related Topics in Physics*, LNP **450** (1995).

[20] R. Kutner, A. Pekalski, K. Sznajd-Weron (Eds.), *Anomalous Diffusion From Basics to Applications*, LNP **519** (1999).

[21] T. Srokowski, Phys. Rev. E **79**, 040104(R) (2009).

[22] Fokker-Planck equations in which only the time derivative has a fractional power have been studied in R. Metzler and J. Klafter, Physics Reports **339** 1-77 (2000).

[23] H. Kleinert and V. Schulte-FrohlindeV. Schulte-Frohlinde, *Critical Phenomena in ϕ^4-Theory*, World Scientific, Singapore, 2001 (`http://klnrt.de/b8`).

[24] H. Kleinert, EPL **100**, 10001 (2012) (`http://klnrt.de/399/399-TAIPEH.pdf`). H. Kleinert, (`http://klnrt.de/403`).

[25] M. M. Meerschaert, A. Sikorskii, *Stochastic Models for Fractional Calculus*, Walter de Gruyter (2011).

[26] G. M. Zaslavsky, *Hamiltonian Chaos and Fractional Dynamics*, OUP Oxford (2005).

[27] R. Hilfer (Ed.), *Applications of Fractional Calculus in Physics*, World Scientific (2000).

[28] E. Barkai, R. Metzler, and J. Klafter, Phys. Rev. E **61**, 132138 (2000).

[29] R.P. Feynman, Phys. Rev. **80**, 440 (1950); R. P. Feynman and A.R. Hibbs, *Quantum Mechanics and Path Integrals* (McGraw-Hill, New York, 1965).

[30] For the so-called Riesz fractional derivative see R. Metzler, E. Barkai, J. Klafter, Phys. Rev. Lett. **82**, 3564 (1999); B.J. West, P. Grigolini, R. Metzler, and T.F. Nonnenmacher, Phys.Rev. E **55**, 99 (1997). For the so-called Weyl derivative. See R.K. Raina and C.L. Koul, Proc. Am. Math. Soc. **73**, 188 (1979).

[31] The relevant functional matrix is $\langle \mathbf{x}|(-\boldsymbol{\nabla}^2)^{\lambda/2}|\mathbf{x}'\rangle = \Gamma[-\lambda/2]^{-1}\int d\sigma\, \sigma^{-\lambda/2-1}(4\pi\sigma)^{-D/2}e^{R^2/4\sigma} = {}^{D}c_{\lambda}R^{-\lambda-D}$, where ${}^{D}c_{\lambda} = 2^{\lambda}\Gamma((D+\lambda)/2)/\pi^{D/2}\Gamma(-\lambda/2)$, and $R \equiv |\mathbf{x}-\mathbf{x}'|$. If λ is close to an even integer, it needs a small positive shift $\lambda \to \lambda_+ \equiv \lambda + \epsilon$ and we can replace $\epsilon R^{\epsilon-1}$ by $\delta(R) = S_D R^{D-1}\delta^{(D)}(\mathbf{R})$, where $S_D = 2\pi^{D/2}/\Gamma(D/2)$. For $A > 0$ we have $|\mathbf{x}'|^{-A} = {}^{D}c^{-1}_{\lambda_A}\langle \mathbf{x}'|(-\boldsymbol{\nabla}^2)^{\lambda_A/2}|\mathbf{0}\rangle$ with $\lambda_A \equiv A - D$, so that we find $\int d^D x' \langle \mathbf{x}|(-\boldsymbol{\nabla}^2)^{\lambda/2}|\mathbf{x}'\rangle|\mathbf{x}'|^{-A} = {}^{D}c^{-1}_{\lambda_A}\langle \mathbf{x}|(-\boldsymbol{\nabla}^2)^{(\lambda+A-D)/2}|\mathbf{0}\rangle = {}^{D}c_{\lambda+A-D}\,{}^{D}c^{-1}_{\lambda_A}|\mathbf{x}|^{-A-\lambda}$.

[32] I. S. Gradshteyn and I. M. Ryzhik, *Table of Integrals, Series, and Products, Seventh Edition*, Elsevier (2007), Formula 3.382.7

[33] A. Erdélyi, W. Magnus, F. Oberhettinger, and F. Tricomi, *Higher Transcendental Functions, Vol. 3*, New York (1981), pp. 206-212.

[34] H. J. Haubold, A. M. Mathai, and R. K. Saxena, J. Appl. Math. 298628 (2011).

[35] More generally, $\hat{H}$ can be a generic time-independent Hamiltonian. In particular, it may contain an additional potential term.

[36] Nolan, J. P., *Multivariate stable distributions: approximation, estimation, simulation and identification*. In R. J. Adler, R. E. Feldman, and M. S. Taqqu (Eds.), *A Practical Guide to Heavy Tails*, pp. 509-526, Birkhauser, Boston (1998).

[37] E. Barkai and R. J. Silbey, J. Phys. Chem. B, 104 (16), pp 38663874 (2000).

[38] Lévy distributions are implemented in WOLFRAM MATHEMATICA 8 under the command *StableDistribution*.

[39] Jun-Sheng Duan, J. Math. Phys. **46**, 013504 (2005).

[40] C. Fox, Trans. Amer. Math. Soc. **98**, 395 (1961).

[41] A. M. Mathai, R. K. Saxena, H. J. Haubold, *The H function: Theory and Applications*, Springer, 2010.

[42] A. A. Kilbas and M. Saigo, Journal of Applied Math. and Stoch. Anal., **12** 2 191-204 (1999).

[43] This technique is explained in Chapters 12 and 19 of Ref. [4]. The pseudotime s resembles the

so-called Schwinger proper time used in relativistic physics.

[44] N. Laskin, (arXiv/1009.5533); Phys.Lett. A **268**, 298 (2000); Phys. Rev. E **62**, 3135 (2000); (ibid.) E **66**, 056108 (2002); Chaos **10**, 780 (2000); Communications in Nonlinear Science and Numerical Simulation **12**, 2 (2007).

[45] I.H. Duru and H. Kleinert, Phys. Lett. B **84**, 30 (1979) (`klnrt.de/65/65.pdf`); Fortschr. Phys. **30**, 401 (1982) (`klnrt.de/83/83.pdf`). See also Chaps. 13 and 14 in [4].

[46] A. Young and C. DeWitt-Morette, Ann. Phys. (N.Y.) **169**, 140 (1984); H. Kleinert and A. Pelster, Phs. Rev. Lett. **78**, 565 (1997).

[47] L.Z.J. Liang, D. Lemmens, and J. Tempere, Phys. Rev. E 83, 056112 (2011) (arxiv:1101.3713).

D Full article: Transport properties of anyons in random topological environments

Journal reference:

V. Zatloukal, L. Lehman, S. Singh, J. K. Pachos, and G. K. Brennen, *Transport properties of anyons in random topological environments*, Phys. Rev. B **90**, 134201 (2014) [arXiv:1207.5000].

This work was done in collaboration with Dr. Jiannis Pachos (University of Leeds), Dr. Gavin Brennen, Dr. Lauri Lehman and Dr. Sukhwinder Singh (Macquarie University, Sydney), and it benefited from my visits to the University of Leeds, and Macquarie University in Sydney during the year 2012.

Co-authorship statement

I confirm that Vaclav Zatloukal contributed by at least 20% to the article

V. Zatloukal, L. Lehman, S. Singh, J. K. Pachos, and G. K. Brennen, *Transport properties of anyons in random topological environments*, Phys. Rev. B **90**, 134201 (2014) [arXiv:1207.5000],

with his main contribution consisting in the analytical treatment of the Abelian case, and in numerical simulations in the non-Abelian case.

February 2016 Dr. Jiannis Pachos, University of Leeds

Transport properties of anyons in random topological environments

V. Zatloukal,[1] L. Lehman,[2] S. Singh,[2] J.K. Pachos,[3] and G.K. Brennen[2,3]

[1]*Faculty of Nuclear Sciences and Physical Engineering, Czech Technical University in Prague, Břehová 7, 115 19 Praha 1, Czech Republic*
[2]*Centre for Engineered Quantum Systems, Department of Physics and Astronomy, Macquarie University, North Ryde, NSW 2109, Australia*
[3]*School of Physics and Astronomy, University of Leeds, Leeds LS2 9JT, UK*

The quasi one-dimensional transport of Abelian and non-Abelian anyons is studied in the presence of a random topological background. In particular, we consider the quantum walk of an anyon that braids around islands of randomly filled static anyons of the same type. Two distinct behaviours are identified. We analytically demonstrate that all types of Abelian anyons localise purely due to the statistical phases induced by their random anyonic environment. In contrast, we numerically show that non-Abelian Ising anyons do not localise. This is due to their entanglement with the anyonic environment that effectively induces dephasing. Our study demonstrates that localisation properties strongly depend on non-local topological interactions and it provides a clear distinction in the transport properties of Abelian and non-Abelian anyons.

I. INTRODUCTION

In systems with physics constrained to two dimensions, point-like particles named anyons can occur which have more general statistics than bosons or fermions [1]. Beyond mere possible existence they were found to be a good description for low lying quasi-particle excitations of fractional quantum Hall (FQH) systems, Majorana edge modes of nanowires, and they exactly describe excitations in various strongly correlated two dimensional spin lattice models [2]. Recently there has been experimental progress in preparation and control of systems capable of exhibiting topological order with the goal to observe anyonic statistics [3, 4]. This is further motivated by the discovery that braiding some types of non-Abelian anyons provides for naturally fault tolerant quantum computing [2, 5]. As we are not yet able to manipulate anyons individually, it would be beneficial to reveal their exotic braiding properties on macroscopic scale. In particular, we are interested in the transport properties of anyons and their possible localisation, that can have direct observable consequences.

Transport properties of anyons in uniform backgrounds were studied in [6] using a discrete-time quantum walk. The dispersion of the walker was found to be quadratic for Abelian anyons, as in the usual quantum walk [7], while for non-Abelian anyons it has been shown to be asymptotically linear [8, 9] just like classical random walks. The essential reason being that entanglement resulting from braiding non-Abelian anyons is sufficient to suppress quantum correlations responsible for the quadratic speed-up.

In this work, we investigate the role of disorder on the propagation of both, Abelian and non-Abelian, anyons. It has been known for more than five decades that randomised local potentials can suppress diffusion of quantum particles — a phenomenon known as Anderson localisation [10]. This mechanism is based on randomisation of phases that correspond to individual particle histories and consequent destructive interference. Here we consider a discrete-time anyonic quantum walk in a disordered topological background. In particular, we consider a walker that braids around islands canonically arranged on a line, where the number of static anyons at a given island assumes a random value. For the Abelian anyons this causes the walker acquiring random *discrete* phases which, as we demonstrate, leads to localisation. For the non-Abelian ones the Hilbert space grows exponentially with the number of anyons and hence, the length of the walk. As this makes long time exact numerics prohibitive we introduce an anyonic Hubbard model and use an anyonic matrix product state evolution to efficiently model continuous time

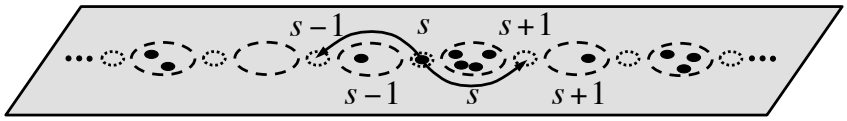

FIG. 1: The quasi one-dimensional quantum walk of an anyon braiding counterclockwise around islands filled with a random number of static anyons of the same type. The islands, denoted with dashed circles, are canonically arranged on the line. The possible positions of the walker are denoted by dotted circles placed in between the islands.

transport. The result is that Ising non-Abelian anyons do not localise. These generic behaviours provide a very clear distinction in the transport properties of Abelian and non-Abelian anyons.

II. THE DISCRETE-TIME MODEL

Our setup consists of n "islands" canonically ordered on the surface and labeled by index s, as shown in Fig. 1. The s-th island is occupied by m_s static anyons ($m_s \geq 0$) and the configuration, represented by vector $\vec{m} = (m_1, \ldots, m_n)$, is supposed to be fixed during the course of the walk. Anyons are labeled within an island from left to right by an index $i_s = 1, \ldots, m_s$. The mobile *walker* anyon hops between neighbouring sites winding counterclockwise around the islands. Hence our system is quasi one-dimensional. We denote possible walker's spatial positions also by s, with the convention that position s lies between islands $s-1$ and s, as shown in Fig. 1. The distance between sites is set to unity, though for purely topological interactions the distance scale is irrelevant. Hopping direction is controlled by the coin state: $|0\rangle$ moves the walker to the left, $|1\rangle$ to the right. The total Hilbert space decomposes as $\mathcal{H} = \mathcal{H}_{\text{space}} \otimes \mathcal{H}_{\text{coin}} \otimes \mathcal{H}_{\text{fusion}}$, where $\mathcal{H}_{\text{space}} = \text{span}_{\mathbb{C}}\{|s\rangle\}_{s=1}^{n}$, $\mathcal{H}_{\text{coin}} = \text{span}_{\mathbb{C}}\{|0\rangle, |1\rangle\}$, and $\mathcal{H}_{\text{fusion}}$ enumerates all distinct measurement outcomes of topological charge when pairs of anyons are fused together [5].

One step of the walk is defined as a composition of two unitary operations, $W = TU$, where $U = \frac{1}{\sqrt{2}}\left(\begin{smallmatrix} 1 & 1 \\ 1 & -1 \end{smallmatrix}\right)$ acts in the coin space, and T is a conditional braiding operator which moves the walker left or right depending on the coin state:

$$T = \sum_{s=1}^{n} |s-1\rangle\langle s| \otimes |0\rangle\langle 0| \otimes \hat{b}_{s-1} + |s+1\rangle\langle s| \otimes |1\rangle\langle 1| \otimes \check{b}_s \ , \tag{1}$$

where $\hat{b}_s = b_{s,1} \cdots b_{s,m_s}$, $\check{b}_s = b_{s,m_s} \cdots b_{s,1}$, and $\hat{b}_s = \check{b}_s = 1$ if $m_s = 0$. The operators $\{b_{s,i_s}\}$, acting on the fusion space $\mathcal{H}_{\text{fusion}}$, form a unitary representation of the r-strand braid group, $r = 1 + \sum_{s=1}^{n} m_s$, which reflects the type of anyons we choose. To make T unitary, we assume periodic boundary conditions ($|0\rangle_{\text{space}} = |n\rangle_{\text{space}}$) but will be concerned with walks satisfying $t < n/2$, where t is the number of steps, so that winding around the surface is not an issue. Note that this model is *chiral*, because only counterclockwise braids are considered. This is in close analogy to edge states in Fractional Quantum Hall (FQH) liquids where the breaking of time-reversal symmetry in the bulk results in a net current in one direction at the edge. Below we also consider a continuous-time model where braiding is allowed in both directions. The qualitative behaviour of the variance in this model is similar to the chiral discrete-time model.

Let the system's initial state be $|\Psi(0)\rangle = |s_0\rangle\,|c_0\rangle\,|\Phi_0\rangle$, where $s_0 = \lceil n/2 \rceil$ is the initial position of the walker, $c_0 = 0$ denotes the initial state of the coin, and Φ_0 depends on the initial state of the anyons. After t iterations of the one step operator W, the state becomes $|\Psi(t)\rangle = W^t\,|\Psi(0)\rangle$ — a superposition over all coin histories $\vec{a} \in \{0,1\}^{\otimes t}$, weighted by appropriate phase factors.

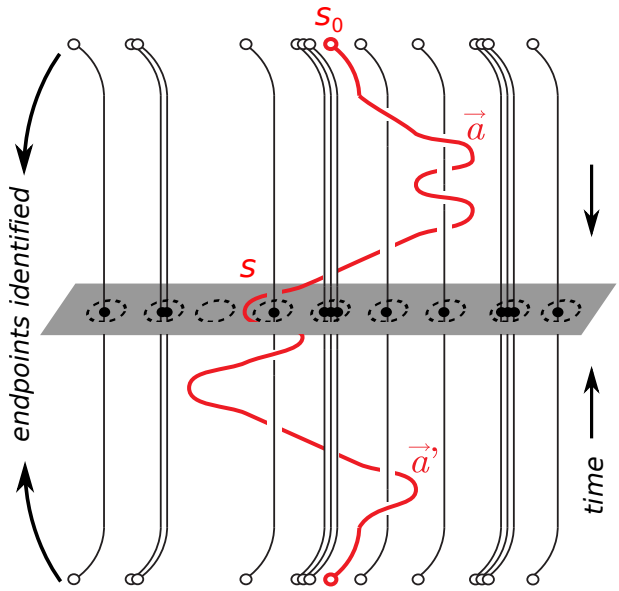

FIG. 2: Worldline of the mobile anyon constructed from a pair of paths $(\vec{a},\vec{a}') \rightsquigarrow s$. Together with the worldlines of the static anyons, they give rise to the link $L_{\vec{a}\vec{a}'}$ via the Markov closure of the braid word $B^\dagger_{\vec{a}'}B_{\vec{a}}$, which identifies the corresponding endpoints. (All the particle worldlines are assumed to have a common orientation.) Linking numbers $\ell_s(\vec{a},\vec{a}')$ as defined in Fig. 3 are easily read off from the figure: e.g., $\ell_s=-1, \ell_{s+1}=0$, etc.

The reduced state of the spatial degree of freedom of the walker is

$$\begin{aligned}\rho_{\rm space}(t) &= {\rm tr}_{\rm coin}{\rm tr}_{\rm fusion}\,|\Psi(t)\rangle\langle\Psi(t)| \\ &= \sum_{\vec{a},\vec{a}'} {\rm tr}\mathcal{U}_{\vec{a}\vec{a}'}{\rm tr}\mathcal{Y}_{\vec{a}\vec{a}'}\,|s_{\vec{a}}\rangle\langle s_{\vec{a}'}|\ ,\end{aligned} \tag{2}$$

where $s_{\vec{a}} = s_0 + \sum_{k=1}^t (2a_k-1)$ is the walker's final position corresponding to the coin history $\vec{a}=(a_1,\ldots,a_t)$; ${\rm tr}\mathcal{U}_{\vec{a}\vec{a}'} = \frac{1}{2^t}(-1)^{z(\vec{a},\vec{a}')}$, with $z(\vec{a},\vec{a}') \equiv \sum_{k=1}^{t-1}(a_ka_{k+1}+a'_ka'_{k+1})$, is a partial trace over the coin degree of freedom (DOF); and $\mathcal{Y}_{\vec{a}\vec{a}'} = B_{\vec{a}}\,|\Phi_0\rangle\langle\Phi_0|\,B^\dagger_{\vec{a}'}$ acts in the fusion space. The braid word $B_{\vec{a}}$ can be constructed recursively from a given coin history $\vec{a}$:

$$B_{\vec{a}^{(k+1)}} = \begin{cases} \hat{b}_{s_{\vec{a}^{(k)}}-1}B_{\vec{a}^{(k)}} & \text{if}\ \ a_{k+1}=0 \\ \check{b}_{s_{\vec{a}^{(k)}}}B_{\vec{a}^{(k)}} & \text{if}\ \ a_{k+1}=1 \end{cases}\ , \tag{3}$$

where $\vec{a}^{(k)}=(a_1,\ldots,a_k)$ is a truncation of $\vec{a}$, $s_{\vec{a}^{(0)}}=s_0$, and $B_{\vec{a}^{(0)}}=1$.

The spatial distribution of the walker after t steps is given by diagonal elements of the reduced density matrix,

$$p_{\vec{m}}(s,t) \equiv \langle s|\,\rho_{\rm space}(t)\,|s\rangle = \frac{1}{2^t}\sum_{(\vec{a},\vec{a}')\rightsquigarrow s}(-1)^{z(\vec{a},\vec{a}')}{\rm tr}\mathcal{Y}_{\vec{a}\vec{a}'}\ , \tag{4}$$

where "$(\vec{a},\vec{a}') \rightsquigarrow s$" denotes the set of pairs of paths $(\vec{a},\vec{a}')$ satisfying $a_t=a'_t$ and $s_{\vec{a}}=s_{\vec{a}'}=s$ (see Figure 2). The subscript $\vec{m}$ indicates a fixed island occupation configuration. Variance of

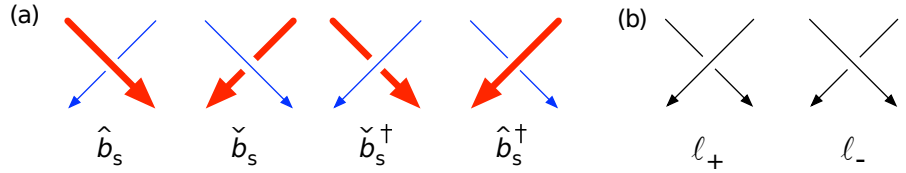

FIG. 3: (a) The linking number between the walker's component (thin blue) and the worldline of an island s (thick red), that collects all components of the island's static anyons, is determined by the relative number of four types of crossings $\ell_s = \frac{-\#\hat{b}_s - \#\check{b}_s + \#\hat{b}_s^\dagger + \#\check{b}_s^\dagger}{2}$. (b) The writhe of a link is the difference of the number of positive crossings and negative crossings: $w(L) = \ell_+ - \ell_-$.

the probability distribution $p_{\vec{m}}(s,t)$ is defined in the usual way:

$$\sigma^2_{\vec{m}}(t) = \sum_s p_{\vec{m}}(s,t)s^2 - \left(\sum_s p_{\vec{m}}(s,t)s\right)^2 . \tag{5}$$

In the studies of transport phenomena in disordered environments, one is interested in quantities that result from averaging over all random background configurations. We shall assume that the island occupation numbers m_s are independent and identically distributed random variables with distribution $W(m_s)$. The probability of occurrence of a configuration $\vec{m}$ is then simply $W_{\vec{m}} = \prod_{s=1}^n W(m_s)$, and we denote configuration average of a quantity $Q_{\vec{m}}$ by $\langle\langle Q\rangle\rangle \equiv \sum_{\vec{m}} W_{\vec{m}} Q_{\vec{m}}$. The average position distribution after a t-step walk is given by

$$\langle\langle p(s,t)\rangle\rangle = \frac{1}{2^t} \sum_{(\vec{a},\vec{a}')\rightsquigarrow s} (-1)^{z(\vec{a},\vec{a}')} \langle\langle \mathrm{tr}\mathcal{Y}_{\vec{a}\vec{a}'}\rangle\rangle \ . \tag{6}$$

The topological quantity $\langle\langle \mathrm{tr}\mathcal{Y}_{\vec{a}\vec{a}'}\rangle\rangle$, that depends on particle statistics, governs the transport of an anyonic walker in random background.

III. ABELIAN ANYONS

For Abelian anyons the braid generators $\{b_{s,i_s}\}$ are all equal to $e^{i\phi}$. We assume the anyonic exchange angle to be $\phi = \pm\frac{\pi}{N}$, $N \in \mathbb{N}$. The fusion space is one-dimensional, $\mathcal{H}_{\text{fusion}} \simeq \mathbb{C}$, and we can choose $|\Phi_0\rangle$ arbitrarily. Upon introducing the linking numbers

$$\ell_s(\vec{a},\vec{a}') = \frac{-\#(\hat{b}_s \text{ and } \check{b}_s \text{ in } B_{\vec{a}}) + \#(\hat{b}_s^\dagger \text{ and } \check{b}_s^\dagger \text{ in } B^\dagger_{\vec{a}'})}{2} \ , \tag{7}$$

that count the number of times the walker's trajectory $(\vec{a},\vec{a}')$ winds around an island s (see Fig. 2 and 3a), $\mathrm{tr}\mathcal{Y}_{\vec{a}\vec{a}'}$ reduces to $\prod_{s=1}^n e^{\mp i 2\frac{\pi}{N} m_s \ell_s(\vec{a},\vec{a}')}$.

For simplicity we consider uniform occupation distribution: $W(m) = 1/N$ for $0 \le m \le N-1$. Then the average position distribution of the walker after t steps, $\langle\langle p^{(\pm\frac{\pi}{N})}(s,t)\rangle\rangle$, is given by (6) with

$$\langle\langle \mathrm{tr}\mathcal{Y}^{(\pm\frac{\pi}{N})}_{\vec{a}\vec{a}'}\rangle\rangle = \prod_{s=1}^n \delta_{0,\ell_s(\vec{a},\vec{a}') \bmod N} \ , \tag{8}$$

where $\delta_{i,j}$ is the Kronecker symbol.

Localization of the distribution can be proven analytically by mapping the model to a variation of the one-dimensional multiple scattering model presented in [11], Section 2. (We base correspondence between the two on physical intuition rather than mathematical rigor.) In that work, scatterers are arranged in line with *continuous* random distances between neighbours. Incoming light undergoes a series of scattering events and eventually localises due to the randomness in phases that individual trajectories accumulate during their passage between consecutive scatterers. In our variation the braiding phases, accumulated when traversing each island populated with random numbers of anyons, take values in the *discrete* set $\{\frac{\pi m}{N}, 0 \leq m \leq N-1\}$, and reflection and transmission coefficients of the scatterers are identified with the entries of the coin operator.

The scattering model is described by Fig. 4. A monochromatic wave incident from the left scatters on a series of scatterers characterized by "from left / from right" reflection and transmission coefficients $r_j, t_j/r'_j, t'_j$. The distance between two successive scatterers j and $j+1$ is random, such that the phase that the wave acquires when traveling between j and $j+1$ is $e^{i\theta_j}$.

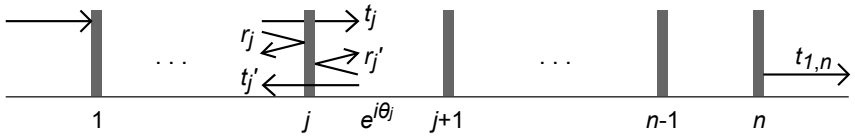

FIG. 4: In the multiple scattering model, the wave approaches (from the left) a series of n scatterers, and is transmitted with the amplitude $t_{1,n}$. The scatterers are arranged in line with random distances between neighbours. Hence, the phases $e^{i\theta_j}$ that the wave acquires during travelling from a scatterer j to $j+1$ are also random. The complex quantities $r_j, t_j/r'_j, t'_j$ are the reflection and transmission amplitudes for the wave impinging from the left / right.

Denote by $t_{1,n}$ the block amplitude of transmission from the "left of scatterer 1" to the "right of scatterer n"; and by $r'_{1,n}$ the reflection amplitude from the block "1 to n" when approaching from the right. $t_{1,n}$ can be expressed by the series

$$\begin{aligned} t_{1,n} &= t_{1,n-1}e^{i\theta_{n-1}} \sum_{k=0}^{\infty} \left(r_n e^{i\theta_{n-1}} r'_{1,n-1} e^{i\theta_{n-1}}\right)^k t_n \\ &= \frac{t_{1,n-1}e^{i\theta_{n-1}} t_n}{1 - r_n r'_{1,n-1} e^{i2\theta_{n-1}}} \ . \end{aligned} \tag{9}$$

The corresponding transmission probability and its logarithm are given by

$$|t_{1,n}|^2 = \frac{|t_{1,n-1}|^2 |t_n|^2}{|1 - r_n r'_{1,n-1} e^{i2\theta_{n-1}}|^2} \ , \tag{10}$$

$$\ln|t_{1,n}|^2 = \ln|t_{1,n-1}|^2 + \ln|t_n|^2 - \ln|1 - r_n r'_{1,n-1} e^{i2\theta_{n-1}}|^2 \ . \tag{11}$$

The reflection and transmission amplitudes $t_{1,n}$, $r'_{1,n}$ are random variables that depend on the configuration of scatterers $1, \ldots, n$, i.e. on the angles $\theta_1, \ldots, \theta_{n-1}$. We assume that θ_j's are identically distributed independent random variables with a uniform distribution over the discrete set $\{\frac{\pi}{N} m \mid m = 0, \ldots, N-1\}$ ($\frac{\pi}{N}$ will be identified with the anyonic exchange angle ϕ) [32]. We shall denote by $\langle\langle(\ldots)\rangle\rangle$ the statistical average over the angles $\theta_1, \ldots, \theta_{n-1}$, i.e.

$$\langle\langle(\ldots)\rangle\rangle \equiv \sum_{m_1=0}^{N-1} \frac{1}{N} \cdots \sum_{m_{n-1}=0}^{N-1} \frac{1}{N} (\ldots) \ . \tag{12}$$

Averaging of (11) leads to

$$\langle\langle \ln|t_{1,n}|^2\rangle\rangle = \langle\langle \ln|t_{1,n-1}|^2\rangle\rangle + \ln|t_n|^2 - \langle\langle \ln|1 - r_n r'_{1,n-1} e^{i2\theta_{n-1}}|^2\rangle\rangle \ . \tag{13}$$

We shall now assume that $t_j = t, r_j = r$ for all j. On the level of the Abelian anyonic quantum walk, this corresponds to a spatially independent coin. Bounds on the value of $\langle\langle \ln|t_{1,n}|^2\rangle\rangle$ are computed in Appendix A 1 (see Eq. (A7)). Exponentiating the resulting bounds results in

$$\begin{aligned} \exp\langle\langle \ln|t_{1,n}|^2\rangle\rangle &\leq (1-|r|^N)^{\frac{2}{N}} e^{-n\left[\ln(1-|r|^N)^{\frac{2}{N}} - \ln|t|^2\right]} \ , \\ \exp\langle\langle \ln|t_{1,n}|^2\rangle\rangle &\geq (1+|r|^N)^{\frac{2}{N}} e^{-n\left[\ln(1+|r|^N)^{\frac{2}{N}} - \ln|t|^2\right]} \ . \end{aligned} \tag{14}$$

Estimates of the localization length ξ_{loc} follow:

$$\frac{1}{\ln(1+|r|^N)^{\frac{2}{N}} - \ln|t|^2} \leq \xi_{loc} \leq \frac{1}{\ln(1-|r|^N)^{\frac{2}{N}} - \ln|t|^2} \ , \tag{15}$$

where the anyonic statistical angle $\phi = \frac{\pi}{N}$. For $N \to \infty$ we have $\xi_{loc} \to -\frac{1}{\ln|t|^2}$.

For the upper bound in (15) to make sense, $-\ln|t|^2 + \frac{1}{N}\ln(1-|r|^N)^2$ has to be a positive number. This leads to the condition

$$|t|^2 < (1-|r|^N)^{\frac{2}{N}} \ , \text{ i.e. } \ |t|^N + |r|^N < 1 \ . \tag{16}$$

Since $|t|^2 + |r|^2 = 1$ (with $|t|, |r| < 1$), the latter is satisfied for $N > 2$.

The case $N = 1$ corresponds to fermions which are known not to localize (their exchange statistics does not induce any interference effects). The marginal case $N = 2$ corresponds to *semions* ($\phi = \pi/2$), but we are unable to decide about their localization within this method. However, numerics for an analogous model involving continuous time hopping of semions on a ladder support localisation [13].

To establish a connection between this scattering model and the Abelian anyonic quantum walk with the coin $U = \frac{1}{\sqrt{2}}\left(\begin{smallmatrix} 1 & 1 \\ 1 & -1 \end{smallmatrix}\right)$, we define

$$t = -\frac{1}{\sqrt{2}} \ , \ t' = \frac{1}{\sqrt{2}} \ , \ r = \frac{1}{\sqrt{2}} \ , \ r' = \frac{1}{\sqrt{2}} \ . \tag{17}$$

The localization length estimate for $N = 8$ ($\frac{\pi}{8}$-anyons) is

$$1.412 \leq \xi_{loc} \leq 1.477 \ . \tag{18}$$

Let us stress that we investigated stationary state of a wave after infinitely many scattering events. This corresponds to the infinite-time asymptotic behavior of the anyonic quantum walk.

The result (15) works for any $N > 2$, thus extending prior work which assumed a continuum of values in the scattering length, i.e. $N \to \infty$ [14, 15], or rationally independent values [16]. Fig. 5 shows numerical results for the case $N = 8$. This case describes statistics for Abelian excitations in the $U(1)_8$ theory for the $\nu = 1/2$ fractional quantum Hall state where charge $2e$ electron pairs form an effective $\nu = 1/8$ bosonic Laughlin state [17] and it is also relevant to the non-Abelian case described below. The variance approaches a constant value and the asymptotic position distribution assumes a characteristic exponential shape, $\langle\langle p^{(\pm\frac{\pi}{N})}(s, t \to \infty)\rangle\rangle \sim e^{-\frac{|s-s_0|}{\xi_{\rm loc}}}$, with the localization length $\xi_{\rm loc} \doteq 1.44$. This is a clear manifestation of the Anderson localization of Abelian anyons.

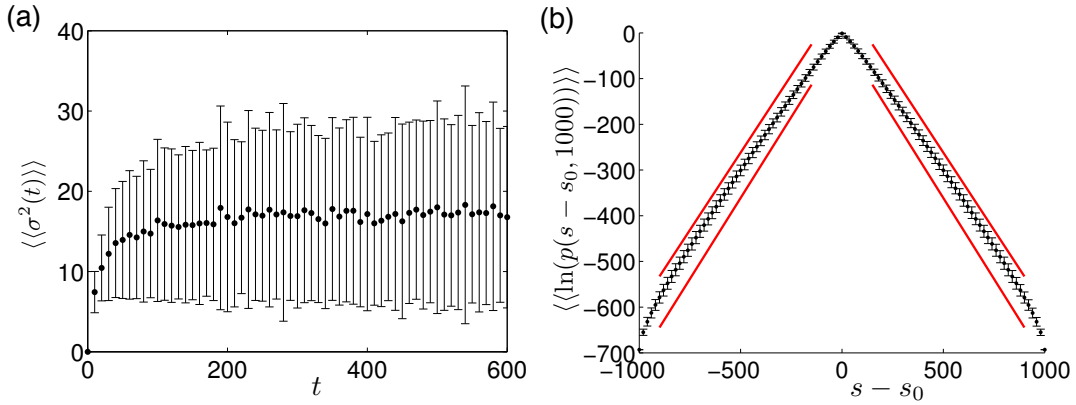

FIG. 5: Numerical results for localisation of Abelian anyons. The exchange statistics is $\phi = \frac{\pi}{8}$ and the statistics is averaged over a random background of island occupations where the distribution in each is uniform over $m_s \in \{0, \ldots, 7\}$. (a) Average variance as a function of time t for up to 600 time steps. The averages are taken over at least 500 charge configurations. (For clarity, only every 10th step is plotted.) (b) Average of the logarithm of probability distribution at time step $t = 1000$, taken over 10000 charge configurations. Red lines correspond to bounds for the localisation length given in Eq. (18). In both (a) and (b), the error bars are given by standard deviation.

IV. ISING NON-ABELIAN ANYONS

We consider the Ising model of non-Abelian anyons. There are three kinds of particles in this model: vacuum, fermion, and non-Abelian anyon. In analogy with [8], the initial fusion state $|\Phi_0\rangle$ describes the vacuum configuration of pairs of anyons with half the members braided to the right. Here, they randomly populate islands (except for the walker) to form a disordered background configuration $\vec{m}$. The braid generators $\{b_{s,i_s}\}$ are now unitary matrices, the dimension of which grows like $d^{|\vec{m}|}$, where $|\vec{m}| \equiv \sum_{s=1}^{n} m_s$, and $d = \sqrt{2}$ is the *quantum dimension* of Ising anyons. This exponential increase in the Hilbert space dimension as well as the non-local character of the total braiding makes the evolution distinct from other quasi 1D systems.

The trace over the fusion degree of freedom can be related to the Kauffman bracket polynomial $\langle L_{\vec{a}\vec{a}'}\rangle$ [18] of a link $L_{\vec{a}\vec{a}'}$ (see Figure 2 above), which arises from the Markov closure of the braid word $B^{\dagger}_{\vec{a}'} B_{\vec{a}}$ [6, 8, 19]. This link corresponds to the world lines (strands) of all the anyons. Moreover, $\langle L_{\vec{a}\vec{a}'}\rangle$ can be expressed in terms of the Jones polynomial $V_{L_{\vec{a}\vec{a}'}}(q)$ [20]. Altogether,

$$\mathrm{tr}\mathcal{Y}_{\vec{a}\vec{a}'} = \frac{\langle L_{\vec{a}\vec{a}'}\rangle(q^{-1/4})}{d^{|\vec{m}|}} = \frac{\left(-q^{-3/4}\right)^{w(L_{\vec{a}\vec{a}'})} V_{L_{\vec{a}\vec{a}'}}(q)}{d^{|\vec{m}|}} \,, \tag{19}$$

where the *writhe* $w(L_{\vec{a}\vec{a}'}) = 2\sum_{s=1}^{n} m_s \ell_s(\vec{a}, \vec{a}')$ is the difference between the number of positive and negative crossings of the anyonic worldlines (see Fig. 3b). For Ising model anyons, which correspond to spin-1/2 irreps of the quantum group $SU(2)_2$ we have specifically $q = i$. Note there are some differences in the braid matrices for the Ising model and $SU(2)_2$ models but it does not affect the results herein as we comment at the end of this section.

The Jones polynomial $V_{L_{\vec{a}\vec{a}'}}(i)$ for the links relevant to the quantum walk can be further

simplified in terms of simple topological characteristics, the arf invariant, through [21]

$$V_{L_{\vec{a}\vec{a}'}}(i) = \sqrt{2}^{|\vec{m}|}(-1)^{arf(L_{\vec{a}\vec{a}'})} \prod_{\substack{s=1 \\ m_s>0}}^{n} \widetilde{\ell}_s \ , \tag{20}$$

where $\widetilde{\ell}_s \equiv \delta_{0,\ell_s \bmod 2}$. The product in the last expression is equal to 1 only if the link $L_{\vec{a}\vec{a}'}$ is *proper*, i.e. the sum of the pairwise linking numbers is even. Furthermore, when the link is *totally proper*, i.e. all pairs of components have an even linking number, and there is no self-linking, then [22]

$$arf(L_{\vec{a}\vec{a}'}) = \sum_{s=1}^{n} m_s c_2(s) + \sum_{1\le s'<s''\le n} m_{s'} m_{s''} \tau(s', s'') \ , \tag{21}$$

where $c_2(s)$ is the cubic coefficient in the *Conway polynomial* of the two-component sublink of $L_{\vec{a}\vec{a}'}$ consisting of strands corresponding to the walker and island s; and $\tau(s', s'')$ is the Milnor triple invariant, which counts the number of Borromean rings (three braided loops that disentangle if just one is removed) between the walker strand and the strands s' and s''. Note there is no self-linking because the links represent world lines of the anyons which move forward in time only. In Ref. [8] it was shown that for a uniformly filled background, for all the links that contribute to the spatial probability distribution, properness implies total properness. For non-uniform filling the same is true for the simple reason that paths that had even linking between the walker and one island anyon will then have multiple pairwise linking when the island has multiple occupancy.

Inserting (20) and (21) into the expression (19) for the fusion space trace we obtain

$$\begin{aligned} \mathrm{tr}\mathcal{Y}_{\vec{a}\vec{a}'} &= (-i^{-\frac{3}{4}})^{w(L_{\vec{a}\vec{a}'})}(-1)^{arf(L_{\vec{a}\vec{a}'})} \prod_{\substack{s=1 \\ m_s>0}}^{n} \widetilde{\ell}_s \\ &= (-1)^{\sum_{s'<s''} m_{s'} m_{s''} \tau(s',s'')} \prod_{\substack{s=1 \\ m_s>0}}^{n} \widetilde{\ell}_s (i)^{\frac{\ell_s}{2} m_s} (-1)^{m_s c_2(s)} \ . \end{aligned} \tag{22}$$

For islands s such that $m_s > 0$ and $\widetilde{\ell}_s = 1$, i.e. $\frac{\ell_s}{2} \in \mathbb{Z}$, we can use a result of [8], and simplify

$$c_2(s) = \frac{\ell_s}{6}(\ell_s^2 - 1) = \frac{\ell_s}{2}\frac{1}{3}\left[4\left(\frac{\ell_s}{2}\right)^2 - 1\right] \overset{mod\ 2}{=} \frac{\ell_s}{2} \ . \tag{23}$$

Hence, our final result for $\mathrm{tr}\mathcal{Y}_{\vec{a}\vec{a}'}$ reads

$$\mathrm{tr}\mathcal{Y}_{\vec{a}\vec{a}'} = \prod_{\substack{s=1 \\ m_s>0}}^{n} \widetilde{\ell}_s (-i)^{\frac{\ell_s}{2} m_s} \prod_{1\le s'<s''\le n} (-1)^{m_{s'} m_{s''} \tau(s',s'')} \ . \tag{24}$$

For uniform background configuration we recover the case studied in [8].

To illustrate the role of disorder in a non-Abelian anyonic quantum walk, we choose uniform island occupation probabilities. As (24) is for $m_s > 0$ 4-periodic in m_s we take $W(m) = 1/4$ for $1 \le m \le 4$ and $W(m) = 0$ otherwise [23]. The average trace over the fusion space for Ising model anyons is calculated as

$$\langle\langle \mathrm{tr}\mathcal{Y}_{\vec{a}\vec{a}'} \rangle\rangle = \sum_{\vec{m}\in\{1,\ldots,4\}^n} \frac{1}{4^n} \prod_{s=1}^{n} \widetilde{\ell}_s (-i)^{\frac{\ell_s}{2} m_s} \prod_{1\le s'<s''\le n} (-1)^{m_{s'} m_{s''} \tau(s',s'')} \ . \tag{25}$$

We observe the following:

$$\langle\langle \mathrm{tr}\mathcal{Y}_{\vec{a}\vec{a}'}\rangle\rangle = \left[\prod_{s=1}^{n}\widetilde{\ell}_s\right]\frac{1}{4^{n-1}}\sum_{\vec{m}\in\{1,\ldots,4\}^{n-1}}\prod_{s=1}^{n-1}(-i)^{\frac{\ell_s}{2}m_s}\prod_{1\le s'<s''\le n-1}(-1)^{m_{s'}m_{s''}\tau(s',s'')}$$
$$\times\frac{1}{4}\sum_{m_n=1}^{4}\left[(-i)^{\frac{\ell_n}{2}}\right]^{m_n}\left[\prod_{s'=1}^{n-1}(-1)^{m_{s'}\tau(s',n)}\right]^{m_n}$$
$$=\ldots\times\begin{cases}1 & \text{if } (-i)^{\frac{\ell_n}{2}}(-1)^{\sum_{s'=1}^{n-1}m_{s'}\tau(s',n)}=1\\ 0 & \text{otherwise}\end{cases} \tag{26}$$

Hence, $\langle\langle \mathrm{tr}\mathcal{Y}_{\vec{a}\vec{a}'}\rangle\rangle = 0$ whenever $\ell_n \neq 0 \bmod 4$ (i.e. when $(-i)^{\frac{\ell_n}{2}}$ is not a real number). Furthermore, if $\ell_n = 4 \bmod 8$, then $\tau(s',n) = 0$ for all $r = 1,\ldots,n-1$ [24], and therefore $(-1)^{\frac{\ell_n}{4}}(-1)^{\sum_{s'=1}^{n-1}m_{s'}\tau(s',n)} = -1$. Hence, $\langle\langle \mathrm{tr}\mathcal{Y}_{\vec{a}\vec{a}'}\rangle\rangle = 0$ whenever $\ell_n \neq 0 \bmod 8$. By the same reasoning, analogous holds for any island $s = 1,\ldots,n$.

Let us define $\widetilde{\widetilde{\ell}}_s \equiv \delta_{0,\ell_s \bmod 8}$. We have

$$\langle\langle \mathrm{tr}\mathcal{Y}_{\vec{a}\vec{a}'}\rangle\rangle = \prod_{s=1}^{n}\widetilde{\widetilde{\ell}}_s\sum_{\vec{m}\in\{1,\ldots 4\}^n}\frac{(-1)^{\sum_{1\le s'<s''\le n}m_{s'}m_{s''}\tau(s',s'')}}{4^n} \tag{27}$$

The expression $(-1)^{m_{s'}m_{s''}\tau(s',s'')}$ is invariant under shifting $m_{s'} \to m_{s'}+2$ or $m_{s''} \to m_{s''}+2$. Therefore, the sum over $\vec{m} \in \{1,\ldots,4\}^n$ contains 2^n classes of 2^n equivalent configurations. Also, $m_j = 0$ is equivalent with $m_j = 2$. We conclude that the average position distribution of the Ising quantum walk after t steps, $\langle\langle p^{(\mathrm{Ising})}(s,t)\rangle\rangle$, is given by (6) with average fusion space trace

$$\langle\langle \mathrm{tr}\mathcal{Y}^{(\mathrm{Ising})}_{\vec{a}\vec{a}'}\rangle\rangle = \left[\prod_{s=1}^{n}\widetilde{\widetilde{\ell}}_s\right]\mathcal{T}_{\vec{a}\vec{a}'}\ . \tag{28}$$

Here

$$\mathcal{T}_{\vec{a}\vec{a}'} = \frac{1}{2^n}\sum_{\vec{m}\in\{0,1\}^n}\prod_{1\le s'<s''\le n}(-1)^{m_r m_s\tau(s',s'')}. \tag{29}$$

which can be interpreted as an arithmetic mean of the quantity $(-1)^{arf(L^*_{\vec{a}\vec{a}'})}$ taken over all sublinks $L^*_{\vec{a}\vec{a}'}$ of a link $L_{\vec{a}\vec{a}'}$.

Comment: while the Ising model anyons correspond to spin$-1/2$ irreps of the quantum group $SU(2)_2$ the braid generators for the two models are not identical. The primary difference relevant to our studies is the $R_{\frac{1}{2}\frac{1}{2}}$ matrix for braiding of two spin1/2 irreps that fuse into spin-0 or spin-1 irreps. For Ising model anyons,

$$R^{\frac{1}{2},\frac{1}{2}}_{\mathrm{Ising}} = e^{-i\frac{\pi}{8}}\begin{pmatrix}1 & 0\\ 0 & i\end{pmatrix} \quad \text{and} \quad R^{\frac{1}{2},\frac{1}{2}}_{SU(2)_2} = iR^{*\frac{1}{2},\frac{1}{2}}_{\mathrm{Ising}}. \tag{30}$$

This implies the relevant braid generators for these models are equivalent up to a phase i and complex conjugation. In disordered walks, the distribution of stationary anyons is non-uniform and the walker may thus pick up non-trivial phases from bra- and ket-evolution. The difference between these phases is given by the writhe w, which is the difference between positive and negative crossings in the link diagram. The total phase difference is then $i^w = i^{2\sum_{s=1}^{N}m_s\ell_s}$. But in view of (20), the trace is zero unless ℓ_s is a multiple of 2, so that $i^w = 1$, and all the results herein hold equivalently for Ising and $SU(2)_2$ anyons.

A. Numerical calculations of non-Abelian anyons

We calculated the evolution numerically using two methods. First, the probability distribution was calculated exactly using Eqs. (4) and (24) up to 23 time steps, and the average variance $\langle\langle\sigma^{2(\mathrm{Ising})}(t)\rangle\rangle$ over at least 100 charge configurations $m_s \in \{1,\ldots,4\}$ was obtained (see Fig. 6(a)). The average variance is approximately a straight line with slope 0.456 from 10 to 23 time steps, but the error bars of the variance, obtained by the standard deviation, overlap with the error bars of the Abelian case, so we cannot distinguish between Abelian and non-Abelian anyons on this short time scale. Considering occupations $m_s \in \{0,\ldots,4\}$ (vacuum charges included), the variance is slightly larger, i.e. the wave packet is diffusing faster (not shown).

To obtain results for longer times, we turn to the continuous-time picture where the time evolution is generated by a Hubbard-type Hamiltonian H and the propagator $e^{-iH\delta t}$ implements an infinitesimal time evolution. The total Hamiltonian is given by the sum of the shift and coin flip terms $H = H_{\mathrm{shift}} + H_{\mathrm{flip}}$, where [25]

$$H_{\mathrm{shift}} = J\sum_s (T^-_{s+1}\hat{b}_s P_1 + T^+_s \check{b}_s P_2) + \mathrm{h.c.} \tag{31}$$

$$H_{\mathrm{flip}} = \sum_s (\kappa\,|2\rangle_s\langle 1| + \kappa^*\,|1\rangle_s\langle 2|) \tag{32}$$

with $J \in \mathbb{R}, \kappa \in \mathbb{C}$ and $T^{\pm}_s = (|1\rangle_{s\pm1}\ {}_s\langle 1| + |2\rangle_{s\pm1}\ {}_s\langle 2|)\otimes I_{\mathrm{fusion}}$ are translation operators between sites s and $s\pm1$, $\hat{b}_s$ are braid generators as defined above for braiding the mobile anyon around anyons in the island between s and $s+1$ (acting on fusion space only) and $P_c = \sum_s |c\rangle_s\langle c|\otimes I_{\mathrm{fusion}}$ are projectors to the coin states. Here $|c\rangle_s$ corresponds to occupation of state c at site s, i.e. $|c=0\rangle_s$ corresponds to no mobile anyon at site s, $|c=1\rangle_s$ ($|c=2\rangle_s$) is a mobile anyon with coin state $|0\rangle$ ($|1\rangle$) at site s. Here we consider only the case where coins are identical on every site.

The above Hamiltonian is the generator of continuous-time evolution for total time T. Running the continuous-time walk for time T simulates the discrete-time quantum walk in a stroboscopic manner, such that the walker makes $T/\delta t$ steps of infinitesimal length δt: $e^{-iHT} = (e^{-iH\delta t})^{T/\delta t}$. In the first order of Suzuki-Trotter expansion, the propagator decomposes to $e^{-iH_{\mathrm{shift}}\delta t}e^{-iH_{\mathrm{flip}}\delta t}$, similarly as the single step operator in the discrete-time quantum walk model.

We perform numerics on an $n = 100$ sized lattice with open (reflecting) boundaries using the "Time-Evolving Block Decimation" (TEBD) [26] algorithm that is based on Matrix Product States (MPS) using $J = \kappa = 1$ to mimic the discrete coin flip. Our implementation of the TEBD algorithm explicitly preserves anyonic charge and also particle number [27] corresponding to the presence of a single walker. Full details of the numerical simulation are given in Ref. [25]. Thus, while the position of the walker and the fusion degrees of freedom of the anyons are entangled during the time evolution, the algorithm preserves distinction between them. This in turn allowed for specification of total anyonic charge and particle number, here we considered the total vacuum sector with one walker. Fig. 6 shows that for non-Abelian anyons the variance grows linearly as a function of time, indicating no signature of localisation.

B. Correlations in time

The absence of localization in the non-Abelian case can be understood heuristically as a decoherence effect. The fusion Hilbert space $\mathcal{H}_{\mathrm{fusion}}$ of the non-Abelian anyons acts as a non-local and highly non-Markovian environment whose dimension grows exponentially as $d^{|\vec{m}|}$. The entanglement between the quantum walk DOFs and fusion DOFs is known to erase the quantum effects

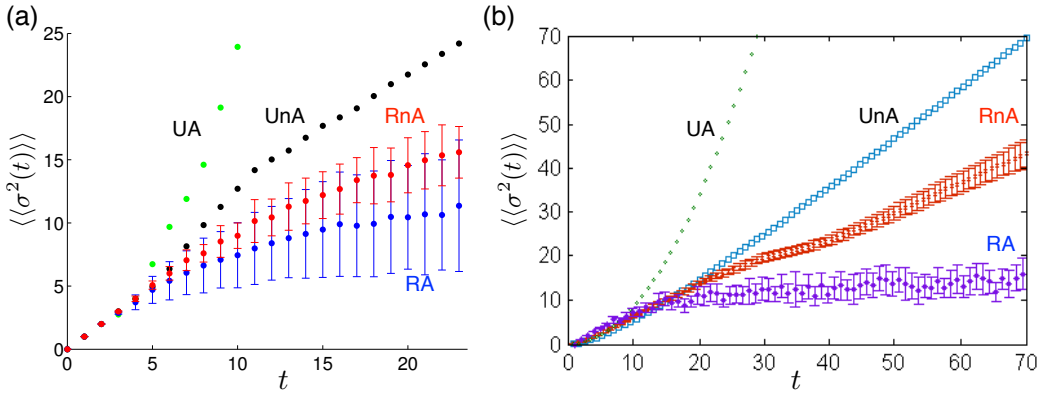

FIG. 6: Numerical results for transport of Abelian and non-Abelian anyons. (a) Exact results for the discrete time quantum walk with anyons over an $n = 46$ sized lattice. Here are plotted the variances for Abelian anyons with $\frac{\pi}{8}$ exchange statistics around a uniform background of islands singly occupied by Abelian anyons (Uniform Abelian=UA), Ising model anyons around a uniform background $m_s = 1 \forall s$ (Uniform non-Abelian=UnA), Abelian anyons with occupation probability uniform over $m_s \in \{0, \ldots, 7\}$ (Random Abelian=RA; averaging over at least 100 configurations), and Ising anyons with $m_s \in \{1, \ldots, 4\}$ (Random non-Abelian=RnA; 50 configurations). (b) Variance of anyons in a Hubbard model on a ladder realising a continuous time anyonic quantum walk over an $n = 100$ sized lattice. Here space and time axes are scaled so that a continuous time classical diffusion would have diffusion coefficient providing $\sigma^2(t) = t$. For the random non-Abelian model, island occupations are with $m_s \in \{0, \ldots, 4\}$ averaged over 50 configurations. The asymptotic slope for the case RnA is 0.54 and it remains positive and less than one within one sigma variance. Numerics are obtained using an approximate method employing real time evolution of an anyonic MPS with bond dimension equal to 100.

in the case of uniform filling [8]. Furthermore, on comparing (28) to the Abelian expression (8) for $N = 8$, they are identical except for the prefactor $\mathcal{T}_{\vec{a}\vec{a}'}$. The key distinguishing feature is decoherence introduced by this factor. Considering Eq. (8) as the coherent expression where the quantum interference of probability amplitudes causes localisation, we argue that the $\mathcal{T}_{\vec{a}\vec{a}'}$ coefficient can be viewed as a noise term due to the dependence on the link invariant τ which fluctuates as the length of braids increases.

As shown in Ref. [28], the quantum walk is diffusive in the presence of both temporal and spatial disorder, in other words localization does not occur in a spatially disordered system if temporal randomness is also present. The effect of $\mathcal{T}_{\vec{a}\vec{a}'}$ is that it multiplies the contribution from each path by the configuration average over $(-1)^{\sum_{1\leq s'<s''\leq n} m_{s'} m_{s''} \tau(s',s'')}$. While this term preserves memory of the whole history of the particle's trajectory, we argue that at short time scales it fluctuates in a disordered manner. The value of τ changes when a new Borromean ring is formed, which requires at least 4 time steps. Also, the formation of a Borromean ring requires a very specific pattern in the particle's trajectory which is in no way periodic. In addition, because of the condition on the last coin outcomes $a_t = a'_t$, there are new path patterns up to $t-1$ time steps introduced on every time step which were not allowed for the previous time step, so these

paths are not correlated to previous evolution at all.

The time correlations of the τ invariant can be tracked by defining the correlator

$$C(t,t') = \frac{\left\langle (-1)^{\tau_t}(-1)^{\tau_{t-t'}}\right\rangle - \left\langle (-1)^{\tau_t}\right\rangle\left\langle (-1)^{\tau_{t-t'}}\right\rangle}{1-\left\langle (-1)^{\tau_t}\right\rangle^2} \tag{33}$$

where $\tau_t = \sum_{1\le s'<s''\le n}\tau(s',s'')$ is the sum of three-component invariants for all sublinks for a path up to t time steps and $\left\langle\ \cdot\ \right\rangle_{(\vec{a},\vec{a}')\rightsquigarrow s_0}$ is the expectation value over all paths leading to the initial site s_0 (the subindex has been suppressed above for clarity). The term in the denominator is a normalization factor, which is defined to be the value of the term in the numerator in the perfectly correlated case $t'=0$. For simplicity, the correlator is calculated only for the uniform filling ($m_s = 1 \quad \forall s$) using the same method as described in [8]. The time correlations can be analysed by keeping the final time t fixed and calculating the correlator for increasing values of t'. The intermediate time value $\tau_{t-t'}$ is calculated by erasing the t' last braid generators from the total braid word, such that braiding is switched off after $t-t'$ time steps. For some braid words, the quantity $\tau(s',s'')$ is not well defined in our method, in which case we set $\tau(s',s'')=0$. The correlator for $t=18$ is plotted in Fig. 7, which shows that the correlations fall off exponentially after one step, indicating that effectively the τ invariant maintains memory only for a short period of time, and the environment is Markovian at long time scales. Note that because of the condition $a_t = a'_t$, the braiding at the last time step can always be trivially undone, therefore the last two time steps are perfectly correlated. The correlator can also be calculated for other sites $s \neq s_0$. In these cases, the rapid falloff is observed for the central region $s_0 - t/\sqrt{2} \le s \le s_0 + t/\sqrt{2}$, and outside this region the falloff becomes linear at the furthest edge sites. The edge behaviour is however irrelevant, as the behaviour of the quantum walk is determined by the central region only.

The fundamental reason for the classical-like behaviour of the walker is the strong entanglement between the quantum walk states and the fusion states, and the highly mixing nature of the fusion space environment. The walker states stay entangled with the fusion states for long time periods, and recurrences where these states become uncoupled happen very rarely.

We have also investigated the effect of temporally random phases introduced to the spatially random Abelian walk. In this model the wave function is multiplied by a random -1 phase with some probability p_{phase} if the walker crosses a site belonging to the temporally fluctuating region of sites. The calculations with different values of p_{phase} and different sizes of the region up to 500 time steps showed that the behaviour becomes diffusive in all these cases.

V. CONCLUSIONS

An experimental demonstration of the disordered anyonic quantum walk could be realized with a chain of quantum double point contacts in FQH liquids, as discussed in some detail in Ref. [29]. There the walker particle is a mobile edge excitation of the 2D FQH liquid, coin mixing is achieved by (weak) tunneling between two edges, and island populations can be changed by creating bulk excitations via top gates. The conductivity between the injection point and the measurement point is proportional to the probability to reach the absorbing boundary when the walker starts localized at the injection point. Experimental control of such double point contact devices and observation of interference between fractional charges was reported in Refs. [30, 31].

Our study provides a new paradigm of disorder that has the ability to override the localisation properties of quasiparticles with anyonic statistics. In a real system with random potentials Abelian anyons that do not localise due to the potentials can be localised just by the presence of a random anyonic environment. On the other hand, non-Abelian $SU(2)_2$ anyons that would

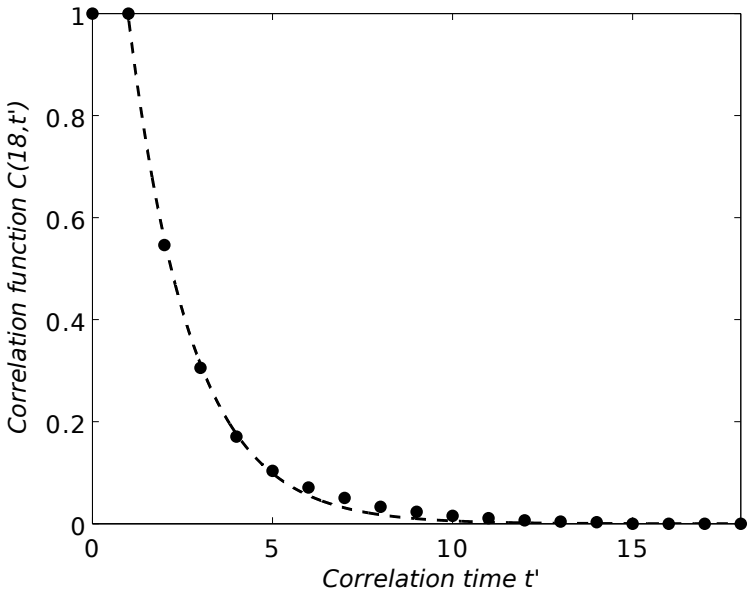

FIG. 7: Correlator $C(t,t')$ as a function of t' with total number of time steps $t = 18$. The line shows the best exponential fit $C(18,t') = 1.77\, e^{-0.58\, t'}$. The value $C(18, t' = 18) \sim 10^{-16}$

localise due to some random potential can be delocalised if a random background of non-Abelian anyons is present.

We expect delocalisation to occur even for more general $SU(2)_k$ non-Abelian anyons due to the entanglement of the walker with the environment. Indeed, it has been demonstrated that the entanglement of the walker with its uniform environment for any $k > 1$ is strong enough to cause the walk to decohere obtaining eventually a classical diffusive behaviour [9].

VI. ACKNOWLEDGEMENTS

We acknowledge helpful discussion with S. Simon and Z. Wang. V.Z. received support from the Grant Agency of the Czech Technical University in Prague, grant No. SGS13/217/OHK4/3T/14, and GAČR Grant No. P402/12/J077, S.S. received support from the MQNS grant by Macquarie University Grant No. 9201200274, G.K.B. received support from the ARC via the Centre of Excellence in Engineered Quantum Systems (EQuS), project number CE110001013, and J.K.P. received support from the EPSRC.

Appendix A: Localization lengths

1. Bounding the localisation length

Here we compute the bounds on the localization length for Abelian anyons with exchange statistics π/N. This is done by computing $\langle\langle \ln |t_{1,n}|^2 \rangle\rangle$, which is the statistical average of the

logarithm of the transition probability amplitude taken over the angles $\theta_1, \theta_2, \ldots, \theta_{n-1}$ which are valued in the discrete set $\{\frac{\pi}{N} m \mid m = 0, \ldots, N-1\}$. To proceed, we carry out the θ_{n-1}-average in the last term of (13),

$$\sum_{m_{n-1}=0}^{N-1} \frac{1}{N} \ln |1 - r_n r'_{1,n-1} e^{i\frac{2\pi}{N} m_{n-1}}|^2 = \frac{1}{N} \ln \left| \prod_{m_{n-1}=0}^{N-1} (1 - r_n r'_{1,n-1} e^{i\frac{2\pi}{N} m_{n-1}}) \right|^2$$
$$= \frac{1}{N} \ln |1 - (r_n r'_{1,n-1})^N|^2 \tag{A1}$$

In the latter equality we used the fact that

$$\prod_{m=0}^{N-1} (1 - C e^{i\frac{2\pi}{N} m}) = 1 - C^N \ , \tag{A2}$$

which can be proven by using the Newton's identities between elementary symmetric polynomials and power sums [12].

The $\theta_1, \ldots, \theta_{n-2}$-average of (A1) becomes trivial once we estimate ($|r'_{1,n-1}| \leq 1$)

$$\begin{aligned} \ln(1 - (|r_n||r'_{1,n-1}|)^N)^2 &\leq \ln |1 - (r_n r'_{1,n-1})^N|^2 \\ &\leq \ln(1 + (|r_n||r'_{1,n-1}|)^N)^2, \qquad \text{(A3)} \\ \ln(1 - |r_n|^N)^2 &\leq \ln |1 - (r_n r'_{1,n-1})^N|^2 \\ &\leq \ln(1 + |r_n|^N)^2 \ . \qquad \text{(A4)} \end{aligned}$$

The upper and lower bounds of relation (13) read

$$\langle\langle \ln |t_{1,n}|^2 \rangle\rangle \leq \langle\langle \ln |t_{1,n-1}|^2 \rangle\rangle + \ln |t_n|^2 - \frac{1}{N} \ln(1 - |r_n|^N)^2 \tag{A5}$$

and

$$\langle\langle \ln |t_{1,n}|^2 \rangle\rangle \geq \langle\langle \ln |t_{1,n-1}|^2 \rangle\rangle + \ln |t_n|^2 - \frac{1}{N} \ln(1 + |r_n|^N)^2 \tag{A6}$$

respectively. When applied repeatedly, these recurrences yield ($t_{1,1} \equiv t_1$)

$$\begin{aligned} \langle\langle \ln |t_{1,n}|^2 \rangle\rangle &\leq \sum_{j=1}^{n} \ln |t_j|^2 - \frac{1}{N} \sum_{j=2}^{n} \ln(1 - |r_j|^N)^2 \ , \\ \langle\langle \ln |t_{1,n}|^2 \rangle\rangle &\geq \sum_{j=1}^{n} \ln |t_j|^2 - \frac{1}{N} \sum_{j=2}^{n} \ln(1 + |r_j|^N)^2 \ , \end{aligned} \tag{A7}$$

where we have omitted the lower index of the averaging brackets $\langle\langle \ldots \rangle\rangle$.

2. Island distributions including N anyons each with exchange statistics $\frac{\pi}{N}$

The argument in the main text assumed anyon occupancies m_j in each of the islands were identically distributed independent random variables drawn from a uniform distribution over the set $\{m = 0, \ldots, N-1\}$. If instead we expand the set to $\{m = 0, \ldots, N\}$ so that we can include

populations having cummulative fermionic exchange phases with the walker, then the results do not change much. By a similar analysis one finds that the localization length satisfies the bounds:

$$\xi_{loc}^{LB}(N) \leq \xi_{loc} \leq \xi_{loc}^{UB}(N) \tag{A8}$$

where

$$\begin{aligned} \xi_{loc}^{UB}(N) &= \frac{1}{\ln[(1-|r|^2)(1-|r|^N)]^{\frac{2}{N+1}} - \ln|t|^2}, \\ \xi_{loc}^{LB}(N) &= \begin{cases} \frac{1}{\ln[(1+|r|^2)^2(|r|^{2N}+2|r|^N+1)]^{\frac{1}{N+1}} - \ln|t|^2} & N \text{ odd} \\ \frac{1}{\ln[(1+|r|^2+2|r|\cos\frac{\pi}{N})(|r|^{2N}+2|r|^N+1)]^{\frac{1}{N+1}} - \ln|t|^2} & N \text{ even} \end{cases} . \end{aligned} \tag{A9}$$

Again these bounds are valid only for $N > 2$. Choosing, as before,

$$t = -\frac{1}{\sqrt{2}} \ , \ t' = \frac{1}{\sqrt{2}} \ , \ r = \frac{1}{\sqrt{2}} \ , \ r' = \frac{1}{\sqrt{2}} \ . \tag{A10}$$

the localization length estimate for $N = 8$ ($\frac{\pi}{8}$-anyons) now has looser bounds

$$1.218 \leq \xi_{loc} \leq 1.906 \ . \tag{A11}$$

Of course, in the limit $N \to \infty$, we have $\xi_{loc} \to -\frac{1}{\ln|t|^2}$.

---

[1] J.M. Leinaas and J. Myrheim, J. Nuovo Cimento Soc. Ital. Fis. B **37**, 1 (1977).
[2] J.K. Pachos, *Introduction to Topological Quantum Computation*, Cambridge Univ. Press (2012).
[3] I. P. Radu, J. B. Miller, C. M. Marcus, M. A. Kastner, L. N. Pfeiffer, and K. W. West, Science **320**, 899 (2008); R. L. Willett, L. N. Pfeiffer, and K. W. West, Proc. Natl. Acad. Sci. **106**, 8853 (2009).
[4] V. Mourik, K. Zuo, S. M. Frolov, S. R. Plissard, E. P. A. M. Bakkers, and L. P. Kouwenhoven, Science **336**, 1003 (2012).
[5] M.H. Freedman, A. Kitaev, M.J. Larsen, and Z. Wang, Bull. Amer. Math. Soc. **40**, 31 (2002).
[6] G.K. Brennen, D. Ellinas, V. Kendon, J.K. Pachos, I. Tsohantjis, and Z. Wang, Ann. Phys. **325**, 664 (2010).
[7] A. Ambainis, E. Bach, A. Nayak, A. Vishwanath and J. Watrous, Proc. 33rd Annual ACM STOC, 37 (2001); A. Nayak and A. Vishwanath, quant-ph/0010117.
[8] L. Lehman, V. Zatloukal, G.K. Brennen, J.K. Pachos, and Z. Wang, Phys. Rev. Lett. **106**, 230404 (2011).
[9] L. Lehman, D. Ellinas, and G.K. Brennen, J. Comput. Theor. Nanosci. 10, 1634 (2013);
[10] P. W. Anderson, Phys. Rev. **109**, 1492 (1958).
[11] C.A. Müller and D. Delande, arXiv:1005.0915v2.
[12] I.G. Macdonald, *Symmetric Functions and Hall Polynomials*, second ed. Oxford: Clarendon Press. (1995).
[13] V. Zatloukal, Master's thesis, Czech Technical University in Prague, 2011 (available online at `http://ssmf.fjfi.cvut.cz/2008.html`).
[14] F. Klopp and K. Pankrashkin, Lett. Math. Phys. **87**, 99 (2009).
[15] J.T. Chalker and S. Siak, J. Phys.: Cond. Matt. **2** 2671 (1990).
[16] H. Schanz and U. Smilansky, Phys. Rev. Lett. **84**, 1427 (2000).
[17] X. Chen, L. Fidkowski, and A. Vishwanath, arXiv:1306.3250.
[18] L.H. Kauffman, Topology **26**, 395 (1987).
[19] D. Aharonov, V. Jones and Z. Landau, Algorithmica **55**, 395 (2009); arXiv:quant-ph/0511096.
[20] V.F.R Jones, Bull. Amer. Math. Soc. **12**, 103 (1985).

[21] H. Murakami, Sem. notes Kobe Univ. **11** 335 (1983).
[22] R. Kirby and P. Melvin, Geometry and Topology Monographs **7**, 213 (2004); arXiv:math/0410358.
[23] If we include the vacuum island occupation and consider a model with $W(m) = 1/5$ for $0 \leq m \leq 4$, numerics show that the variance of the resulting walker's position distribution grows even faster.
[24] Recall that $\tau(s', s'')$ can be nonzero only if $\ell_{s'}, \ell_{s''} = 0$.
[25] S. Singh, R.N.C. Pfeifer, G. Vidal and G. Brennen, Phys. Rev. B **89**, 075112 (2014).
[26] G. Vidal, Phys. Rev. Lett. **93**, 040502 (2004).
[27] S. Singh, R. N. C. Pfeifer and G. Vidal, Phys. Rev. B **83**, 115125 (2011); arXiv:1008.4774 [cond-mat.str-el] (2010).
[28] A. Albrecht, C. Cedzich, R. Matjeschk, V. B. Scholz, A. H. Werner, and R. F. Werner, Quantum Inf. Process. **11**, 1219 (2012).
[29] V. Zatloukal, L.J. Lehman, J.K. Pachos, and G.K. Brennen, Quantum Computers and Computing **12** (1), 51 (2012).
[30] R. L. Willett, L. N. Pfeiffer, and K. W. West. Measurement of filling factor 5/2 quasiparticle interference with observation of charge e/4 and e/2 period oscilla- tions. Proc. Nat. Acad. Sci. **106**, 8853 (2009).
[31] R. L. Willett, L. N. Pfeiffer, and K. W. West. Phys. Rev. B **82**, 205301 (2010).
[32] Allowing for total island charge that is Fermonic, i.e. $m_j \in \{0, \ldots, N\}$, does not change the results much (see Appendix A 2).